

IFT - UNESP
INSTITUTO DE FÍSICA TEÓRICA

M. Sc. dissertation

IFT-T.000/99

Femtoscopic studies of $D^0 D^0$ and $\bar{D}^0 \bar{D}^0$ correlations

Isabela Maietto Silvério

Advisor

Prof. Sandra dos Santos Padula

Co-advisor

Prof. Gastão Inácio Krein

August 2021

S587f Silvério, Isabela Maietto
Femtoscopic studies of D^0D^0 and $\bar{D}^0\bar{D}^0$ correlations / Isabela Maietto
Silvério. – São Paulo, 2021
86 f.

Dissertação (mestrado) – Universidade Estadual Paulista (Unesp),
Instituto de Física Teórica (IFT), São Paulo
Orientador: Sandra dos Santos Padula
Coorientador: Gastão Inácio Krein

1. Partículas (Física nuclear). 2. Correlações entre partículas. 3.
Interações quark-gluon. I. Título

Sistema de geração automática de fichas catalográficas da Unesp. Biblioteca
do Instituto de Física Teórica (IFT), São Paulo. Dados fornecidos pelo
autor(a).

*Dedico esta dissertação em memória de Rodrigo Tambellini,
de Lorryne Rodrigues e de meu avô "Lavinho" Silvério.*

Agradecimentos

Primeiramente, agradeço à minha família, em especial, aos meus pais Ivete e Irley por acreditarem em mim e nos meus sonhos, por lutarem comigo e torná-los possíveis, e também à minha irmã Júlia por torcer por mim em todos os momentos.

Agradeço à minha orientadora Profa. Sandra dos Santos Padula por me aceitar como aluna e permitir a realização deste trabalho, por todas as discussões e conselhos, tantos profissionais quanto pessoais, mas principalmente, por me mostrar a física com olhos tão encatados e inspiradores! Agradeço ao meu co-orientador Prof. Gastão Krein por toda a ajuda e a disposição ao longo do meu mestrado, e por sempre me incentivar a pensar em física além da minha zona de conforto, isso foi essencial para a minha formação e vou levar sempre comigo!

Aproveito para agradecer aos demais professores e trabalhadores do Instituto de Física Teórica da UNESP. Agradeço ao Prof. Sérgio Novaes por me aceitar como integrante do grupo SPRACE e proporcionar essa oportunidade incrível! Agradeço a todos os outros professores do SPRACE, Prof. Pedro, Prof. Thiago, Prof. Eduardo e Prof. César, e também aos meus colegas Dener, Ana, Túlio, João e Felipe, por contribuírem individualmente com a minha formação. Agradeço também aos organizadores do "*Internacional Masterclass hands on particle physics*", Profa. Sandra, Profa. Cleide, Profa. Valéria, Prof. Nelson, Prof. Pedro e Prof. Fernando, por confiarem em mim e me proporcionarem o privilégio de contribuir com esse evento que atinge tantas pessoas!

Agradeço ao meu colega de profissão, e companheiro Breno por toda a ajuda e suporte nesse período! Aos meus colegas de faculdade e agora amigos para a vida Bruno, Gabriela, Mariana e Gabriel. Agradeço aos meus colegas do IFT, em especial ao Matheus Martins, Bruno, Gabriel Sousa, Matheus Hrabowec, Raul, Vinicius e Gabriel Vidal por todas as (muitas) horas de estudo e por todos os bons momentos que compartilhamos. Agradeço também à Ana Julia por toda a atenção e por me incentivar a buscar sempre o meu melhor.

O presente trabalho foi realizado com o apoio da Coordenação de Aperfeiçoamento de Pessoal de Nível Superior – Brasil (CAPES) – Código de financiamento 001.

Resumo

A femtoscopia é conhecida como uma ferramenta para investigar as dimensões espaço-temporais da região de onde as partículas são emitidas em colisões de alta energia. Embora originalmente proposta para descrever correlações de estatística quântica para partículas idênticas, é sensível também às interações de estado final, como a interação de Coulomb, ao considerar partículas carregadas e a interação forte entre hádrons. A correlação de duas partículas, em função do momentum relativo do par, pode ser descrita em termos da norma ao quadrado da função de onda total das partículas correlacionadas. Neste estudo, foram desenvolvidos dois códigos para realizar o cálculo numérico resolvendo as equações de Schrödinger e Lippmann-Schwinger com modelos de potenciais para obter a função de onda. Nesta dissertação, foi realizada a validação do código resolvendo a equação de Schrödinger usando dois tipos de partículas correlacionadas próton-lambda ($p\Lambda$) e lambda-lambda ($\Lambda\Lambda$), cuja interações já são conhecidas na literatura. Essas correlações foram medidas pela colaboração ALICE, no LHC, e pela colaboração STAR, no RHIC. A ausência de dados experimentais e de descrição teórica das correlações D^0D^0 e $\bar{D}^0\bar{D}^0$, motivou o desenvolvimento de um código que resolvesse a equação de Lippmann-Schwinger com um potencial não-local para obter a função de onda espalhada e, posteriormente, a respectiva função de correlação de duas partículas. A descrição numérica desenvolvida neste trabalho pode ser usada para estudos de correlação de D^0D^0 e $\bar{D}^0\bar{D}^0$ em experimentos em colisores de partículas, como um possível guia.

Palavras Chaves: Correlação de partículas; Femtoscopia; Interação forte.

Áreas do conhecimento: Física; Física de partículas.

Abstract

Femtoscopy is a powerful tool to investigate the space-time dimensions of the region from which particles are emitted, in high energy collisions. Although originally derived to describe identical particle quantum statistical correlations, it is sensitive also to final state interactions, such as Coulomb interactions, when considering charged particles and strong interactions between hadrons. The two-particle correlation is written as a function of the pair relative momentum, and can be described in terms of the norm squared of the total wave function of the correlating particles. In this study, two codes were developed to perform the numerical calculation solving the Schrödinger and the Lippmann-Schwinger equations with potential models to obtain the wave function. In this dissertation, the validation of the code solving the Schrödinger equation was performed, using two types of correlating particles proton-lambda ($p\Lambda$) and lambda-lambda ($\Lambda\Lambda$), whose those interactions is already available in the literature. Such correlations were measured by the ALICE collaboration at the LHC and by the STAR collaboration at RHIC. The absence of experimental data and theoretical description of D^0D^0 and $\bar{D}^0\bar{D}^0$ correlations motivated the development of a code that solves the Lippmann-Schwinger equation with a non-local potential to obtain the scattered wave function and, afterwards, the respective two-particle correlation function. Furthermore, the numerical description elaborated in this work might be used to investigate correlations of D^0D^0 and $\bar{D}^0\bar{D}^0$ in particle collider experiments, as a guideline.

Keywords: Particles correlation; Femtoscopy; Strong interaction.

Knowledge Areas: Physics; Particle Physics.

Contents

1	Introduction	1
2	Introduction to femtoscopy	4
2.1	Identical particles correlation	5
2.1.1	Pairs of identical particles	12
2.2	Final state interactions	14
2.2.1	Coulomb interactions	16
2.2.2	Strong interactions	16
2.3	Joint effects	24
2.3.1	Two identical particles	24
2.3.2	Two non-identical particles	25
3	Scattering wave function	26
3.1	Schrödinger equation	26
3.1.1	Euler method	29
3.2	Lippmann-Schwinger equation	30
3.2.1	Partial wave analysis	32
3.2.2	Numerical description	37
3.3	Equivalence of the approaches	38
3.3.1	Yukawa potential	39
3.4	Extension: other potential models	41
3.4.1	Potentials models for describing $\Lambda\Lambda$ interaction	41
3.4.2	Usmani potential	43
3.4.3	Meson-meson potential	45
4	Numerical results	49
4.1	Validation of the codes	49
4.1.1	$\Lambda\Lambda$ correlation	49
4.1.2	$p\Lambda$ correlation	56
4.2	$D^0D^0, \bar{D}^0\bar{D}^0$ correlation	60
5	Conclusions and final remarks	70

A Elements of the meson-meson potential	72
A.1 Short-range contribution	72
A.2 Long-range contribution	80
Bibliography	82

Chapter 1

Introduction

One of the most important advances in science in the last century was the development of the theory that describes the fundamental particles and their interactions, the Standard Model (SM) of elementary particles. The composition of matter has been an intriguing question for a long time. The findings of the last century showed that matter is composed of elementary particles, quarks and leptons (fermions, half-integer spin particles), and particles that intermediate the fundamental interactions (bosons, integer spin particles), i.e, electromagnetic (mediated by photons), weak (mediated by W^+ , W^- and Z) and strong interaction (mediated by gluons). In particular, the strong force is responsible for the interaction between quarks and gluons, described by quantum chromodynamics (QCD), in which a new type of charge, or quantum number, called color, was introduced. There are six flavors of quarks known: up (u), down (d), strange (s), charm (c), top (t), and bottom (b). One of the characteristics of QCD is the color confinement, implying that quarks seem to be permanently confined in bound states, the hadrons, which can be further divided into two categories, the baryons and the mesons. The first group corresponds to particles composed of three quarks and the second, to those composed of a quark-antiquark pair. These configurations must have a neutral color charge, since no colored hadrons have been observed so far. To be able to investigate and/or test some of the hypotheses of the SM a substantial development in particle accelerators and detectors was needed to reach an ever increasing collision energy.

Around the middle of the last century, a technique was proposed in radio astronomy, by the engineer Robert Hanbury-Brown and the mathematician Richard Q. Twiss, to measure the angular diameter of a star using the correlation between two photons emitted from it. This was the first study and measurement of identical particles correlation that lead to the *intensity interferometry* or **Hanbury-Brown-Twiss (HBT) effect**. However, in the sixties, without any knowledge of the HBT effect, a similar effect was accidentally observed, when considering the momentum

correlation of identical pions originated from proton-antiproton collisions, while the experiment searched for the ρ meson. After these findings, it was possible to study the correlation between particles within very short life-times. One insight that came from the interferometry studies, is that it was possible to measure some properties of the emission source of the correlated particles, for example, its dimensions.

This last information was of great interest for heavy-ion physics and collisions, since the field aims to probe and to understand better the strongly interacting matter at extreme conditions, such as high temperature and energy density. The method applied to high energy collisions, which is called **femtoscopy**, is sensitive not only to quantum statistics, but also to the underlying dynamics, like the source expansion, and to final state interactions, such as Coulomb interactions, when considering charged particles, and strong interactions between hadrons.

A relevant topic nowadays of study in high energy collisions is the correlation function of baryons and mesons, via femtoscopy. This is being investigated by the STAR (the Solenoidal Tracker at RHIC) collaboration at Relativistic Heavy Ion Collider (RHIC), the CMS (Compact Muon Solenoid), and the ALICE (Large Ion Collider Experiment) collaboration at the Large Hadron Collider (LHC). Experimentally, the two-particle correlation function can be obtained as the ratio of the signal distribution, which is the distribution of pairs from the same events, over the reference distribution, for instance, the distribution of pairs from mixed events. For theoretical calculations, the correlation function of two particles, as a function of their relative momentum, can be written in terms of the norm squared of the total wave function of the correlated particles. The total wave function, containing the effect of a potential region, is written in terms of an incident plane wave and the scattered wave function. The scattered contribution can be numerically obtained using methods that solve differential equation, such as the Schrödinger equation, or integrals equations, such as the Lippmann-Schwinger equation, depending on the type of the interaction.

In this work, the description of the femtoscopy tool is made in Chapter 2, where a study of the correlation of identical particles, that gives rise to the contribution of quantum statistics, is done. The contributions to the final state interactions are presented, with a focus on the strong interaction, since the particle correlations

studied in this dissertation describe only electrically neutral particle pairs. The joint effects of the contributions were displayed for correlations of identical spin-1/2 baryons and identical spin-zero mesons.

In Chapter 3, a study in scattering theory was carried out to understand the mechanism of obtaining the total wave function numerically. The Schrödinger equation and its solution are presented, as well as a numerical method for solving it, which works for the case of local potentials. The Lippmann-Schwinger equation is explored in order to expand the formalism to the cases of non-local potentials and momentum-dependent potentials.

In Chapter 4, the validation of the code that solves the Schrödinger equation using two types of interactions, proton-lambda ($p\Lambda$) and lambda-lambda ($\Lambda\Lambda$), is performed by comparing the calculated correlation function with data and also by obtaining the scattering observables and comparing with theoretical results that are already available in the literature. The absence of experimental data and numerical description for D^0D^0 and $\bar{D}^0\bar{D}^0$ correlations, where the mesons are composed of a light quark u and heavy quark c , motivated the development of a code that solves the Lippmann-Schwinger equation with a non-local potential part to obtain the scattered wave function and, afterwards, the respective two-particle correlation function. This procedure can contribute for heavy particle correlations studies and to investigate new exotic bound states of matter, as molecular states arising from the interaction. From the code, it was possible to also obtain the scattering observables. In addition, a comparative study with the Lednicky-Lyuboshitz model for describing final state interactions was developed.

At last in, Chapter 5, a brief discussion is presented regarding the results obtained, together with the conclusion of the studies of this work.

Chapter 2

Introduction to femtoscopy

The studies of identical particles correlations started in the mid-fifties, with Robert Hanbury-Brown and Richard Q. Twiss performing a measurement of the angular diameter of a star using the correlation between two photons emitted from it [1–3]. The probability of detecting two coincident photons will be the correlation with respect to the relative separation across two detectors. When thinking of a system of identical particles, the correlation associates the intensity of a particle at a space-time point and the intensity of the other particle at another point in space-time, both measured coincidentally. This leads to the *intensity interferometry* or **Hanbury-Brown-Twiss (HBT) effect** which provides an estimate of the correlation between identical particles from the same source.

Later in 1960, G. Goldhaber, S. Goldhaber, W. Y. Lee and A. Pais [4], unaware of the HBT method, performed an experiment intended to discover the ρ meson by measuring charged pions in proton-antiproton collisions at $\sqrt{s} = 1.05$ GeV. The study showed that the momentum correlation of two identical pions from the same event could be described as the Fourier transform of a function of the phase space distribution of the emission source, this giving information about source dimensions. However, it was later demonstrated that the method applied to high energy collisions is sensitive not only to quantum statistics [5], but also to the underlying dynamics, like the source expansion, and to final state interactions, such as Coulomb interactions, when considering charged particles, and strong interactions between hadrons.

In this chapter, the construction of the correlation function will be discussed. First, the construction of the description for the quantum statistics (QS) contributions is shown. Then, the introduction of contributions to the final state interactions will be addressed, focusing mainly on the strong interactions (SI), since in this work the pair of particles of interest are electrically neutral. The formalism is, then, also extended for non-identical particles. In the end, the joint effects are

presented, gathering together the QS and SI contribution for identical spin-zero mesons and identical spin-1/2 baryons. Natural units are used throughout this work ($\hbar = c = 1$).

2.1 Identical particles correlation

In this section, the identical particles correlations, i.e., the **Quantum Statistics** (QS) contribution to the two-particle correlation function will be discussed.

First, for example consider a pion particle, which is a boson, emitted from the space-time point $x = (t, \mathbf{x})$ with four-momentum $k = (k^0, \mathbf{k})$ that is detected in the space-time point $x' = (t', \mathbf{x}')$. The probability amplitude for the propagation of the emitted free pion from x to x' [6] is

$$\begin{aligned}\psi(t' - t, \mathbf{x}' - \mathbf{x}) &= A(k, x) e^{i\phi(x)} e^{i[k^0(t'-t) - \mathbf{k} \cdot (\mathbf{x}' - \mathbf{x})]} \\ &= A(k, x) e^{i\phi(x)} e^{ik \cdot (x' - x)},\end{aligned}\quad (2.1)$$

with $A(k, x)$ being the probability amplitude for emitting a particle of momentum k at position x and $\phi(x)$ an emission phase. Hence, the complete probability amplitude $\psi(k : x \rightarrow x')$ for a pion of momentum k to be emitted at the source point x , propagated along the classical trajectory and arrive at x' is

$$\psi(k : x \rightarrow x') = A(k, x) e^{i\phi(x)} e^{ik \cdot (x' - x)}. \quad (2.2)$$

However, the pion emission can occur at any other point in the extended source, therefore, the total amplitude for the detection of a pion at x' is the sum over all source points.

$$\psi(k : \{\text{all } x \text{ points}\} \rightarrow x') = \sum_x A(k, x) e^{i\phi(x)} e^{ik \cdot (x' - x)}. \quad (2.3)$$

The probability $P(k)$ for a pion to be produced at the source and travel to the detector at a point x' , also called single-particle momentum distribution, is the absolute square of the total probability amplitude

$$\begin{aligned}P(k) &= |\psi(k : \{\text{all } x \text{ points}\} \rightarrow x')|^2 \\ &= \left| \sum_x A(k, x) e^{i\phi(x)} e^{ik \cdot (x' - x)} \right|^2.\end{aligned}\quad (2.4)$$

Taking into account all the random phases, $P(k)$ is:

$$P(k) = \sum_x A^2(k, x) + \sum_{x \neq y} A(k, x)A(k, y)e^{i\phi(x)}e^{-i\phi(y)}e^{ik \cdot x}e^{-ik \cdot y}. \quad (2.5)$$

The second term of $P(k)$ can be considered zero because the large number of terms with slowly varying magnitudes are multiplied by rapidly fluctuating random phases that cancel each other out in the sum. Thus, Eq. (2.5) becomes

$$P(k) = \sum_x A^2(k, x). \quad (2.6)$$

Converting the discrete notation to a continuous one, changing the summation into an integral, provides

$$\sum_x \rightarrow \int dx \rho(x).$$

Therefore, the single-particle momentum distribution is then written as

$$P(k) = \int dx \rho(x) A^2(k, x). \quad (2.7)$$

The same formalism can be used to discuss the momentum correlations in the detection of two identical pions from a general source. Consider a pion with four-momentum k_1 emitted from the source point x_1 and detected at x'_1 , and another pion with four-momentum k_2 emitted from the source point x_2 and detected at x'_2 , illustrated on Figure (2.1). The probability amplitude for this process, analogous to Eq. (2.2), is

$$\Psi\{k_1 k_2 : \text{all } x_1 x_2 \text{ points} \rightarrow x'_1 x'_2\} \approx \psi(k_1 : x_1 \rightarrow x'_1) \psi(k_2 : x_2 \rightarrow x'_2), \quad (2.8)$$

where the probability for emitting two pions simultaneously from the same source point is considered negligible. Writing Eq. (2.8) more explicitly, and neglecting any effects of final state interactions, then

$$\Psi\{k_1 k_2 : x_1 x_2 \rightarrow x'_1 x'_2\} \approx A(k_1, x_1) e^{i\phi(x_1)} A(k_2, x_2) e^{i\phi(x_2)} e^{ik_1 \cdot (x_1 - x'_1)} e^{ik_2 \cdot (x_2 - x'_2)}. \quad (2.9)$$

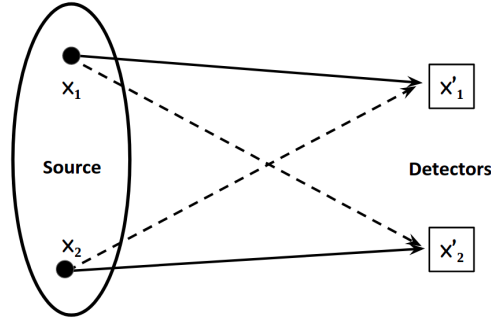


Figure 2.1: Illustration of the emission of a pion with four-momentum k_1 from a source point x_1 and detected at a point x'_1 and another identical pion with four-momentum k_2 from a point x_2 and detected at a point x'_2 [6]. Since the pions are identical, the cross possibility has also to be taken into account.

However, being identical pions, the crossed possibility should also be considered. In other words, the pion with four-momentum k_1 detected at x'_1 could also be emitted at x_2 instead, and propagate from x_2 to x'_1 , and the other pion of momentum k_2 detected at x'_2 could be emitted at x_1 and propagate from x_1 to x'_2 . This can be expressed by the following probability amplitude

$$\Psi\{k_1 k_2 : x_2 x_1 \rightarrow x'_1 x'_2\} \approx A(k_1, x_2) e^{i\phi(x_2)} A(k_2, x_1) e^{i\phi(x_1)} e^{ik_1 \cdot (x_2 - x'_1)} e^{ik_2 \cdot (x_1 - x'_2)}. \quad (2.10)$$

Summing Eq. (2.9) and Eq. (2.10), since both cases can occur:

$$\begin{aligned} \Psi(k_1 k_2 : \{\text{all } x_1 x_2 \text{ points}\} \rightarrow x'_1 x'_2) &= \frac{1}{\sqrt{2}} \sum_{x_1, x_2} e^{i\phi(x_1)} e^{i\phi(x_2)} \\ &\times \left\{ A(k_1, x_1) A(k_2, x_2) e^{ik_1 \cdot (x_1 - x'_1)} e^{ik_2 \cdot (x_2 - x'_2)} \right. \\ &\left. + A(k_1, x_2) A(k_2, x_1) e^{ik_1 \cdot (x_2 - x'_1)} e^{ik_2 \cdot (x_1 - x'_2)} \right\}, \end{aligned} \quad (2.11)$$

for which the two-particle momentum distribution $P(k_1, k_2)$ is written as

$$P(k_1, k_2) = \frac{1}{2} |\Psi(k_1, k_2 : \{\text{all } x_1 x_2 \text{ points}\} \rightarrow x'_1 x'_2)|^2. \quad (2.12)$$

Considering that the source is chaotic and the emissions are independent from

each other, an average over the emission phases should be taken to estimate the two-particle momentum distribution [7]

$$\begin{aligned}
P(k_1, k_2) &= \frac{1}{2} \sum_{x_1, x_2} \left\{ A^2(k_1, x_1) A^2(k_2, x_2) + A^2(k_1, x_2) A^2(k_2, x_1) \right. \\
&+ A(k_1, x_1) A(k_2, x_2) A(k_1, x_2) A(k_2, x_1) \left[e^{i(k_1 - k_2) \cdot (x_1 - x_2)} + e^{-i(k_1 - k_2) \cdot (x_1 - x_2)} \right] \left. \right\} \\
&\times \left\langle e^{i(\phi(x_1) + \phi(x_2) - \phi'(x_1) - \phi'(x_2))} \right\rangle. \tag{2.13}
\end{aligned}$$

The average over the random results is¹

$$\left\langle e^{i(\phi_1 + \phi_2 - \phi'_1 - \phi'_2)} \right\rangle = \delta_{\phi_1 \phi'_1} \delta_{\phi_2 \phi'_2} + \delta_{\phi_1 \phi'_2} \delta_{\phi_2 \phi'_1}. \tag{2.14}$$

Inserting Eq. (2.14) into (2.13), and recollecting that the particles are identical, the exchange symmetry between the two identical bosons, with four-momenta k_1 and k_2 , respectively, emitted from x_1 and x_2 , can be used so that the amplitudes can be written as: $A(k_1, x_1) = A(k_1, x_2)$ and $A(k_2, x_1) = A(k_2, x_2)$. This leads to

$$P(k_1, k_2) = \sum_{x_1, x_2} A^2(k_1, x_1) A^2(k_2, x_2) \left\{ 1 + \frac{1}{2} \left[e^{i(k_1 - k_2) \cdot (x_1 - x_2)} + e^{-i(k_1 - k_2) \cdot (x_1 - x_2)} \right] \right\}. \tag{2.15}$$

Defining $\rho(x)$ as the source density, and changing the discrete notation to a continuous one by replacing the summation by an integral, results

$$\begin{aligned}
P(k_1, k_2) &= \int dx_1 dx_2 \rho(x_1) \rho(x_2) A^2(k_1, x_1) A^2(k_2, x_2) \\
&\times \left\{ 1 + \frac{1}{2} \left[e^{i(k_1 - k_2) \cdot (x_1 - x_2)} + e^{-i(k_1 - k_2) \cdot (x_1 - x_2)} \right] \right\}. \tag{2.16}
\end{aligned}$$

Assuming the following expressions for $S(x_i, k_i)$ [8, 9]

$$S(x_1, k_1) = \rho(x_1) A^2(k_1, x_1), \quad S(x_2, k_2) = \rho(x_2) A^2(k_2, x_2). \tag{2.17}$$

¹To simplify consider $\phi(x_i) = \phi_i$ and $\phi'(x_i) = \phi'_i$.

Therefore, Eq. (2.16) can be rewritten as

$$P(k_1, k_2) = \int dx_1 dx_2 S(k_1, x_1) S(k_2, x_2) \times \left\{ 1 + \frac{1}{2} \left[e^{i(k_1 - k_2) \cdot (x_1 - x_2)} + e^{-i(k_1 - k_2) \cdot (x_1 - x_2)} \right] \right\}. \quad (2.18)$$

Defining the pair relative momentum q and the average pair momentum K of the two identical pions, with four-momentum k_1 and four-momentum k_2 , as

$$q = k_1 - k_2, \quad K = \frac{k_1 + k_2}{2}, \quad (2.19)$$

then, Eq. (2.18) becomes ²

$$P(k_1, k_2) = P(k_1)P(k_2) \left[1 + \left| \int dx \frac{\sqrt{S(x, k_1)S(x, k_2)}}{\sqrt{P(k_1)P(k_2)}} e^{iq \cdot x} \right|^2 \right], \quad (2.20)$$

where according to Eq. (2.7)

$$P(k_1) = \int dx_1 S(k_1, x_1), \\ P(k_2) = \int dx_2 S(k_2, x_2).$$

The two-particle correlation function $C(k_1, k_2)$ is defined as

$$C(k_1, k_2) = \frac{P(k_1, k_2)}{P(k_1)P(k_2)}. \quad (2.21)$$

Using Eq. (2.20), the two-particle correlation function can be written as

$$C(k_1, k_2) = 1 + \frac{\left| \int dx \sqrt{S(x, k_1)S(x, k_2)} e^{iq \cdot x} \right|^2}{\int dx S(x, k_1) \int dy S(y, k_2)}, \quad (2.22)$$

or,

$$C(k_1, k_2) = 1 + \frac{\int dx_1 dx_2 S(x_1, k_1) S(x_2, k_2) \cos [q \cdot (x_1 - x_2)]}{\int dx_1 S(x_1, k_1) \int dx_2 S(x_2, k_2)}. \quad (2.23)$$

The expression above for $C(k_1, k_2)$ is suited to describe the identical bosons correlation, i.e. the Bose-Einstein statistic contribution for spin-zero bosons. In the case of

²Here, it was used the property: $g(k_i, x_i) + g^*(k_i, x_i) = 2\text{Re} [g(k_i, x_i)]$

identical fermions, the very minimal modification is to replace the "+" (plus) sign by a "-" (minus) sign in the expression above, and thus to obtain the Fermi-Dirac Statistic contribution. However, more accurately, the spin composition of the particles involved should be taken into account.

It is very common in the literature to rewrite the Eq. (2.20) into the form of Eq. (2.22). Now, it is immediate to show from Eq. (2.19), $k_1 = K + q/2$ and $k_2 = K - q/2$. Next, considering that the region of interest for interferometry, i.e., where the identical particle correlation signal is stronger, corresponds to small values of the pair relative momentum (with $q \ll K$), the so-called *smoothness approximation* [10] can be applied by expanding the $S(x, k_i)$ with respect to $S(x, K)$, i.e.,

$$\begin{aligned} S(x, k_1) &= S(x, K + q/2) = S(x, K) + \frac{q}{2} \left. \frac{\partial S(x, k')}{\partial k'} \right|_{k'=K} + \mathcal{O}(q^2), \\ S(x, k_2) &= S(x, K - q/2) = S(x, K) - \frac{q}{2} \left. \frac{\partial S(x, k')}{\partial k'} \right|_{k'=K} + \mathcal{O}(q^2). \end{aligned}$$

The product between the $S(x, k_i)$ functions is

$$S(x, k_1)S(x, k_2) = S^2(x, K) + \frac{q}{2} S(x, K) \left[\left. \frac{\partial S(x, k')}{\partial k'} \right|_{k'=K} - \left. \frac{\partial S(x, k')}{\partial k'} \right|_{k'=K} \right] + \mathcal{O}(q^2) \quad (2.24)$$

Therefore, desconsidering higher order powers of q , the two-particle correlation function, from Eq. (2.22), can be written as

$$C(K, q) = 1 + \frac{|\int dx S(x, K) e^{iq \cdot x}|^2}{[\int dx S(x, K)]^2}. \quad (2.25)$$

This interesting result shows that the two-particle correlation function, depending on the pair relative momentum and containing the contribution from the Quantum Statistics (QS) only, is related to the Fourier transform of the source function. Thus, the width of the correlation function is related to the space-time extensions of the emitting source, which is the most common application for identical particle correlation. Nevertheless, it should be noticed that this description applies to purely static sources. In cases of sources produced in high energy collisions, however, the expansion of the source breaks this approximation, introducing a dependence on the average momentum of the pair K , besides the dependence on q .

It is useful to write Eq. (2.23) in the reference frame that will be used throughout this work. For an on-shell pair of identical particles with four-momenta k_1 and k_2 , and using the definition of q and K , the so-called "on-shell" constraint holds, i.e.,

$$q \cdot K = q^\mu K_\mu \equiv (k_1 - k_2) \cdot \frac{1}{2}(k_1 + k_2) = \frac{1}{2}(k_1^2 - k_2^2) = \frac{1}{2}(m_1^2 - m_2^2) = 0, \quad (2.26)$$

then

$$q \cdot K = (q_0, -\mathbf{q}) \cdot (K^0, \mathbf{K}) = 0 \Rightarrow q_0 = \frac{1}{K^0} \mathbf{K} \cdot \mathbf{q}. \quad (2.27)$$

This means that q_0 is not an independent variable and can be eliminated in the pair rest frame (PRF), where $\mathbf{K} = \frac{1}{2}(\mathbf{k}_1 + \mathbf{k}_2) = 0$. Therefore, in this reference frame,

$$q \cdot x = (q_0, -\mathbf{q}) \cdot (x^0, \mathbf{r}) = -\mathbf{q} \cdot \mathbf{r}, \quad (2.28)$$

where $\mathbf{r} = \mathbf{x}_1 - \mathbf{x}_2$. Applying the above conditions in the smootheness approximation and considering the PRF, Eq. (2.23) becomes

$$C(q) = 1 + \frac{\int dx_1 dx_2 S(x_1, K) S(x_2, K) \cos(\mathbf{q} \cdot \mathbf{r})}{\int dx_1 S(x_1, K) \int dx_2 S(x_2, K)}. \quad (2.29)$$

The equation above can be rearrange to

$$C(q) = \frac{\int dx_1 dx_2 S(x_1, K) S(x_2, K) [1 + \cos(\mathbf{q} \cdot \mathbf{r})]}{\int dx_1 S(x_1, K) \int dx_2 S(x_2, K)}, \quad (2.30)$$

Consider now the function $\mathcal{S}(r)$

$$\mathcal{S}(r) = \frac{\int dx_1 dx_2 S(x_1, K) S(x_2, K) \delta^4(r - x_1 + x_2)}{\int dx_1 S(x_1, K) \int dx_2 S(x_2, K)}, \quad (2.31)$$

then, Eq. (2.30) becomes

$$C(q) = \int d\mathbf{r} [1 + \cos(\mathbf{q} \cdot \mathbf{r})] \int dt \mathcal{S}(r). \quad (2.32)$$

Assuming that the particles are emitted simultaneously in the pair rest frame, which is called *equal time approximation* [5, 11], it is possible to define a source function as

$$S(\mathbf{r}) = \int dt \mathcal{S}(r), \quad (2.33)$$

also imposing that $S(\mathbf{r})$ normalized to the unity, Eq. (2.30) becomes

$$C(q) = \int d\mathbf{r} S(\mathbf{r}) [1 + \cos(\mathbf{q} \cdot \mathbf{r})]. \quad (2.34)$$

Throughout the work the source function is a Gaussian distribution given by

$$S(r) = \frac{e^{-r^2/4R^2}}{(4\pi R^2)^{3/2}}, \quad (2.35)$$

where R is the source width and $|\mathbf{r}| = r$.

2.1.1 Pairs of identical particles

From now on, r and q will represent the modulus of the vectors \mathbf{r} and \mathbf{q} , respectively. Now, to write the two-particle correlation function for specific pairs of identical particles it is convenient to rewrite $C(q)$ introducing the spin dependence, as it follows

$$C_{QS}(q) = \sum_S \rho_S C_S(q), \quad (2.36)$$

where $\rho_S = \frac{(2S+1)}{(2s_1+1)(2s_2+1)}$ is the statistical weight, with $S = |s_1 - s_2|, \dots, s_1 + s_2$ as the total spin. Consider a pair of **identical spin-zero mesons**, where $\rho_S = 1$, the integral of Eq. (2.34) is written as

$$C_{QS}(q) = 1 + 2\pi \int_0^\infty \int_0^\pi d\theta dr r^2 \sin \theta \frac{e^{-r^2/4R^2}}{(4\pi R^2)^{3/2}} \cos(qr \cos \theta), \quad (2.37)$$

where the scalar product is reduced to $\mathbf{q} \cdot \mathbf{r} = qr \cos \theta$, and $S(r)$ is normalized to unity. Then, the two-particle correlation function for identical spin-zero mesons is

$$C_{QS}(q) = 1 + e^{-q^2 R^2}. \quad (2.38)$$

Next, consider the case of **identical spin-1/2 baryons**, it is necessary to take into account the contributions for the different spin states: the singlet state ($S = 0$) and the triplet state ($S = 1$), where S is the total spin of the system. The spin-singlet case corresponding to spin-1/2 identical fermions has the same expression as for spin-zero mesons, Eq. (2.38), i.e.,

$$C_{S=0}(q) = 1 + e^{-q^2 R^2}. \quad (2.39)$$

However, in the triplet case, it is necessary to apply the anti-symmetrization, which is represented as

$$C_{S=1}(q) = 1 - 2\pi \int_0^\infty \int_0^\pi d\theta dr r^2 \sin\theta \frac{e^{-r^2/4R^2}}{(4\pi R^2)^{\frac{3}{2}}} \cos(qr \cos\theta). \quad (2.40)$$

This leads to

$$C_{S=1}(q) = 1 - e^{-q^2 R^2}. \quad (2.41)$$

The two-particle correlation function for spin-1/2 baryons is then the sum of both contributions

$$C_{QS}(q) = \frac{1}{4}C_{S=0}(q) + \frac{3}{4}C_{S=1}(q). \quad (2.42)$$

Therefore, the final expression for the correlation function of a spin-1/2 fermion is given by

$$C_{QS}(q) = 1 - \frac{1}{2}e^{-q^2 R^2}. \quad (2.43)$$

Fig. 2.2 shows the behavior of both quantum statistics contributions in the two-particle correlation function, discussed in this section.

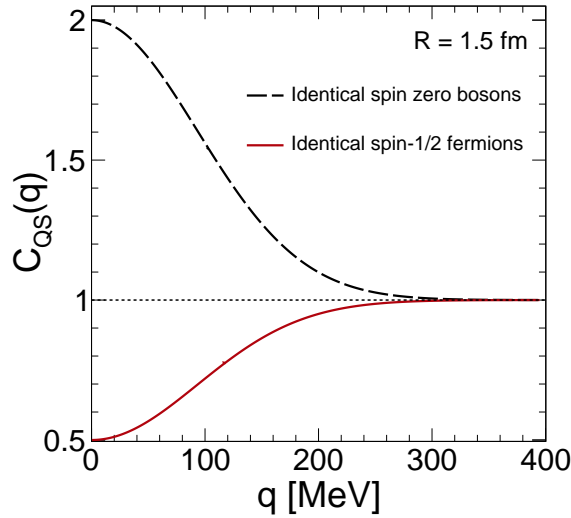


Figure 2.2: Illustration of the quantum statistics contribution for the case of identical spin-zero bosons (black, dashed line), Eq. (2.38), and the case of identical spin-1/2 fermions (red, full line), Eq. (2.43), using the source width as $R = 1.5$ fm.

For comparing the theoretical results with data it is necessary to be careful, since there are additional constraints to be taken into account: they are related, for instance, to detector effects in the description of the collision final objects, to the

uncertainty on the object properties, among others. The λ factor is an empirical parameter introduced in the two-particle correlation function as

$$C(q) = 1 + \lambda C'_{\text{QS}}(q) \quad (2.44)$$

where $C'_{\text{QS}}(q) = C_{\text{QS}}(q) - 1$ is the quantum statistics contribution. For the theoretical discussion in the rest of this Chapter $\lambda = 1$ is considered.

Later developments of the method and applications to high energy collisions, showed that the two-particle correlation function is not only sensitive to the effects of QS, but also to the final state interactions, as will be discussed in the next section.

2.2 Final state interactions

In Sec. 2.1, the effect of the final state interactions was not taken into account. Nevertheless, further studies of Femtoscopy in high energy collisions revealed that the effects of the final state interactions between correlating particles could not be neglected, such as **Coulomb interactions** and **Strong Interactions (SI)** [12]. This leads to the possibility of extending applications of the femtoscopic method to non-identical particles. Therefore, the effects of final state interactions in particle correlations in femtoscopy are introduced in the method below.

To adjust the formalism for including final state interactions, firstly, it will be convenient to use the *on-shell* constraint, elaborated in the previous section, considering pairs of non-identical particles. Define the center-of-mass four-coordinate and the relative separation of the pair, respectively, as [13]

$$R = \frac{(k_1 \cdot K)x_1 + (k_2 \cdot K)x_2}{K^2}, \quad r = x_1 - x_2, \quad (2.45)$$

then the average pair four-momentum and the relative pair four-momentum can be constructed, respectively as,

$$K = \frac{1}{2}(k_1 + k_2), \quad q = (k_1 - k_2) - \frac{(k_1 - k_2) \cdot K}{K^2} K. \quad (2.46)$$

The scalar product $q \cdot K$ follows as

$$\begin{aligned}
 q \cdot K &= \left[(k_1 - k_2) - \frac{(k_1 - k_2) \cdot K}{K^2} K \right] \cdot \left[\frac{1}{2} (k_1 + k_2) \right] \\
 &= \frac{1}{2} (m_1^2 - m_2^2) - \frac{(k_1 - k_2) \cdot K}{K^2} K^2 \\
 &= \frac{1}{2} (m_1^2 - m_2^2) - \frac{1}{2} (m_1^2 - m_2^2) = 0.
 \end{aligned} \tag{2.47}$$

Therefore, it is possible to eliminate the q_0 variable, as it was done in Eq. (2.28). In the pair rest frame, $\mathbf{K} = 0$,

$$q \cdot x = (q_0, -\mathbf{q}) \cdot (x^0, \mathbf{r}) = -\mathbf{q} \cdot \mathbf{r}, \tag{2.48}$$

where $\mathbf{r} = \mathbf{x}_1 - \mathbf{x}_2$.

From Eq. (2.34), and remembering that the source function, Eq. (2.35), is normalized to unity, the two-particle correlation function is rewritten as

$$\begin{aligned}
 C(q) &= \int d\mathbf{r} S(\mathbf{r}) [1 + \cos(\mathbf{q} \cdot \mathbf{r})] \\
 &= \int d\mathbf{r} S(\mathbf{r}) \left[1 + \frac{e^{i\mathbf{q} \cdot \mathbf{r}} + e^{-i\mathbf{q} \cdot \mathbf{r}}}{2} \right],
 \end{aligned} \tag{2.49}$$

where the terms in square brackets is equivalent to the norm squared of the symmetrized free wave function, since

$$\Psi_{\text{sym}}(\mathbf{q}, \mathbf{r}) = \frac{1}{\sqrt{2}} e^{2i\mathbf{K} \cdot \mathbf{R}} \left(e^{i\frac{\mathbf{q}_1 \cdot \mathbf{r}}{2}} + e^{-i\frac{\mathbf{q}_2 \cdot \mathbf{r}}{2}} \right). \tag{2.50}$$

From the above discussion, it is straightforward to extend the description of the two-particle correlation function to include the final state interactions occurring after the particles are emitted from the source. The total wave function, which includes the scattered contribution, gives information about the final state interactions. This can be written by using the *Koonin-Pratt* formula [14, 15] given by

$$C(\mathbf{q}) = \int d\mathbf{r} S(\mathbf{r}) |\Psi(\mathbf{q}, \mathbf{r})|^2, \tag{2.51}$$

where $\Psi(\mathbf{q}, \mathbf{r})$ is the total two-particle wave function. This formulation can now be easily extended to the case of non-identical particles correlations.

In the following sections, the contribution to the correlation function originated from Coulomb and strong interactions are discussed.

2.2.1 Coulomb interactions

The Coulomb interactions should be taken into account when considering electrically charged particles in interferometric analyses. The wave function corresponding to the Coulomb interaction can be written as [9, 11, 16]

$$\Psi(\mathbf{k}, \mathbf{r}) = \Gamma(1 + i\eta) e^{-\frac{1}{2}\pi\eta} e^{i\mathbf{k}\cdot\mathbf{r}} F(-i\eta; 1; iz), \quad (2.52)$$

where $F(-i\eta; 1; iz)$ is a hypergeometric function, $z = (kr - \mathbf{k}\cdot\mathbf{r})$ and $\eta = \pm \frac{m\alpha_{\text{QED}}}{k}$, with α_{QED} is the fine structure constant and m the particle mass. The positive (negative) sign applies for equally (oppositely) charged particles, corresponding to the repulsion (attraction) case. From now on, the average pair momentum will be denoted as $\mathbf{k} = \frac{\mathbf{q}}{2}$. When correcting to the correlation function for Coulomb final state interaction in proton-proton collisions the Gamov factor, $G(\eta)$, is a reasonably good approximation.

$$|\Psi(k, r = 0)|^2 = \frac{2\pi\eta}{e^{2\pi\eta} - 1} = G(\eta). \quad (2.53)$$

In more general cases, the full correction given in Eq. (2.52) should be applied. Using the Koonin-Pratt formula, Eq. (2.51), the two-particle correlation function for the Coulomb interaction contribution is

$$C(\mathbf{k}) = \int d\mathbf{r} S(\mathbf{r}) G(\eta) |F(-i\eta; 1; iz)|^2. \quad (2.54)$$

In the following sections, the contribution to the correlation function originated from the strong interactions are discussed.

2.2.2 Strong interactions

In this section, the formulation of the two-particle correlation function that includes the effects of **Strong Interactions (SI)** is discussed, along with the introduction of a method called the **Lednicky-Lyuboshitz model (LL)** [17].

The derivation starts by considering the Koonin-Pratt correlation function, Eq.

(2.51), according to which

$$C(\mathbf{k}) = \int d\mathbf{r} S(\mathbf{r}) |\Psi(\mathbf{k}, \mathbf{r})|^2, \quad (2.55)$$

where $\Psi(\mathbf{k}, \mathbf{r})$ is the two-particle wave function, that is affected by the interaction. It can be expanded in a *partial wave decomposition* (PWD) [18], as

$$\Psi(\mathbf{k}, \mathbf{r}) = \sum_{l=0}^{\infty} \psi_l(k, r) P_l(\cos \theta), \quad (2.56)$$

where $P_l(\cos \theta)$ is the Legendre polynomial of order l , that is the quantum number associated with the orbital angular momentum [19]. The notation from now on is $k = |\mathbf{k}|$ and $r = |\mathbf{r}|$.

Supposing that the pair is composed of unlike particles and that only the s-wave (i.e., angular momentum $l = 0$) part of the two-particle wave function $\Psi(\mathbf{k}, \mathbf{r})$ is affected by the interaction,

$$\Psi(\mathbf{k}, \mathbf{r}) = \psi_0(k, r) + \sum_{l=1}^{\infty} \psi_l^{\text{free}}(k, r) P_l(\cos \theta), \quad (2.57)$$

with $\psi_0(k, r)$ being the scattered wave function. Summing and subtracting the $l = 0$ component for the free wave function, then

$$\Psi(\mathbf{k}, \mathbf{r}) = \psi_0(k, r) + \sum_{l=0}^{\infty} \psi_l^{\text{free}}(k, r) P_l(\cos \theta) - \psi_0^{\text{free}}(k, r), \quad (2.58)$$

where the second term of the equation above is the free-particle wave function $e^{i\mathbf{k}\cdot\mathbf{r}}$ and the third term is the free-particle wave function for the s-wave, which is the spherical Bessel function [20], i.e., $j_0(kr) = \sin(kr)/kr$. The total wave function can be rewritten as

$$\begin{aligned} \Psi(\mathbf{k}, \mathbf{r}) &= \psi_0(k, r) + e^{i\mathbf{k}\cdot\mathbf{r}} - j_0(kr) \\ &= e^{i\mathbf{k}\cdot\mathbf{r}} + \phi(k, r), \end{aligned} \quad (2.59)$$

and it can be put inside expression (2.55):

$$C(\mathbf{k}) = \int d\mathbf{r} S(\mathbf{r}) + \int d\mathbf{r} S(\mathbf{r}) \left[e^{-i\mathbf{k}\cdot\mathbf{r}} \phi(k, r) + e^{i\mathbf{k}\cdot\mathbf{r}} \phi^*(k, r) \right] + \int d\mathbf{r} S(\mathbf{r}) |\phi(k, r)|^2 \quad (2.60)$$

Replacing Eq. (2.59) in Eq. (2.55), splitting the integral in three terms and assuming that the source function is spherically symmetric (i.e., $S(\mathbf{r}) = S(r)$) and normalized, leads to

- First term $I_1^{(i)}$:

$$I_1^{(i)} = \int d\mathbf{r} S(\mathbf{r}) = 1, \quad (2.61)$$

- Second term $I_2^{(i)}$:

$$I_2^{(i)} = 4\pi \int dr r^2 S(r) j_0(kr) [\psi_0(k, r) + \psi_0^*(k, r) - 2j_0(kr)], \quad (2.62)$$

- Third term $I_3^{(i)}$:

$$I_3^{(i)} = 4\pi \int dr r^2 S(r) [|\psi_0(k, r)|^2 - j_0(kr) (\psi_0(k, r) + \psi_0^*(k, r)) + j_0^2(kr)]. \quad (2.63)$$

Gathering all the terms results in the two-particle correlation function for non-identical particles

$$C_{SI}(q) = 1 + 4\pi \int_0^\infty dr r^2 S(r) [|\psi_0(k, r)|^2 - j_0^2(kr)]. \quad (2.64)$$

The effect of the interaction in the scattered wave function $\psi_0(k, r)$ is to add a phase shift δ_0 [21] to the previously free wave function $\psi_0^{\text{free}}(k, r)$, i.e.,

$$\psi_0(k, r) = \frac{1}{kr} \sin(kr + \delta_0). \quad (2.65)$$

In order to obtain the scattering observables, one can use the definition of the S-matrix [22]

$$S_l = e^{2i\delta_l} = 1 + 2ikf_l(k), \quad (2.66)$$

to rewrite the scattered wave function as

$$\begin{aligned} \psi_0(k, r) &= \frac{1}{2ikr} \left(e^{i(kr+\delta_0)} - e^{-i(kr+\delta_0)} \right) \\ &= \frac{e^{-i\delta_0}}{kr} \left(\sin kr + kf_0(k) e^{ikr} \right), \end{aligned} \quad (2.67)$$

where $f_0(k)$ is the scattering amplitude.

Thus, the two-particle correlation function becomes

$$C(k) = 1 + 4\pi |f_0(k)|^2 \int_0^\infty dr S(r) + 4\pi \int_0^\infty dr S(r) \frac{1}{k} \sin kr \left[f_0^*(k) e^{-ikr} + f_0(k) e^{ikr} \right]. \quad (2.68)$$

If the source function $S(r)$ is described by a Gaussian distribution [11],

$$S(r) = \frac{e^{-r^2/4R^2}}{(4\pi R^2)^{\frac{3}{2}}}, \quad (2.69)$$

where R is the width of the Gaussian source, it is possible to evaluate each term of Eq. (2.68) separately, as *Second term* $I_2^{(ii)}$:

$$I_2^{(ii)} = 4\pi |f_0(k)|^2 \int_0^\infty dr \frac{e^{-r^2/4R^2}}{(4\pi R^2)^{\frac{3}{2}}} = \frac{|f_0(k)|^2}{2R^2}. \quad (2.70)$$

Third term $I_3^{(ii)}$:

$$\begin{aligned} I_3^{(ii)} &= \frac{4\pi}{k} \int_0^\infty dr S(r) \sin kr [(f_0^* + f_0) \cos kr - i(f_0^* - f_0) \sin kr] \\ &= \frac{4\pi}{k} \int_0^\infty dr S(r) \sin kr [2\text{Re}f_0(k) \cos kr - 2\text{Im}f_0(k) \sin kr]. \end{aligned} \quad (2.71)$$

Now, from the first term of the right-hand side of $I_3^{(ii)}$

$$I_{3a}^{(ii)} = \frac{8\pi \text{Re}f_0(k)}{k} \int_0^\infty dr \frac{e^{-r^2/4R^2}}{(4\pi R^2)^{\frac{3}{2}}} \sin kr \cos kr = \frac{8\pi \text{Re}f_0(k)}{k} \frac{D(2kR)}{(4\pi)^{\frac{3}{2}} R^2}, \quad (2.72)$$

where $D(2kR) = \int_0^{2kR} e^{t^2 - (2kR)^2} dt$ is the Dawson function, expression (2.72) can be rewritten more simply as

$$\begin{aligned} I_{3a}^{(ii)} &= \frac{8\pi \text{Re}f_0(k)}{k} \frac{D(2kR)}{(4\pi)^{\frac{3}{2}} R^2} = \frac{2\text{Re}f_0(k)}{\sqrt{\pi} R} \frac{D(2kR)}{2kR} \\ &= \frac{2\text{Re}f_0(k)}{\sqrt{\pi} R} F_1(2kR), \end{aligned} \quad (2.73)$$

where $F_1(2kR) = \frac{D(2kR)}{2kR} = \int_0^{2kR} \frac{e^{t^2 - (2kR)^2}}{(2kR)} dt$. The integral of the second term of $I_3^{(ii)}$

will be

$$\begin{aligned} I_{3b}^{(ii)} &= \frac{8\pi \text{Im}f_0(k)}{k} \int_0^\infty dr \frac{e^{-r^2/4R^2}}{(4\pi R^2)^{3/2}} \sin^2 kr = \frac{8\pi \text{Im}f_0(k)}{k} \frac{(1 - e^{4k^2 R^2})}{16\pi R^2} \\ &= \frac{\text{Im}f_0(k)}{R} F_2(2kR), \end{aligned} \quad (2.74)$$

where $F_2(2kr) = \frac{1 - e^{-(2kr)^2}}{2kr}$.

From expressions above, $I_{3a}^{(ii)}$ and $I_{3b}^{(ii)}$, Eq. (2.71) becomes

$$\begin{aligned} I_3^{(ii)} &= 4\pi \int_0^\infty dr S(r) \frac{\sin kr}{k} (f_0^* e^{-ikr} + f_0 e^{ikr}) \\ &= \frac{2\text{Re}f_0(k)}{\sqrt{\pi}R} F_1(2kR) - \frac{\text{Im}f_0(k)}{R} F_2(2kR). \end{aligned} \quad (2.75)$$

Summing all the contributions

$$C(k) = 1 + \frac{|f_0(k)|^2}{2R^2} + \frac{2\text{Re}f_0(k)}{\sqrt{\pi}R} F_1(2kR) - \frac{\text{Im}f_0(k)}{R} F_2(2kR). \quad (2.76)$$

Nevertheless, pairs of particles are also produced in a spatial region where the short range nuclear interaction potential is non-zero, i.e. $V(r) \neq 0$. In this region the wave function deviates from its asymptotic form. In the Lednicky model the contribution from the non-asymptotic wave function is taken into account in the form of an extra term that is calculated considering the distance of the pair to be equal to 0, i.e., the source function is reduced to $S(r=0) = \frac{1}{(4\pi R^2)^{3/2}}$. Therefore, the correction term is [17]

$$\Delta C_{\text{non-asym}}(k) = 4\pi S(r=0) \frac{|f(q)|^2}{2k} \frac{d}{dk} \left(\frac{1}{f(k)} \right) = \frac{r_0}{4\sqrt{\pi}R^3} |f(k)|^2. \quad (2.77)$$

The scattering amplitude $f_0(k)$ can be written as

$$f_0(k) = [k \cot \delta_0 - ik]^{-1}. \quad (2.78)$$

A commonly used approximation is to use the *effective range expansion* (ERE) for $f_0(k)$ [21]

$$f_0(k) \approx \left[-\frac{1}{a_0} + \frac{1}{2} r_0 k^2 - ik \right]^{-1}, \quad (2.79)$$

where a_0 is the *scattering length* and r_0 is the *effective range*, which together with the

phase shift δ_0 are the *scattering observables* that will be explored further during this work.

Finally, using Eq. (2.76), Eq. (2.77), and Eq. (2.79), the **LL model** [17], for describing the strong interaction contribution in the correlation function, is given by

$$C_{\text{LL}}(k) = 1 + \sum_S \rho_S \left[\frac{|f_0^S(k)|^2}{2R^2} \left(1 - \frac{r_0^S}{2\sqrt{\pi}R} \right) + \frac{2\text{Re}f_0^S(k)}{\sqrt{\pi}R} F_1(2kr) - \frac{\text{Im}f_0^S(k)}{R} F_2(2kR) \right] \quad (2.80)$$

with the spin dependence $\rho_S = \frac{(2S+1)}{(2s_1+1)(2s_2+1)}$, introduced in the previous section Eq. (2.36), and

$$F_1(z) = \int_0^z \frac{e^{t^2-z^2}}{z} dt; \quad F_2(z) = \frac{(1 - e^{-z^2})}{z}, \quad z = 2kR \quad (2.81)$$

Keeping in mind that this result is for the case of non-identical particles only. For the case of identical particles, one needs to be more careful with the (anti) symmetrization contributions.

For the case of **identical spin-1/2 baryons**, it is necessary to take into account the singlet and the triplet state as it was done in the Sec. 2.1. The total wave function for the singlet state can be written in terms of symmetric spatial wave function $\varphi_{\text{sym}}(\mathbf{k}, \mathbf{r})$ and a anti-symmetric spin part $\chi_{\text{anti-sym}}(S, M)$, given by

$$\Psi_{\text{tot}}(\mathbf{k}, \mathbf{r}) = \varphi_{\text{sym}}(\mathbf{k}, \mathbf{r}) \cdot \chi_{\text{anti-sym}}(S, M). \quad (2.82)$$

To symmetrize the spatial wave function it can be done applying $\mathbf{r} \rightarrow -\mathbf{r}$ [23], which leads to

$$\begin{aligned} \varphi_{\text{sym}}(\mathbf{k}, \mathbf{r}) &= \frac{1}{\sqrt{2}} [\varphi(\mathbf{k}, \mathbf{r}) + \varphi(\mathbf{k}, -\mathbf{r})] \\ &= \sqrt{2} [\cos(\mathbf{k} \cdot \mathbf{r}) + \psi_0(k, r) - j_0(kr)]. \end{aligned} \quad (2.83)$$

Replacing Eq. (2.83) in the integral for $C(k)$, Eq. (2.55), the two-particle correlation function for singlet state is given by

$$C_{S=0}(k) = 1 + e^{-4k^2R^2} + 8\pi \int dr r^2 S(r) \left[|\psi_0(k, r)|^2 - j_0^2(kr) \right]. \quad (2.84)$$

where the strong interaction contribution for $S = 0$ is the third term of the previous equation, written as

$$C_{\text{SI}}^{S=0}(k) = 1 + 8\pi \int dr r^2 S(r) \left[|\psi_0(k, r)|^2 - j_0^2(kr) \right]. \quad (2.85)$$

The total wave function for the triplet state can be written in terms of anti-symmetric spatial wave function $\varphi_{\text{anti-sym}}(\mathbf{k}, \mathbf{r})$ and a symmetric spin part $\chi_{\text{sym}}(S, M)$, given by

$$\Psi_{\text{tot}}(\mathbf{k}, \mathbf{r}) = \varphi_{\text{anti-sym}}(\mathbf{k}, \mathbf{r}) \cdot \chi_{\text{sym}}(S, M), \quad (2.86)$$

where

$$\begin{aligned} \varphi_{\text{anti-sym}}(\mathbf{k}, \mathbf{r}) &= \frac{1}{\sqrt{2}} [\varphi(\mathbf{k}, \mathbf{r}) - \varphi(\mathbf{k}, -\mathbf{r})] \\ &= \frac{1}{\sqrt{2}} [e^{i\mathbf{k} \cdot \mathbf{r}} - e^{-i\mathbf{k} \cdot \mathbf{r}}], \end{aligned} \quad (2.87)$$

which does not have any contribution for the interaction since it does not have s-wave interaction. Replacing Eq. (2.87) in the integral for $C(k)$, Eq. (2.55), the two-particle correlation function for triplet state is given by

$$C_{S=1}(k) = 1 - e^{-4k^2 R^2}. \quad (2.88)$$

Now, taking into account the respective statistical weight for each spin state, the two-particle correlation function for identical spin-1/2 baryons is given by

$$C_{\text{tot}}(k) = \frac{1}{4} C_{S=0}(k) + \frac{3}{4} C_{S=1}(k), \quad (2.89)$$

$$C_{\text{tot}}(k) = 1 - \frac{1}{2} e^{-4k^2 R^2} + 2\pi \int_0^\infty dr r^2 S(r) \left[|\psi_0(k, r)|^2 - j_0^2(kr) \right], \quad (2.90)$$

where the strong interaction (SI) contribution is

$$C_{\text{SI}}(k) = 1 + 2\pi \int_0^\infty dr r^2 S(r) \left[|\psi_0(k, r)|^2 - j_0^2(kr) \right], \quad (2.91)$$

which is similar to Eq. (2.64) only by a factor of 1/2. Substituting the asymptotic expression for the wave function $\psi_0(k, r)$ Eq. (2.65), and neglecting the quantum

statistics term, the **LL model** for identical spin-1/2 baryons is

$$C_{LL}(k) = 1 + \frac{1}{2} \left[\frac{|f_0(k)|^2}{2R^2} \left(1 - \frac{r_0}{2\sqrt{\pi}R} \right) + \frac{2\text{Re}f_0(k)}{\sqrt{\pi}R} F_1(2kr) - \frac{\text{Im}f_0(k)}{R} F_2(2kR) \right]. \quad (2.92)$$

For **identical spin-zero mesons** the total wave function can be written in terms of symmetric spatial wave function $\varphi_{\text{sym}}(\mathbf{k}, \mathbf{r})$, since for spin-zero there is not a spin part. Therefore,

$$\begin{aligned} \varphi_{\text{sym}}(\mathbf{k}, \mathbf{r}) &= \frac{1}{\sqrt{2}} [\varphi(\mathbf{k}, \mathbf{r}) + \varphi(\mathbf{k}, -\mathbf{r})] \\ &= \sqrt{2} [\cos(\mathbf{k} \cdot \mathbf{r}) + \psi_0(k, r) - j_0(kr)]. \end{aligned} \quad (2.93)$$

Replacing Eq. (2.93) in the integral for $C(k)$, Eq. (2.55), taking into account the respective statistical weight, the two-particle correlation function for identical spin-zero mesons is given by

$$C_{\text{tot}}(k) = 1 + e^{-4k^2R^2} + 2\pi \int_0^\infty dr r^2 S(r) \left[|\psi_0(k, r)|^2 - j_0^2(kr) \right], \quad (2.94)$$

where the strong interaction (SI) contribution is

$$C_{\text{SI}}(k) = 1 + 2\pi \int_0^\infty dr r^2 S(r) \left[|\psi_0(k, r)|^2 - j_0^2(kr) \right], \quad (2.95)$$

which is similar to Eq. (2.64) differing only by a factor of 2. Substituting the asymptotic expression for the wave function $\psi_0(k, r)$ (Eq. (2.65)), and neglecting the Bose-Einstein statistics term, one can recover the **LL model** for identical spin-zero mesons

$$C_{LL}(k) = 1 + 2 \left[\frac{|f_0(k)|^2}{2R^2} \left(1 - \frac{r_0}{2\sqrt{\pi}R} \right) + \frac{2\text{Re}f_0(k)}{\sqrt{\pi}R} F_1(2kr) - \frac{\text{Im}f_0(k)}{R} F_2(2kR) \right] \quad (2.96)$$

Notice that, for comparing the theoretical results with data, it is necessary to introduce again the λ factor, as it was done in Eq. (2.44), taken into account now also the final state interaction contribution, as

$$C(q) = 1 + \lambda [C'_{\text{QS}}(q) + C'_{\text{SI}}(q)] \quad (2.97)$$

where $C'_{\text{QS}}(q) = C_{\text{QS}}(q) - 1$ is the quantum statistics contribution, when considering identical particles, $C'_{\text{SI}}(q) = C_{\text{SI}}(q) - 1$ is the strong interactions contribution

and for the theoretical discussion in the rest of this work $\lambda = 1$.

These expressions will be useful to validate the results coming from the scattered wave function.

2.3 Joint effects

After presenting the possible contributions that compose the two-particle correlation function, it is necessary to group these effects to obtain a **total correlation function** for the systems of interest, which are: identical and non-identical spin-1/2 baryons and spin-zero mesons.

2.3.1 Two identical particles

In this section, the two-particle correlation function is reviewed for the case of two identical spin-1/2 baryons and two identical spin-zero mesons, where the quantum statistics and the strong interactions contribution are brought together to compose the total two-particle correlation function.

Baryons

The correlation function for two identical spin-1/2 baryons is composed of a spin-singlet and a spin-triplet part. The spin-singlet part of the correlation function is the joint of quantum statistics, Eq. (2.38), and strong interaction contributions, Eq. (2.85) which is

$$C_{S=0}(k) = 1 + e^{-4k^2R^2} + 2\pi \int_0^\infty dr r^2 S(r) \left[|\psi_0(k, r)|^2 - j_0^2(kr) \right]. \quad (2.98)$$

The spin-triplet part of the correlation function is only the quantum statistics contribution, Eq. (2.41), as it was shown before, Eq. (2.87),

$$C_{S=1}(k) = 1 - e^{-4k^2R^2}. \quad (2.99)$$

Therefore, the total two-particle correlation function for two identical spin-1/2 baryons is

$$C_{\text{tot}}(k) = \frac{1}{4}C_{S=0}(k) + \frac{3}{4}C_{S=1}(k) \quad (2.100)$$

$$C_{\text{tot}}(k) = 1 - \frac{1}{2}e^{-4k^2R^2} + \frac{1}{2} \int_0^\infty dr r^2 S(r) \left[|\psi_0(k, r)|^2 - j_0^2(kr) \right]. \quad (2.101)$$

Mesons

The correlation function for two identical spin-zero mesons is composed of the quantum statistics, Eq. (2.38), and the strong interactions, Eq. (2.95), contributions, given by

$$C(k) = 1 + e^{-4k^2R^2} + 8\pi \int dr r^2 S(r) \left[|\psi_0(k, r)|^2 - j_0^2(kr) \right], \quad (2.102)$$

2.3.2 Two non-identical particles

In this section, the two-particle correlation function is reviewed for the case of two non-identical spin-1/2 baryons and two non-identical spin-zero mesons, where only the strong interactions contribution is taken into account.

Baryons

The total two-particle correlation function for non-identical spin-1/2 baryons is obtained as it was done in the previous section with Eq. (2.64),

$$C(k) = 1 + 4\pi \sum_S \rho_S \int_0^\infty dr r^2 S(r) \left[|\psi_0^S(k, r)|^2 - j_0^2(kr) \right]. \quad (2.103)$$

Mesons

Since the following calculations will be performed considering pseudo-scalar mesons, the expression for $C(k)$ will be almost the same as in Eq. (2.103), with the difference that the statistical weight will be one since the particles in question have $S = 0$:

$$C(k) = 1 + 4\pi \int_0^\infty dr r^2 S(r) \left[|\psi_0(k, r)|^2 - j_0^2(kr) \right]. \quad (2.104)$$

As shown in this chapter, by the expressions (2.101), (2.102), (2.103) and (2.104), the total correlation function depends on the contribution of the scattered wave function. In the following chapter, it will be shown how the scattered wave function is obtained numerically, based on two distinct formalisms, and the subsequent correlation function for specific correlating particles.

Chapter 3

Scattering wave function

In the previous section the formalism of femtoscopy was discussed and the Koonin-Pratt formula, Eq. (2.55), was presented for the two-particle correlation function $C(k)$. To obtain the correlation function, the total wave function $\Psi(\mathbf{r}, \mathbf{k})$ of the correlating pair must be determined. It is composed of two parts: a free wave function and a scattered wave function. The former corresponds to the plane wave $e^{i\mathbf{k}\cdot\mathbf{r}}$, whereas the latter contains all the information about the interactions of interest, i.e., the final-state interactions. These interactions can be described by a local potential defined as $V(\mathbf{r}) \rightarrow V(\mathbf{p} - \mathbf{p}')$, where \mathbf{r} is the relative distance of the pair, \mathbf{p}' is the pair incident relative momentum and \mathbf{p} is the pair outgoing relative momentum. However, not every scattering problem is described by a local potential, and a non-local potential is needed when the potential is described as $V(\mathbf{p}, \mathbf{p}') \rightarrow V(\mathbf{r}, \mathbf{r}')$, i.e., the outgoing relative distance \mathbf{r}' of the pair is different than the incoming one \mathbf{r} .

In this Chapter, the calculation of the scattered wave function is discussed with a numerical description on how to solve the Schrödinger equation for the case of local or \mathbf{r} dependent potentials, which is the case for the potentials that describes the $\Lambda\Lambda$ and $p\Lambda$ interactions, and the Lippmann-Schwinger equation for the case of non-local or momentum dependent potentials, which is the case for the potential that describes the D^0D^0 , $\bar{D}^0\bar{D}^0$ interactions. Natural units are used throughout this work ($\hbar = c = 1$).

3.1 Schrödinger equation

The scattered wave function is given by the solution of the Schrödinger equation in the presence of a potential $V(\mathbf{r})$. Considering its time-independent form in

the Dirac notation

$$\hat{H} |\psi_{\mathbf{k}}\rangle = E |\psi_{\mathbf{k}}\rangle, \quad (3.1)$$

where \hat{H} is the Hamiltonian of the system and it can be written as

$$\hat{H} = \hat{H}_0 + \hat{V}(\mathbf{r}), \quad (3.2)$$

and $\hat{H}_0 = \frac{\hat{\mathbf{p}}^2}{2\mu}$ is the free-particle Hamiltonian operator, and $\hat{H}_0 |\phi_{\mathbf{k}}\rangle = E_0 |\phi_{\mathbf{k}}\rangle$, with eigenvalue $= \frac{k^2}{2\mu}$. The Eq. (3.1) becomes

$$\left(\frac{\hat{\mathbf{p}}^2}{2\mu} + \hat{V}(\mathbf{r}) \right) |\psi_{\mathbf{k}}\rangle = E |\psi_{\mathbf{k}}\rangle. \quad (3.3)$$

To obtain the wave function, the definition of the coordinate space wave function is recalled, i.e.,

$$\langle \mathbf{r} | \psi_{\mathbf{k}} \rangle = \psi(\mathbf{k}, \mathbf{r}). \quad (3.4)$$

The Schrödinger equation in coordinate space is given by

$$-\frac{1}{2\mu} \nabla^2 \psi(\mathbf{k}, \mathbf{r}) + V(r) \psi(\mathbf{k}, \mathbf{r}) = E \psi(\mathbf{k}, \mathbf{r}), \quad (3.5)$$

where μ is the reduced mass, $V(r)$ is a potential with r dependence and E is the total energy of the system. The notation from now on is simplified as $\psi(\mathbf{k}, \mathbf{r}) = \psi(\mathbf{r})$, since only the \mathbf{r} dependence will be useful to solve the problem. Equation (3.5) can be rewritten in spherical coordinates as

$$-\frac{1}{2\mu} \left[\frac{1}{r^2} \frac{\partial}{\partial r} \left(r^2 \frac{\partial}{\partial r} \right) + \frac{1}{r^2 \sin \theta} \frac{\partial}{\partial \theta} \sin \theta \frac{\partial}{\partial \theta} + \frac{1}{r^2 \sin^2 \theta} \frac{\partial^2}{\partial \phi^2} \right] \psi(\mathbf{r}) + V(r) \psi(\mathbf{r}) = E \psi(\mathbf{r}). \quad (3.6)$$

A method to solve this partial differential equation is *separation of variables*, in which $\psi(\mathbf{r})$ is

$$\psi(r, \theta, \phi) = R(r) Y(\theta, \phi), \quad (3.7)$$

where $Y(\theta, \phi)$ is the angular part with the solutions as the spherical harmonics [19] and $R_l(r)$ is the solution for the radial Schrödinger equation [24], which is

$$\frac{d}{dr} \left[r^2 \frac{d}{dr} R_l(r) \right] - 2\mu r^2 [V(r) - E] R_l(r) = l(l+1) R_l(r). \quad (3.8)$$

Defining $u_l(r) \equiv rR_l(r)$, Eq. (3.8) becomes

$$\frac{d^2}{dr^2}u_l(r) - \left[\frac{l(l+1)}{r^2} + 2\mu V(r) \right] u_l(r) = -k^2 u_l(r), \quad (3.9)$$

where $k^2 = 2\mu E$. In case of $V(r) = 0$, Eq. (3.9) is reduced to

$$\frac{d^2}{dr^2}u_l(r) = \frac{l(l+1)}{r^2}u_l(r) - k^2 u_l(r). \quad (3.10)$$

The solutions of this equation are proportional to the spherical Bessel functions $j_l(kr)$ [20]

$$u_l(r) \propto rj_l(kr). \quad (3.11)$$

In the case $V(r) \neq 0$, the problem returns to Eq. (3.9)

$$\frac{d^2}{dr^2}u_l(r) = \frac{l(l+1)}{r^2}u_l(r) + \left[2\mu V(r) + k^2 \right] u_l(r), \quad (3.12)$$

with solutions for the asymptotic region ($r \rightarrow \infty$) are given by

$$u_l^v(r) = \frac{i}{2} \left[\exp \left(-i \left(kr - \frac{l\pi}{2} \right) \right) - S_l \exp \left(i \left(kr - \frac{l\pi}{2} \right) \right) \right], \quad (3.13)$$

where S_l is the S-matrix, defined in Eq. (2.66), for elastic scattering $S_l = \exp(i2\delta_l(k))$, and δ_l is the phase shift. Assuming that an interaction only have contributions coming from the s-channel, that is $l = 0$, the radial solution is

$$u_{l=0}^v(r) \propto \sin(kr + \delta_0). \quad (3.14)$$

Returning to the wave function $\psi(\mathbf{r})$, it can be expressed in terms of a *partial wave decomposition* (PWD), as [18]

$$\psi(\mathbf{r}) \rightarrow \psi_l(r) = \sum_{l=0}^{\infty} \sum_{m=-l}^l 4\pi i^l \frac{u_l(r)}{kr} Y_{lm}(\Omega_{\hat{\mathbf{r}}}) Y_{lm}^*(\Omega_{\hat{\mathbf{k}}}), \quad (3.15)$$

where $Y_{lm}(\Omega_{\hat{\mathbf{r}}})$ and $Y_{lm}(\Omega_{\hat{\mathbf{k}}})$ are the spherical harmonics, $\Omega_{\hat{\mathbf{r}}}$ and $\Omega_{\hat{\mathbf{k}}}$ are the solid angles for the $\hat{\mathbf{r}}$ and $\hat{\mathbf{k}}$ unit vectors, respectively. The addition theorem of spherical harmonics (or Legendre additional theorem) states that [19]

$$\sum_{m=-l}^l Y_{lm}(\Omega_{\hat{\mathbf{r}}}) Y_{lm}^*(\Omega_{\hat{\mathbf{k}}}) = \frac{(2l+1)}{4\pi} P_l(\Omega_{\hat{\mathbf{r}}} \cdot \Omega_{\hat{\mathbf{k}}}), \quad (3.16)$$

where $P_l(\cos \gamma)$ is the Legendre's polynomial of order l , with l being the quantum number associated with the orbital angular momentum, and

$$P_l(\Omega_{\hat{r}} \cdot \Omega_{\hat{k}}) = P_l(\cos \gamma) = P_l(x),$$

and $x = \cos \gamma = \cos \theta_1 \cos \theta_2 + \cos(\phi_1 - \phi_2) \sin \theta_1 \sin \theta_2$. Then, Eq. (3.15) can be rewritten as

$$\psi_l(r) = \sum_l (2l+1) i^l \frac{u_l(r)}{kr} P_l(\cos \gamma). \quad (3.17)$$

For $l = 0$,

$$\psi_{l=0}(r) = \frac{u_{l=0}(r)}{kr}. \quad (3.18)$$

Since not always there is an analytical solution for the potential under study, a numerical approach to solve this differential equation is needed. The traditional method used throughout this work is the Euler method.

3.1.1 Euler method

The radial Schrödinger equation is a second order ordinary differential equation. One way to solve it numerically is by using the *Euler method*, which is a formalism that discretizes the derivatives. Defining $\frac{du}{dr} \equiv w$, for the first derivative of $u(r)$:

$$\frac{du}{dr} \approx \frac{u(i+1) - u(i)}{\Delta} \rightarrow u(i+1) = u(i) + \frac{du}{dr} \Delta, \quad (3.19)$$

$$u(i+1) = u(i) + w\Delta. \quad (3.20)$$

where Δ is the step of the algorithm. Defining $\frac{d^2u}{dr^2} \equiv z$, for the second derivative of $u(r)$

$$\frac{d^2u}{dr^2} \approx \frac{w(i+1) - w(i)}{\Delta} \rightarrow w(i+1) = w(i) + \frac{d^2u}{dr^2} \Delta, \quad (3.21)$$

$$w(i+1) = w(i) + z\Delta, \quad (3.22)$$

where $z = \frac{dw}{dr} = [2\mu V - k^2] u$, for $l = 0$.

Through the Euler method, one can obtain the numerical values for the scattering wave function that can be compared to the free wave function, providing information about the scattering observables.

Scattering observables

One way to obtain measurements related to the interactions, subject to a potential V , is by using the scattering observables. The numerical solutions for the scattering wave function in two different positions are $u^{n_1}(r_1)$ and $u^{n_2}(r_2)$. The analytical expressions for the same positions, from Eq. (3.14), are

$$\begin{aligned} u^{a_1}(r_1) &= A_0 \sin(kr_1 + \delta_0), \\ u^{a_1}(r_2) &= A_0 \sin(kr_2 + \delta_0), \end{aligned}$$

where A_0 is an amplitude.

Comparing the numerical u^{n_i} and the analytical u^{a_i} solutions

$$\text{const.} \equiv \frac{u^{n_2}}{u^{n_1}} = \frac{u^{a_2}}{u^{a_1}} \Rightarrow \text{const.} = \frac{\sin(kr_2 + \delta_0)}{\sin(kr_1 + \delta_0)}. \quad (3.23)$$

One of the goals of a numerical code written to extract the scattered wave function is to calculate $\text{const.} \equiv \frac{u^{n_2}}{u^{n_1}}$ and, therefore, the phase shift δ_0 , that is given by

$$\delta_0 = \arctan \left[\frac{\text{const.} \sin(kr_1) - \sin(kr_2)}{\cos(kr_2) - \text{const.} \cos(kr_1)} \right]. \quad (3.24)$$

Hence, the normalized wave function can be obtained as

$$\mathcal{N} = \frac{\sin(kr_i + \delta_0)}{u^{n_i}} \rightarrow u_{l=0}(r) = \mathcal{N} \frac{u^n(r)}{kr}. \quad (3.25)$$

In addition, from the phase shift it is possible to obtain two other scattering observables: the *scattering length* a_0 and the *effective range* r_0 , from the expression of the *effective range expansion* [21, 25]

$$k \cot \delta_0 \approx -\frac{1}{a_0} + \frac{1}{2}r_0k^2. \quad (3.26)$$

However, not every scattering system has a local potential. To solve this type of problem, a distinct formalism is needed to obtain the wave function.

3.2 Lippmann-Schwinger equation

It has been shown that the eigenvalue equation that is relevant for the particle scattering in the presence of a potential is the Schrödinger Equation, such as (3.1)

and (3.5). Rearranging Eq. (3.3) in a way to see the effects of the potential, i.e.,

$$(E - H_0) |\psi_{\mathbf{k}}\rangle = \hat{V} |\psi_{\mathbf{k}}\rangle, \quad (3.27)$$

leads to a solution of the form

$$|\psi_{\mathbf{k}}\rangle = |\phi_{\mathbf{k}}\rangle + \frac{1}{E - H_0 \pm i\epsilon} \hat{V} |\psi_{\mathbf{k}}\rangle. \quad (3.28)$$

In this expression an infinitesimal quantity ϵ is added to the denominator to avoid divergencies when $E - H_0$ is equal to zero, in which case the solution diverges, ϵ specifies how to go around the pole in the complex plane. Therefore, Eq. (3.28) becomes

$$|\psi_{\mathbf{k}}\rangle = |\phi_{\mathbf{k}}\rangle + \hat{G}(k^2) \hat{V} |\psi_{\mathbf{k}}\rangle, \quad (3.29)$$

where

$$\hat{G}(k^2) = \frac{1}{E - H_0 \pm i\epsilon} = \frac{1}{k^2/2\mu - \mathbf{p}^2/2\mu \pm i\epsilon}, \quad (3.30)$$

is the Green function [18]. Multiplying both sides of Eq. (3.29) from the left by \hat{V}

$$\hat{V} |\psi_{\mathbf{k}}\rangle = \hat{V} |\phi_{\mathbf{k}}\rangle + \hat{V} \hat{G}(k^2) \hat{V} |\psi_{\mathbf{k}}\rangle. \quad (3.31)$$

The transition operator $\hat{T}(k^2)$ is defined by the relation [22]

$$\hat{V} |\psi_{\mathbf{k}}\rangle = \hat{T}(k^2) |\phi_{\mathbf{k}}\rangle. \quad (3.32)$$

Replacing Eq. (3.32) in Eq. (3.31)

$$\hat{T}(k^2) |\phi_{\mathbf{k}}\rangle = \hat{V} |\phi_{\mathbf{k}}\rangle + \hat{V} \hat{G}(k^2) \hat{T}(k^2) |\phi_{\mathbf{k}}\rangle, \quad (3.33)$$

an equation for $\hat{T}(k^2)$ can be obtained as [18]

$$\hat{T}(k^2) = \hat{V} + \hat{V} \hat{G}(k^2) \hat{T}(k^2). \quad (3.34)$$

Now, performing the projection of $\hat{T}(k^2)$ and \hat{V} in the momentum eigenstates, $|\phi_{\mathbf{p}}\rangle$ and $|\phi_{\mathbf{p}'}\rangle$ ¹, as follows

$$T(\mathbf{p}, \mathbf{p}'; k^2) = \langle \phi_{\mathbf{p}} | \hat{T}(k^2) | \phi_{\mathbf{p}'} \rangle, \quad (3.35)$$

¹Here \mathbf{p}' is the pair incident relative momentum and \mathbf{p} is the pair outgoing relative momentum

$$V(\mathbf{p}, \mathbf{p}') = \langle \phi_{\mathbf{p}} | \hat{V} | \phi_{\mathbf{p}'} \rangle. \quad (3.36)$$

The Green function $\hat{G}(k^2)$ ² can be rewritten as

$$\hat{G}(k^2) = \frac{1}{k^2/2\mu - \mathbf{p}^2/2\mu \pm i\epsilon} \int d^3k' |\phi_{\mathbf{k}'}\rangle \langle \phi_{\mathbf{k}'}| = \int d^3k' \frac{|\phi_{\mathbf{k}'}\rangle \langle \phi_{\mathbf{k}'}|}{k^2/2\mu - k'^2/2\mu \pm i\epsilon}. \quad (3.37)$$

The momentum-space Lippmann-Schwinger equation is obtained by replacing Eq. (3.35), Eq. (3.36) and Eq. (3.37) in Eq. (3.34)

$$T(\mathbf{p}, \mathbf{p}'; k^2) = V(\mathbf{p}, \mathbf{p}') + \int d^3k' \frac{V(\mathbf{p}, \mathbf{k}')T(\mathbf{k}', \mathbf{p}'; k^2)}{(k^2 - k'^2)/2\mu \pm i\epsilon}. \quad (3.38)$$

The scattering wave function in coordinate space can be related to the \hat{T} matrix elements, similar to what was done in Eq. (3.4). From Eq. (3.29), Eq. (3.32) and Eq. (3.37), and $\psi_{\mathbf{k}}(\mathbf{r})$ can be found as

$$\begin{aligned} \psi(\mathbf{k}, \mathbf{r}) &= \langle \mathbf{r} | \phi_{\mathbf{k}} \rangle + \langle \mathbf{r} | \hat{G}(k^2) V | \psi_{\mathbf{k}} \rangle, \\ &= \phi(\mathbf{k}, \mathbf{r}) + \int d^3k' \frac{\langle \mathbf{r} | \phi_{\mathbf{k}'} \rangle \langle \phi_{\mathbf{k}'} | \hat{V} | \psi_{\mathbf{k}} \rangle}{(k^2 - k'^2)/2\mu \pm i\epsilon}, \\ &= \phi(\mathbf{k}, \mathbf{r}) + \int d^3k' \frac{\phi(\mathbf{k}', \mathbf{r}) \langle \phi_{\mathbf{k}'} | \hat{T}(k^2) | \phi_{\mathbf{k}} \rangle}{(k^2 - k'^2)/2\mu \pm i\epsilon}, \end{aligned} \quad (3.39)$$

that is, the scattering wave function can be obtained from the matrix element $T(\mathbf{k}', \mathbf{k}; k^2)$

$$\psi(\mathbf{k}, \mathbf{r}) = \phi(\mathbf{k}, \mathbf{r}) + \int d^3k' \frac{\phi(\mathbf{k}', \mathbf{r}) T(\mathbf{k}', \mathbf{k}; k^2)}{(k^2 - k'^2)/2\mu \pm i\epsilon}. \quad (3.40)$$

For this derivation to be analogous to what was performed in section (3.1) the observables, written in the *partial wave decomposition* (PWD) form are needed.

3.2.1 Partial wave analysis

The aim of this discussion is to find an expression for a momentum-dependent potential, for the transition operator $T(k^2)$ and for the scattering wave function $\psi(\mathbf{k}, \mathbf{r})$, written in terms of the PWD. Starting with the state vector $|\phi_{\mathbf{k}}\rangle$ [18]

$$|\phi_{\mathbf{k}}\rangle = |\mathbf{k}\rangle = \sqrt{\frac{2}{\pi}} \sum_{l=0}^{\infty} \sum_{m=-l}^l Y_{lm}^*(\Omega_{\hat{\mathbf{k}}}) |klm\rangle, \quad (3.41)$$

²The momentum eigenstate $|\phi_{\mathbf{k}}\rangle$ form a complete orthonormal set: $\int d^3k' |\phi_{\mathbf{k}'}\rangle \langle \phi_{\mathbf{k}'}| = 1$.

where $|klm\rangle$ is a simultaneous eigenstate of \hat{H}_0 , \mathbf{L}^2 and L_z (free-particle Hamiltonian, orbital angular momentum squared and z-projection of orbital angular momentum, respectively) and $Y_{lm}(\Omega_{\hat{\mathbf{k}}})$ is the spherical harmonics. Starting with the expression for the momentum-dependent potential, Eq. (3.36),

$$V(\mathbf{p}, \mathbf{p}') = \frac{2}{\pi} \sum_{l=0}^{\infty} \sum_{m=-l}^l Y_{lm}(\Omega_{\hat{\mathbf{p}}}) \sum_{l'=0}^{\infty} \sum_{m'=-l'}^{l'} Y_{l'm'}^*(\Omega_{\hat{\mathbf{p}'}}) \langle plm | \hat{V} | p'l'm' \rangle, \quad (3.42)$$

where

$$\langle plm | \hat{V} | p'l'm' \rangle = \delta_{ll'} \delta_{mm'} V_l(p, p'), \quad (3.43)$$

and substituting into Eq. (3.42), then

$$V(\mathbf{p}, \mathbf{p}') = \frac{2}{\pi} \sum_{l=0}^{\infty} \sum_{m=-l}^l Y_{lm}(\Omega_{\hat{\mathbf{p}}}) Y_{lm}^*(\Omega_{\hat{\mathbf{p}'}}) V_l(p, p'). \quad (3.44)$$

Applying the addition theorem, Eq. (3.16), to the potential matrix elements, leads to

$$V(\mathbf{p}, \mathbf{p}') = \frac{2}{\pi} \sum_{l=0}^{\infty} \frac{(2l+1)}{4\pi} P_l(x) V_l(p, p'). \quad (3.45)$$

Multiplying both sides of equation above by $P_{l'}(x)$, integrating over x and using the orthogonality relation for the Legendre polynomials³, the PWD for a momentum-dependent potential is then

$$V_l(p, p') = \pi^2 \int_{-1}^1 dx P_l(x) V(\mathbf{p}, \mathbf{p}'). \quad (3.46)$$

Likewise, the PWD of the $\hat{T}(k^2)$ operator matrix element is given by

$$T(\mathbf{p}, \mathbf{p}'; k^2) = \frac{2}{\pi} \sum_{l=0}^{\infty} \sum_{m=-l}^l Y_{lm}(\Omega_{\hat{\mathbf{p}}}) Y_{lm}^*(\Omega_{\hat{\mathbf{p}'}}) T_l(p, p', k^2). \quad (3.47)$$

³Orthogonality relation for the Legendre polynomials [19]: $\int_{-1}^1 dx P_{l'}(x) P_l(x) = \frac{2}{(2l+1)} \delta_{ll'}$

Using the results from Eq. (3.38), Eq. (3.42), Eq. (3.47) and the orthonormality of the spherical harmonics ⁴, the PWD of the $\hat{T}(k^2)$ operator can be rewritten as

$$\begin{aligned}
T(\mathbf{p}, \mathbf{p}'; k^2) &= \frac{2}{\pi} \sum_{l=0}^{\infty} \sum_{m=-l}^l Y_{lm}(\Omega_{\hat{\mathbf{p}}}) Y_{lm}^*(\Omega_{\hat{\mathbf{p}}'}) T_l(p, p'; k^2) \\
&= \frac{2}{\pi} \sum_{l=0}^{\infty} \sum_{m=-l}^l Y_{lm}(\Omega_{\hat{\mathbf{p}}}) Y_{lm}^*(\Omega_{\hat{\mathbf{p}}'}) \\
&\quad \times \left[V_l(p, p') + \frac{2}{\pi} \int dk' k'^2 \frac{V_l(p, k') T_l(k', p'; k^2)}{(k^2 - k'^2)/2\mu \pm i\epsilon} \right],
\end{aligned} \tag{3.48}$$

finally leads to

$$T_l(p, p'; k^2) = V_l(p, p') + \frac{2}{\pi} \int dk' k'^2 \frac{V_l(p, k') T_l(k', p'; k^2)}{(k^2 - k'^2)/2\mu \pm i\epsilon}. \tag{3.49}$$

The PWD of the scattering wave function is similar to the description in Sec. 3.1 by Eq.(3.17). However, now the symmetry under ϕ is not imposed, i.e.,

$$\psi(\mathbf{k}, \mathbf{r}) = \frac{1}{(2\pi)^{3/2}} \sum_{l=0}^{\infty} \sum_{m=-l}^l 4\pi i^l \psi_l(k, r) Y_{lm}^*(\Omega_{\hat{\mathbf{k}}}) Y_{lm}(\Omega_{\hat{\mathbf{r}}}), \tag{3.50}$$

and $\phi_{\mathbf{k}}(\mathbf{r})$ becomes

$$\phi(\mathbf{k}, \mathbf{r}) = \frac{1}{(2\pi)^{3/2}} \sum_{l=0}^{\infty} \sum_{m=-l}^l 4\pi i^l j_l(k, r) Y_{lm}^*(\Omega_{\hat{\mathbf{k}}}) Y_{lm}(\Omega_{\hat{\mathbf{r}}}). \tag{3.51}$$

To obtain the PWD for the scattering wave function $\psi(\mathbf{k}, \mathbf{r})$ in terms of the transition operator it is necessary to insert Eq. (3.50), (3.51), (3.47) into Eq. (3.40) and

⁴Orthonormality relation of the spherical harmonics [19]: $\int d\Omega_{\hat{\mathbf{k}}'} Y_{lm}^*(\Omega_{\hat{\mathbf{k}}'}) Y_{l'm'}(\Omega_{\hat{\mathbf{k}}'}) = \delta_{ll'} \delta_{mm'}$

consider the orthonormality of the spherical harmonics, which leads to

$$\begin{aligned}
\psi(\mathbf{k}, \mathbf{r}) &= \frac{1}{(2\pi)^{3/2}} \sum_{l=0}^{\infty} \sum_{m=-l}^l 4\pi i^l \psi_l(k, r) Y_{lm}^*(\Omega_{\hat{\mathbf{k}}}) Y_{lm}(\Omega_{\hat{\mathbf{r}}}) \\
&= \frac{1}{(2\pi)^{3/2}} \sum_{l=0}^{\infty} \sum_{m=-l}^l 4\pi i^l Y_{lm}^*(\Omega_{\hat{\mathbf{k}}}) Y_{lm}(\Omega_{\hat{\mathbf{r}}}) \\
&\quad \times \left[j_l(kr) + \frac{2}{\pi} \int dk' k' \frac{4\pi i^l j_l(k'r) T_l(k', k; k^2)}{(k^2 - k'^2)/2\mu \pm i\epsilon} \right].
\end{aligned} \tag{3.52}$$

The PWD of the scattering wave function in terms of the T -matrix operator is then written as

$$\psi_l(k, r) = j_l(kr) + \frac{2}{\pi} \int dk' k'^2 \frac{j_l(k'r) T_l(k', k; k^2)}{(k^2 - k'^2)/2\mu \pm i\epsilon}. \tag{3.53}$$

R -matrix

However, to obtain the observables numerically it is convenient to solve the Lippmann-Schwinger equation for the *reaction matrix* $R_l(p, p'; k^2)$, instead of $T_l(p, p'; k^2)$, since the R -matrix is totally real. The Lippmann-Schwinger equation for $R_l(p, p'; k^2)$ is given by [26]

$$R_l(p, p'; k^2) = V_l(p, p') + \frac{2}{\pi} \text{P} \int_0^{\infty} dk' \frac{V_l(p, k') R_l(k', p'; k^2)}{(k^2 - k'^2)/2\mu}, \tag{3.54}$$

where P indicates the integral *principal value*. The expression that relates the $T_l(p, p'; k^2)$ and $R_l(p, p'; k^2)$ matrices are [27]

$$T_l(p, p'; k^2) = R_l(p, p'; k^2) - \frac{2\mu ik R_l(p, k; k^2) R_l(k, p'; k^2)}{1 + 2\mu ik R_l(k, k; k^2)}. \tag{3.55}$$

From, Eqs. (3.54) and (3.55) it is possible to obtain a relation between the on-shell ($p = p' = k$) $T_l(k, k; k^2) \equiv T_l(k^2)$ and $R_l(k, k; k^2) \equiv R_l(k^2)$ matrix elements and the phase shifts, given by

$$T_l(k^2) = \frac{R_l(k^2)}{1 + 2\mu ik R_l(k^2)} = -\frac{1}{2\mu k} e^{i\delta_l(k)} \sin \delta_l(k), \tag{3.56}$$

or

$$R_l(k^2) = \frac{R_l(k^2)}{1 + 2\mu ik T_l(k^2)} = -\frac{1}{2\mu k} \tan \delta_l(k). \quad (3.57)$$

To calculate the scattering wave function $\psi_l(k, r)$ in terms of the R -matrix elements $R(k', k; k^2)$, one starts from Eq. (3.53). Using that, for $k > 0$ and $k' > 0$

$$\frac{1}{(k^2 - k'^2)/2\mu \pm i\epsilon} = \text{P} \frac{1}{(k^2 - k'^2)/2\mu} - i\pi \frac{2\mu}{2k'} \delta(k - k'). \quad (3.58)$$

Equation (3.53) can be rewritten as

$$\psi_l(k, r) = j_l(kr) + \frac{2}{\pi} \text{P} \int_0^\infty dk' k'^2 \frac{j_l(k'r) T_l(k', k; k^2)}{(k^2 - k'^2)/2\mu} - 2i\mu k j_l(kr) T_l(k^2). \quad (3.59)$$

From Eq. (3.55), for $p = k'$ and $p' = k$, then

$$T_l(k', k; k^2) = \frac{R_l(k', k; k^2)}{1 + 2i\mu k R_l(k^2)}, \quad (3.60)$$

which, when Eq. (3.56), Eq. (3.57) and Eq. (3.60) are inserted into Eq. (3.59), leads to

$$\begin{aligned} \psi_l(k, r) &= j_l(kr) \left(1 + i e^{i\delta_l(k)} \sin \delta_l(k) \right) \\ &+ \frac{2}{\pi} \text{P} \int_0^\infty dk' k'^2 \frac{j_l(k'r)}{(k^2 - k'^2)/2\mu} \frac{R_l(k', k; k^2)}{1 - i \tan \delta_l(k)}. \end{aligned} \quad (3.61)$$

To simplify the previous equation, it is possible to use

$$\begin{aligned} 1 + i e^{i\delta_l(k)} \sin \delta_l(k) &= e^{i\delta_l(k)} \cos \delta_l(k), \\ \frac{1}{1 - i \tan \delta_l(k)} &= e^{i\delta_l(k)} \cos \delta_l(k), \end{aligned}$$

Therefore, Eq. (3.61) can be finally be rewritten as

$$\begin{aligned} \psi_l(k, r) &= e^{i\delta_l(k)} \cos \delta_l(k) \left(j_l(kr) + \frac{2}{\pi} \text{P} \int_0^\infty dk' k'^2 j_l(k'r) \frac{R_l(k', k; k^2)}{(k^2 - k'^2)/2\mu} \right) \\ &= e^{i\delta_l(k)} \cos \delta_l(k) \psi_l^R(k, r), \end{aligned} \quad (3.62)$$

where $e^{i\delta_l(k)}$ is a global phase and $\psi_l^R(k, r)$ is the wave function given in terms of the half-off-shell R -matrix element. In this work, it will be considered that all interactions will be affected by the s-wave contribution only, i.e., $l = 0$. Then, the

expression above becomes

$$\psi_0(k, r) = \cos \delta_0(k) \left(j_0(kr) + \frac{2}{\pi} P \int_0^\infty dk' k'^2 j_0(k'r) \frac{R_0(k', k; k^2)}{(k^2 - k'^2)/2\mu} \right). \quad (3.63)$$

Adopting a procedure analogous to that employed in Sec. 3.1, the solution of the Lippmann-Schwinger equation can be obtained numerically.

3.2.2 Numerical description

To solve the Lippmann-Schwinger equation and obtain the scattering wave function numerically, a method was used from Ref. [26] to transform the problem from the continuum spectrum into a discrete matrix problem. First, applying the properties of the principal-value integral [26] :

$$P \int_0^\infty dk' \frac{f(k')}{k^2 - k'^2} = \int_0^\infty dk' \frac{f(k') - f(k)}{k^2 - k'^2}. \quad (3.64)$$

Replacing this result to the expression for the R -matrix, in Eq. (3.54), dropping the subscript "l" for simplicity and taking $p' = k$, that is, $R_l(p, k; k^2) = R(p, k)$ and $V_l(p, k) = V(p, k)$, then

$$R(p, k) = V(p, k) + \frac{2}{\pi} \int_0^\infty dk' \left[k'^2 \frac{V(p, k')R(k', k)}{(k^2 - k'^2)/2\mu} - k^2 \frac{V(p, k)R(k, k)}{(k^2 - k'^2)/2\mu} \right]. \quad (3.65)$$

Next, to transform Eq. (3.65) into a discrete linear equation, the integral is approximated by a Gauss quadrature as a sum over N integration points

$$\int_0^\infty dp f(p) \approx \sum_{j=1}^N w_j f(p_j), \quad (3.66)$$

where p_j are the Gauss points with corresponding weights w_j . Thus,

$$R(p, k) \approx V(p, k) + \frac{2}{\pi} \sum_{j=1}^N \frac{w_j k_j^2 V(p, k_j) R(k_j, k)}{(k^2 - k_j^2)/2\mu} - \frac{2}{\pi} k^2 V(p, k) R(k, k) \sum_{m=1}^N \frac{w_m}{(k^2 - k_m^2)/2\mu}. \quad (3.67)$$

This equation contains the $N + 1$ unknown $R(p_j, k)$: for $j = 1, N$, namely half-on-shell matrix elements, plus for $j = N + 1$ the on-shell matrix element $R(k, k)$. This can be transformed into $N + 1$ unknown $R_i \equiv R(k_i, k)$ simultaneous equations by evaluating it $i = 1, \dots, N$ in the Gauss grid plus $i = N + 1$ for an observable

momentum:

$$p = p_i = \begin{cases} p_j, & j = 1, \dots, N \quad \text{in the Gauss grid} \\ k, & i = N + 1 \quad \text{observable momentum } k \end{cases}$$

Then, the expression in terms of the matrix elements is written as

$$R(k_i, k) = R_i = V_i + \frac{2}{\pi} \sum_{j=1}^N \frac{w_j k_j^2}{(k^2 - k_j^2)/2\mu} V_{ij} R_j - \frac{2}{\pi} k^2 V_{ii} R_{N+1} \sum_{m=1}^N \frac{w_m}{(k^2 - k_m^2)/2\mu}. \quad (3.68)$$

This equation can be written in matrix form as $\mathbf{Ax} = \mathbf{b}$ by combining the denominators and weights into a single vector D , with components:

$$D_i = \begin{cases} \frac{2}{\pi} \frac{w_i k_i^2}{(k^2 - k_i^2)/2\mu}, & \text{for } i = 1, \dots, N \\ -\frac{2}{\pi} k^2 \sum_{j=1}^N \frac{w_j}{(k_0^2 - k_j^2)/2\mu}, & \text{for } i = N + 1 \end{cases}$$

Rewriting Eq. (3.68), in terms of the vector \mathbf{D} , the matrix equations becomes

$$R = V + DVR \rightarrow R - DVR = V \rightarrow [1 - DV]R = V \quad (3.69)$$

Then,

$$R = F^{-1}V, \quad F_{ij} = \delta_{ij} - D_j V_{ij} \quad (3.70)$$

where the solution for R will be via the inversion of the matrix F .

A similar relation can be defined for the $\psi_0(k, r)$, Eq. (3.63), and therefore the scattering wave function $\psi_0(k, r)$ can be written as

$$\psi_0(r) \rightarrow \psi_{N+1}(r) = \cos \delta_0(k_{N+1}) \left(j_{N+1}(r) + \sum_{i=1}^{N+1} j_i(r) D_i R_{N+1} \right). \quad (3.71)$$

3.3 Equivalence of the approaches

The codes developed in Sec. (3.1) and Sec. (3.2) corresponding to the Schrödinger and the Lippmann-Schwinger cases, respectively, are validated in this section by comparing their numerical results with the analytical solution of the problem. The equivalence of the two approaches is shown by comparing the results from both codes for the Yukawa potential, from Ref. [28].

3.3.1 Yukawa potential

In this study, the Yukawa potential adopted for describing the proton-proton interaction, expressed as in Ref. [28],

$$V(r) = -V_0 \frac{e^{-mr}}{r}, \quad (3.72)$$

with $V_0 = 65.246 \text{ MeV}\cdot\text{fm}$, and $m = 0.6329 \text{ fm}^{-1}$. The expression for the Yukawa potential $V(r)$ in the momentum space and decomposed in partial waves, similar to Eq. (3.46), is

$$V_l(k, k') = \pi^2 \int_{-1}^1 dx P_l(x) \langle \mathbf{k} | V | \mathbf{k}' \rangle, \quad (3.73)$$

where $\langle \mathbf{k} | V | \mathbf{k}' \rangle$ is the Fourier transform of the potential,

$$\langle \mathbf{k} | V | \mathbf{k}' \rangle = \int \frac{dr^3}{(2\pi)^3} V(r) e^{i(\mathbf{k}-\mathbf{k}') \cdot \vec{r}}. \quad (3.74)$$

The scalar product can be written as $(\mathbf{k} - \mathbf{k}') \cdot \mathbf{r} = |\mathbf{k} - \mathbf{k}'| |\mathbf{r}| \cos \theta$, and Eq. (3.73) becomes:

$$V_l(k, k') = \pi^2 \int_{-1}^1 dx P_l(x) \left[\int \frac{dr^3}{(2\pi)^3} V(r) e^{i|\mathbf{k}-\mathbf{k}'| |\mathbf{r}| \cos \theta} \right]. \quad (3.75)$$

Considering only the effects of the s-wave ($l = 0$) contribution, $V_0(k, k')$ can be written as

$$\begin{aligned} V_{l=0}(k, k') &= -\pi^2 \int_{-1}^1 dx \int_0^\infty \frac{dr^3}{(2\pi)^3} \left[V_0 \frac{e^{-mr}}{r} \right] e^{i|\mathbf{k}-\mathbf{k}'| |\mathbf{r}| \cos \theta} \\ &= -\frac{V_0}{4kk'} \ln \left[\frac{m^2 + (k + k')^2}{m^2 + (k - k')^2} \right]. \end{aligned} \quad (3.76)$$

The phase shifts can be obtained from Eq. (3.24) using the code that solves the Schrödinger equation and from Eq. (3.57) using the code that solves the Lippmann-Schwinger equation. The results for the scattering wave function and the phase shifts for the Schrödinger and for the Lippmann-Schwinger equations are shown in Fig. 3.1 and Figure 3.2, respectively.

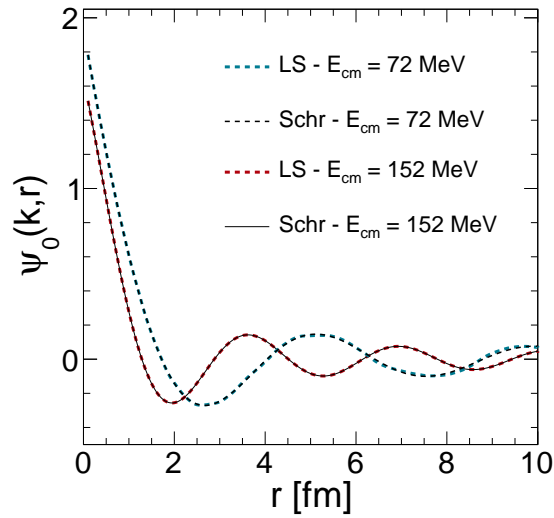


Figure 3.1: Comparison of $\psi_0(k, r)$ versus r numerical results between the Schrödinger (Schr) equation for values of the center-of-mass energy (E_{cm}) of 72 MeV (black, dashed line) and 152 MeV (black, full line) and the Lippmann-Schwinger (LS) equation for values of the center-of-mass energy (E_{cm}) of 72 MeV (blue, dashed line) and 152 MeV (red, dashed line).

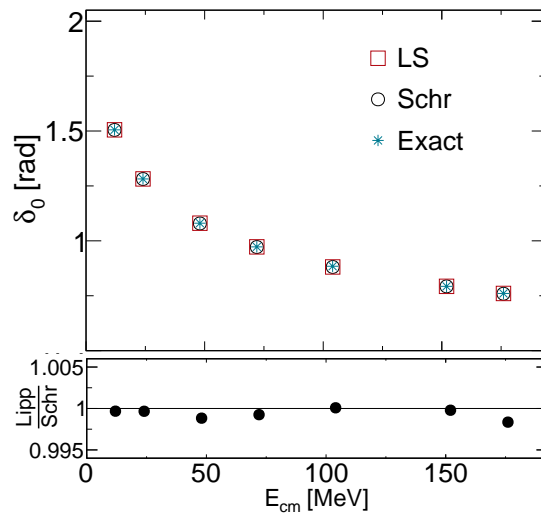


Figure 3.2: Comparison of results for δ_0 versus E_{cm} obtained by solving the Schrödinger equation, Schr (black, empty circle dots), the Lippmann-Schwinger equation, LS (red, empty square dots), and from the analytical derivation of δ_0 , Exact (blue, asterisk dots), from Ref. [28].

3.4 Extension: other potential models

In the previous sections, the formalism to obtain the expressions for the scattered wave function $\psi_0(k, r)$ was derived. This is a necessary step for obtaining the two-particle correlation function. Naturally, regardless the method that is adopted, the expression for the potential representing the interaction is necessary. Some examples of potential models are discussed in the following, corresponding to the type of particle whose correlation is being studied.

3.4.1 Potentials models for describing $\Lambda\Lambda$ interaction

In the case of $\Lambda\Lambda$ interactions, the experimental information is still limited, but there are several proposed models, as can be seen in Ref. [29]. In this work, four distinct models are selected, two of them are of the type *two-range Gaussian* potentials, which the parameters are in Table (3.4.1), NF50, a Nijmegen potential [30] and fss2, quark model potential [31], models

$$V_{\Lambda\Lambda}(r) = V_1 e^{-\frac{r^2}{\mu_1}} + V_2 e^{-\frac{r^2}{\mu_2}}, \quad (3.77)$$

Table 3.1: Parameters for the *two-range Gaussian* potentials, extracted from [29].

Model	V_1 (MeV)	μ_1 (fm)	V_2 (MeV)	μ_2 (fm)
NF50	-2007.35	0.60	5678.97	0.45
fss2	-103.9	0.92	658.2	0.41

and the other two are of the type *three-range Gaussian* potentials, whose parameters are in Table (3.4.1), the Hiyama-Kamimura-Motoba-Yamada-Yamamoto (HKMYY) [32] and Filikhin-Gal (FG) [33] models,

$$V_{\Lambda\Lambda}(r) = V_1 e^{-\frac{r^2}{\mu_1}} + V_2 e^{-\frac{r^2}{\mu_2}} + V_3 e^{-\frac{r^2}{\mu_3}}. \quad (3.78)$$

The expressions (3.77) and (3.78) can be easily transformed to the momentum-space and can be applied to the Schrödinger equation and to the Lippmann-Schwinger equation. From the expression (3.75), the Fourier transform and the

Table 3.2: Parameters for the *three-range Gaussian* potentials, extracted from [29].

Model	V_1 (MeV)	μ_1 (fm)	V_2 (MeV)	μ_2 (fm)	V_3 (MeV)	μ_3 (fm)
HKMYY	-10.96	1.342	-141.75	0.78	2136.6	0.35
FG	-21.49	1.342	-250.13	0.78	9324.0	0.35

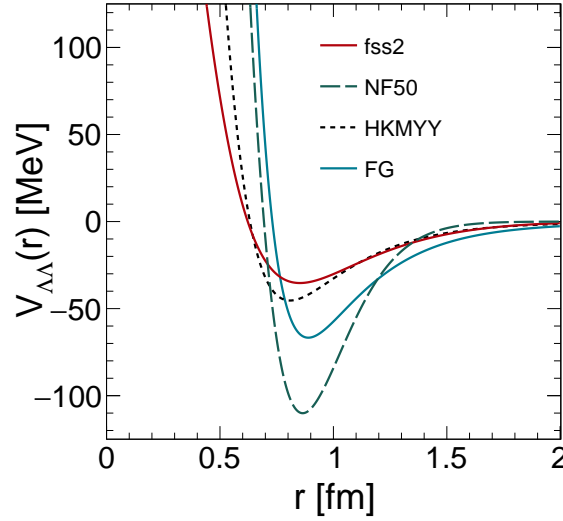


Figure 3.3: The $\Lambda\Lambda$ potentials $V_{\Lambda\Lambda}(r)$, fss2 (red, full line), NF50 (green, long dashed line), HKMYY (black, short dashed line) and FG (blue, full line), with the parameters expressed in Table (3.4.1) and Table (3.4.1) with respect to the relative distance r .

PWD for the s-wave of the *two-range Gaussian* potential and the *three-range Gaussian* potential models are given, respectively, by

$$\begin{aligned}
 V_{l=0}(k-k') &= \frac{\sqrt{\pi}}{4kk'} \left[V_1\mu_1 \left(e^{-\frac{\mu_1^2}{4}(k-k')^2} - e^{-\frac{\mu_1^2}{4}(k+k')^2} \right) \right. \\
 &\quad \left. + V_2\mu_2 \left(e^{-\frac{\mu_2^2}{4}(k-k')^2} - e^{-\frac{\mu_2^2}{4}(k+k')^2} \right) \right], \quad (3.79)
 \end{aligned}$$

and

$$\begin{aligned}
V_{l=0}(k-k') &= \frac{\sqrt{\pi}}{4kk'} \left[V_1 \mu_1 \left(e^{-\frac{\mu_1^2}{4}(k-k')^2} - e^{-\frac{\mu_1^2}{4}(k+k')^2} \right) \right. \\
&+ V_2 \mu_2 \left(e^{-\frac{\mu_2^2}{4}(k-k')^2} - e^{-\frac{\mu_2^2}{4}(k+k')^2} \right) \\
&\left. + V_3 \mu_3 \left(e^{-\frac{\mu_3^2}{4}(k-k')^2} - e^{-\frac{\mu_3^2}{4}(k+k')^2} \right) \right]. \quad (3.80)
\end{aligned}$$

The expressions above, together with Eq. (3.77) and Eq. (3.78), can be used as validators for both codes. Here, only the potential models are introduced. The results obtained for the wave function and then for the correlation function, using the formalism described previously, are presented in Chapter 4.

3.4.2 Usmani potential

In the case of $p\Lambda$ interactions, the Usmani potential is usually employed, since it describes the nucleon-hyperon interaction in the form of a two-pion exchange (TPE) mechanism from the one-pion exchange (OPE) transition potentials [34], i.e,

$$V_{\Lambda p} = V_C - \left(\bar{V} - \frac{1}{4} V_\sigma \sigma_\Lambda \cdot \sigma_p \right) T_\pi^2, \quad (3.81)$$

where V_C is a Woods-Saxon repulsive core,

$$V_C = W_C \left[1 + \exp\left(\frac{r-R}{d}\right) \right]^{-1}, \quad (3.82)$$

with $W_C = 2137$ MeV, $R = 0.5$ fm and $d = 0.2$ fm. The T_π term is a modified OPE tensor potential

$$T_\pi = \left(1 + \frac{3}{x} + \frac{3}{x^2} \right) \frac{e^{-x}}{x} \left(1 - e^{-cr^2} \right)^2, \quad (3.83)$$

being $x = 0.7r$ and $c = 2 \text{ fm}^{-2}$. Also, \bar{V} is the spin-independent part of the attractive potential and V_σ is the spin-dependent part. Both contributions are used in the literature as $\bar{V} = 6.2 \pm 0.05$ MeV and $V_\sigma = 0.25 \pm 0.25$ MeV [35]. Since the proton and Λ particle are non-identical spin-1/2 fermions the contribution from the spin tensor $\sigma_\Lambda \cdot \sigma_p$ is -3 for the singlet state ($S = 0$) and $+1$ for the triplet state

($S = 1$), according to the matrix element of the tensor product

$$\begin{aligned}\langle S = 0; m_S = 0 | \sigma_\Lambda \cdot \sigma_p | S = 0; m_S = 0 \rangle &= -3, \\ \langle S = 1; m_S = -1, 0, 1 | \sigma_\Lambda \cdot \sigma_p | S = 1, m_S = -1, 0, 1 \rangle &= +1.\end{aligned}\quad (3.84)$$

Then, for the singlet state

$$V_{p\Lambda}^{S=0} = V_C - \left(\bar{V} + \frac{3}{4} V_\sigma \right) T_\pi^2, \quad (3.85)$$

and for the triplet state

$$V_{p\Lambda}^{S=1} = V_C - \left(\bar{V} - \frac{1}{4} V_\sigma \right) T_\pi^2, \quad (3.86)$$

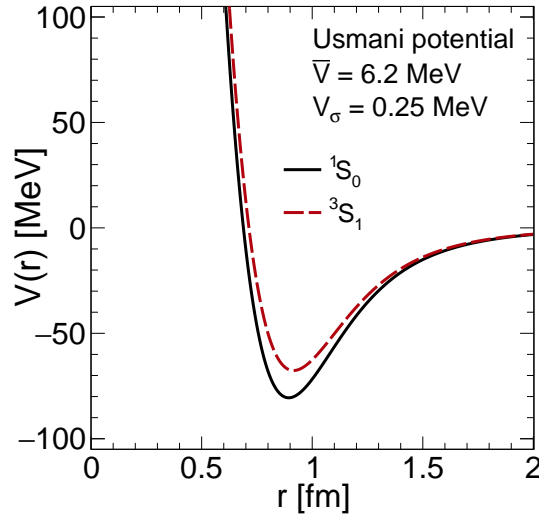


Figure 3.4: Usmani potential $V_{p\Lambda}(r)$ with respect to the relative distance r , with fixed values of $\bar{V} = 6.2$ MeV and $V_\sigma = 0.25$ MeV, for the singlet state, 1S_0 (black, full line), and the triplet state, 3S_1 (red, dashed line).

As mentioned above, the terms \bar{V} and V_σ in the potential, Eq. (3.81), have uncertainties, so, in Figure 3.5, the effect of the variation of these parameters is shown in the final curve for the two-particle correlation function. To make it simple, as is already done in the literature [35, 36], in all the results discussed in this dissertation the values of these two parameters will be fixed to $\bar{V} = 6.2$ MeV and $V_\sigma = 0.25$ MeV.

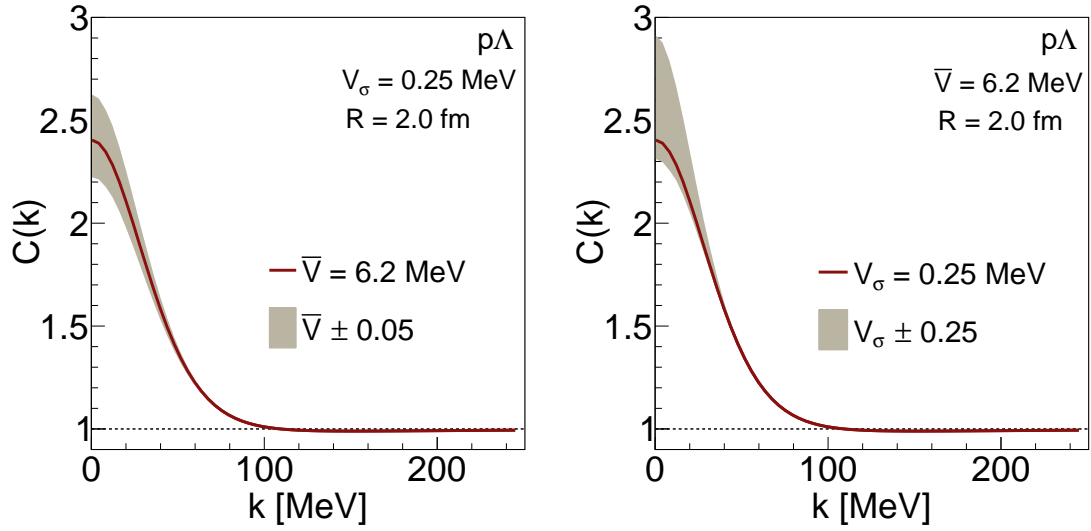


Figure 3.5: The plots show the ranges of the uncertainties (grey, shade region) of the parameters \bar{V} (left) and V_σ (right) in the Usmani potential, around the fixed central values (red, full line) of these parameters, with respect to relative momentum k .

3.4.3 Meson-meson potential

To describe the interaction between the D^0 mesons a quark-model potential was employed, based on Sergio Szpigel's PhD Thesis [37] "*Interação Méson-méson no formalismo Fock-Tani*" and published in Ref. [38]. This model was proposed to describe pions and kaons interactions, however, in this work, the meson-meson potential was extended to also describe the interaction between charmed mesons by adjusting the mesonic states in a Fock space composed by a quark-antiquark pair. Consider now the meson-meson scattering

$$\gamma + \delta \rightarrow \alpha + \beta. \quad (3.87)$$

The potential will be given by the matrix element between the final and the initial state of this process,

$$V_{mm}(\alpha\beta; \gamma\delta) = \langle M_\alpha M_\beta | \left(\hat{V}_{q\bar{Q}} + \hat{V}_{qq} + \hat{V}_{\bar{Q}\bar{Q}} \right) | M_\gamma M_\delta \rangle, \quad (3.88)$$

where $\hat{V}_{q\bar{Q}}$ is the quark-antiquark interaction term, \hat{V}_{qq} is the quark-quark interaction term and $\hat{V}_{\bar{Q}\bar{Q}}$ is the antiquark-antiquark term. The evaluation of this expression results in six non-zero terms that represent the contribution for the

short-range interactions

$$V_{\text{mm}}^{\text{short-range}}(\alpha\beta; \gamma\delta) = V^1(\alpha\beta; \gamma\delta) + V^2(\alpha\beta; \gamma\delta) + V^3(\alpha\beta; \gamma\delta) \\ + V^4(\alpha\beta; \gamma\delta) + V^5(\alpha\beta; \gamma\delta) + V^6(\alpha\beta; \gamma\delta), \quad (3.89)$$

with

$$V^j(\alpha\beta; \gamma\delta) = I_0^j I_{\text{spin}}^j(\alpha\beta; \gamma\delta) I_{\text{flavor}}^j(\alpha\beta; \gamma\delta) I_{\text{color}}^j(\alpha\beta; \gamma\delta) I_{\text{spatial}}^j(\alpha\beta; \gamma\delta). \quad (3.90)$$

There is also a non-zero contribution for the long-range interactions given as

$$V_{\text{mm}}^{\text{long-range}}(\alpha\beta; \gamma\delta) = I_0^{\text{long-range}}(\alpha\beta; \gamma\delta) I_{\text{spatial}}^{\text{long-range}}(\alpha\beta; \gamma\delta). \quad (3.91)$$

The explicit calculation of these matrix elements of the potential are in the Appendices A.1 and A.2, and gives rise to two terms that compose the meson-meson potential: a spin-spin (hyperfine) as the short-range term contribution, V_{hyp} , and a meson exchange as the long-range term contribution, $V_{\text{long-range}}$. The spin-spin term is

$$V^{\text{hyp}}(\mathbf{p}_1, \mathbf{p}'_1) = -\frac{1}{(2\pi)^3} \frac{8\pi\alpha_s}{3m_q m_Q} (\sigma_{s'_1, s_1} \cdot \sigma_{s'_2, s_2}), \quad (3.92)$$

where m_q is the light quark mass, m_Q is the heavy quark mass and $\sigma_{s'_1, s_1} \cdot \sigma_{s'_2, s_2}$ is the spin-tensor. The long-range term is

$$V^{\text{long-range}}(\mathbf{p}_1 - \mathbf{p}'_1) = -\frac{g^2}{(2\pi)^3} \frac{1}{(\mathbf{p}_1 - \mathbf{p}'_1)^2 + m_\sigma^2}, \quad (3.93)$$

with $\frac{g^2}{4\pi} \approx 0.375$ and $m_\sigma = 600$ MeV from Ref. [39].

After some calculations, that are discussed in details in Appendix A.1, each $V^j(\alpha\beta; \gamma\delta)$ is rewritten as

$$V^1(\mathbf{p}, \mathbf{p}') = \left(\frac{1}{2}\right) \left(\frac{1}{9}\right) \frac{8}{3\sqrt{3}} \left(\frac{1}{(2\pi)^3} \frac{8\pi\alpha_s}{m_q m_Q}\right) \\ \times \exp\left[-\frac{1}{2b^2} \left(2\eta^2(\mathbf{p}^2 + \mathbf{p}'^2) + (1 - 2\eta)(\mathbf{p} + \mathbf{p}')^2\right)\right] \\ \times \exp\left[\frac{1}{2b^2} \frac{1}{3}(\mathbf{p} + (1 - 2\eta)\mathbf{p}')^2\right], \quad (3.94)$$

$$\begin{aligned}
V^2(\mathbf{p}, \mathbf{p}') &= \left(\frac{1}{2}\right) \left(\frac{1}{9}\right) \frac{8}{3\sqrt{3}} \left(\frac{1}{(2\pi)^3} \frac{8\pi\alpha_s}{m_q m_Q}\right) \\
&\times \exp\left[-\frac{1}{2b^2} \left(2\eta^2(\mathbf{p}^2 + \mathbf{p}'^2) + (1-2\eta)(\mathbf{p} + \mathbf{p}')^2\right)\right] \\
&\times \exp\left[\frac{1}{2b^2} \frac{1}{3} (\mathbf{p} + (1-2\eta)\mathbf{p}')^2\right], \tag{3.95}
\end{aligned}$$

$$\begin{aligned}
V^3(\mathbf{p}, \mathbf{p}') &= \left(\frac{1}{2}\right) \left(\frac{1}{9}\right) \frac{8}{3\sqrt{3}} \left(\frac{1}{(2\pi)^3} \frac{8\pi\alpha_s}{m_q m_Q}\right) \\
&\times \exp\left[-\frac{1}{2b^2} \left(2\eta^2(\mathbf{p}^2 + \mathbf{p}'^2) + (1-2\eta)(\mathbf{p} + \mathbf{p}')^2\right)\right] \\
&\times \exp\left[\frac{1}{2b^2} \frac{1}{3} ((1-2\eta)\mathbf{p} + \mathbf{p}')^2\right], \tag{3.96}
\end{aligned}$$

$$\begin{aligned}
V^4(\mathbf{p}, \mathbf{p}') &= \left(\frac{1}{2}\right) \left(\frac{1}{9}\right) \frac{8}{3\sqrt{3}} \left(\frac{1}{(2\pi)^3} \frac{8\pi\alpha_s}{m_q m_Q}\right) \\
&\times \exp\left[-\frac{1}{2b^2} \left(2\eta^2(\mathbf{p}^2 + \mathbf{p}'^2) + (1-2\eta)(\mathbf{p} + \mathbf{p}')^2\right)\right] \\
&\times \exp\left[\frac{1}{2b^2} \frac{1}{3} ((1-2\eta)\mathbf{p} + \mathbf{p}')^2\right], \tag{3.97}
\end{aligned}$$

$$\begin{aligned}
V^5(\mathbf{p}, \mathbf{p}') &= \left(\frac{1}{9}\right) \left(\frac{1}{(2\pi)^3} \frac{8\pi\alpha_s}{m_q m_Q}\right) \\
&\times \exp\left[-\frac{1}{2b^2} \left(\eta^2(\mathbf{p} - \mathbf{p}')^2\right)\right], \tag{3.98}
\end{aligned}$$

$$\begin{aligned}
V^6(\mathbf{p}, \mathbf{p}') &= \left(\frac{1}{9}\right) \left(\frac{1}{(2\pi)^3} \frac{8\pi\alpha_s}{m_Q m_Q}\right) \\
&\times \exp\left[-\frac{1}{2b^2} \left((1-\eta)^2(\mathbf{p} + \mathbf{p}')^2\right)\right], \tag{3.99}
\end{aligned}$$

$$V^{\text{long-range}}(\mathbf{p} - \mathbf{p}') = -\frac{g^2}{(2\pi)^3} \frac{e^{-\frac{1}{2b^2}\eta^2(\mathbf{p}-\mathbf{p}')^2}}{(\mathbf{p} - \mathbf{p}')^2 + m_\sigma^2}. \tag{3.100}$$

Summing all the equations expressions, an expression for the meson-meson potential can be obtained as

$$V_{\text{mm}}^{\text{total}} = V_{\text{mm}}^{\text{hyp}} + V_{\text{mm}}^{\text{long-range}} \tag{3.101}$$

Specially, for the case of D^0 mesons, that are composed of a light quark u and a heavy quark c [40], the contributions are

- Spin-spin term:

$$\begin{aligned}
V_{\text{mm}}^{\text{hyp}}(\mathbf{p}, \mathbf{p}') &= \frac{1}{(2\pi)^3} \frac{8\pi\alpha_s}{9} \left\{ \right. \\
&\times \frac{8}{3\sqrt{3}} \frac{1}{m_u m_c} \left[e^{-\frac{1}{2b^2} (2\eta^2(\mathbf{p}^2 + \mathbf{p}'^2) + (1-2\eta)(\mathbf{p} + \mathbf{p}')^2 - \frac{1}{3}(\mathbf{p} + (1-2\eta)\mathbf{p}')^2)} \right. \\
&+ e^{-\frac{1}{2b^2} (2\eta^2(\mathbf{p}^2 + \mathbf{p}'^2) + (1-2\eta)(\mathbf{p} + \mathbf{p}')^2 - \frac{1}{3}((1-2\eta)\mathbf{p} + \mathbf{p}')^2)} \left. \right] \\
&+ \left. \frac{1}{m_u^2} e^{-\frac{1}{2b^2} \eta^2(\mathbf{p} - \mathbf{p}')^2} + \frac{1}{m_c^2} e^{-\frac{1}{2b^2} (1-\eta)^2(\mathbf{p} + \mathbf{p}')^2} \right\}. \tag{3.102}
\end{aligned}$$

- Long-range term:

$$V_{\text{mm}}^{\text{long-range}}(\mathbf{p} - \mathbf{p}') = -\frac{g^2}{(2\pi)^3} \frac{e^{-\frac{1}{2b^2} \eta^2(\mathbf{p} - \mathbf{p}')^2}}{(\mathbf{p} - \mathbf{p}')^2 + m_\sigma^2}. \tag{3.103}$$

From Refs. [37] and [39] the parameters are

$$\begin{aligned}
\alpha_s &= 0.6; \quad \frac{g^2}{4\pi} = 0.375 \\
m_c &= 1670 \text{ MeV}; \quad m_u = 330 \text{ MeV} \\
\eta &= \frac{m_c}{m_c + m_u} = \frac{1670}{1670 + 330} = 0.835 \\
b &= 383.5 \text{ MeV} \tag{3.104}
\end{aligned}$$

In the next chapter the expressions in Eqs. (3.77), (3.78), (3.81) and (3.101) will be used to obtain the scattered wave-function and subsequently correlation function for the systems of interest.

Chapter 4

Numerical results

Employing the numerical methods described in the last chapter, Sec. 3.1 and 3.2, an investigation was conducted to study the correlation function for different correlating systems: $\Lambda\Lambda$, $p\Lambda$ and D^0D^0 and $\bar{D}^0\bar{D}^0$. Besides the correlation function, the scattering observables for each system is obtained and compared with the literature. Notice, however, that for the D^0D^0 and $\bar{D}^0\bar{D}^0$ meson correlation there are no theoretical or experimental guidelines in femtoscopy yet.

4.1 Validation of the codes

In the following sections, Sec. 4.1.1 and 4.1.2, the validation of the code that solves the Schrödinger equation using the $\Lambda\Lambda$ and $p\Lambda$ particles correlations was performed comparing the theoretical and experimental results available in the literature. It was also possible to use the $\Lambda\Lambda$ correlations to certify if the code that solves the Lippmann-Schwinger equation was working properly.

4.1.1 $\Lambda\Lambda$ correlation

The $\Lambda\Lambda$ correlation function can be obtained by the two-particle correlation function for identical spin-1/2 fermions derived on Chapter 2 and described in Eq. (2.101). In this expression the quantum statistics (QS) contribution is written as

$$C_{\text{QS}}(k) = 1 - \frac{1}{2}e^{-4k^2R^2}, \quad (4.1)$$

and the strong interaction (SI) contribution is written as

$$C_{\text{SI}}(k) = 1 + 2\pi \int_0^\infty dr r^2 S(r) \left[|\psi_0(k, r)|^2 - j_0^2(kr) \right], \quad (4.2)$$

where the total contribution (QS+SI) is detailed in Eq. (2.101).

All the contributions for a fixed value of the source width, $R = 2$ fm, using the

NF50 potential model for the *two-range Gaussian* potential, Eq. (3.77), and the HKMYY potential model for the *three-range Gaussian* potential, Eq. (3.78), is shown in Figure 4.1. From these figures, it can be seen that the curve corresponding to the quantum statistics contribution goes below unity, which corresponds, in femtoscopy to a "repulsive" correlation, in association with the behavior of QS correlations between identical spin-1/2 fermions, as shown in Fig. 2.2. The strong interaction contribution goes above one, which is related to the attractive character of the NF50 and HKMYY potentials.

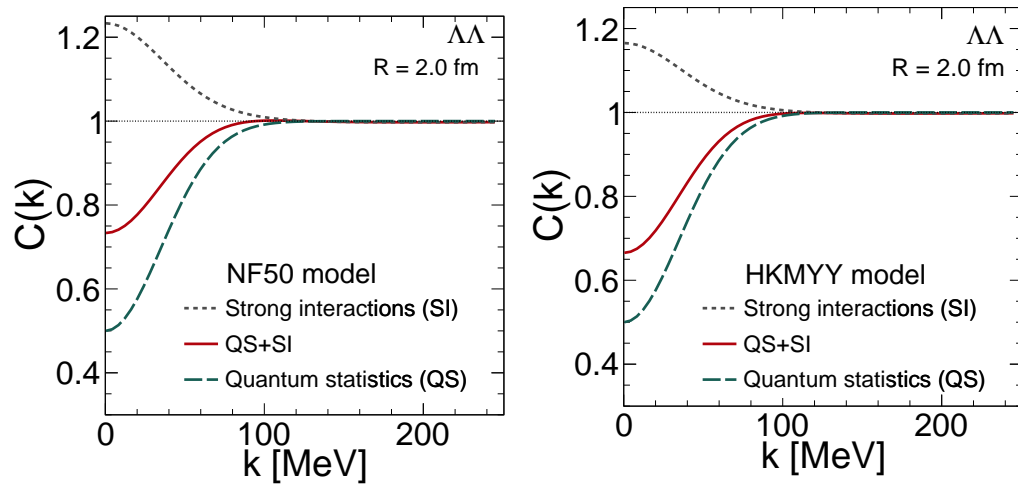


Figure 4.1: The contributions to the two-particle correlation function contributions for $\Lambda\Lambda$ particles, from strong interaction (grey, short dashed line), total (red, full line) and quantum statistics (green, long dashed line), shown as a function of the momentum k , using the NF50 model (left) and HKMYY model (right).

As discussed in Chapter 3, the expression for the $\Lambda\Lambda$ potential can be easily transformed into the momentum space, and then inserted in the Lippmann-Schwinger equation to extract the scattered wave function and, subsequently, the two-particle correlation function. Therefore, through this double application can be used to validate both codes, as can be seen in Figure 4.2. Notice that in Figure 4.2 the curves are in agreement with the results that are shown in Refs. [29, 36].

From Fig. 4.2, can be seen that the curves from the code that solves the Schrödinger and Lippmann-Schwinger equations are in agreement, showing that the LS code reproduces well the results from the Schr code, such as the scattering observables in Table 4.1, and then can be used to elaborate some predictions, as will be done in the Sec. 4.2, for the case of the D^0D^0 , $\bar{D}^0\bar{D}^0$ correlation, since, in

this case, the potential model depends on a non-local potential part.

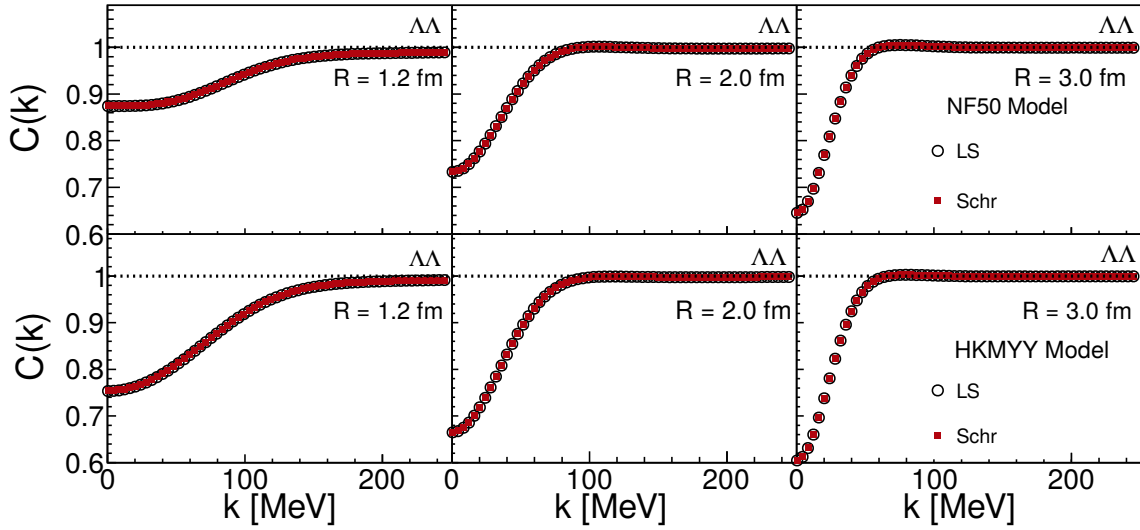


Figure 4.2: Comparison of numerical results for the correlation function from the code that solves the Lippmann-Schwinger equation, LS (black, empty circle dots), and the code that solves the Schrödinger equation, Schr (red, square dots), as a function of the relative momentum k of the $\Lambda\Lambda$ pair, using the NF50 model (top plot) and the HKMYY model (bottom plot) for three values of source width R .

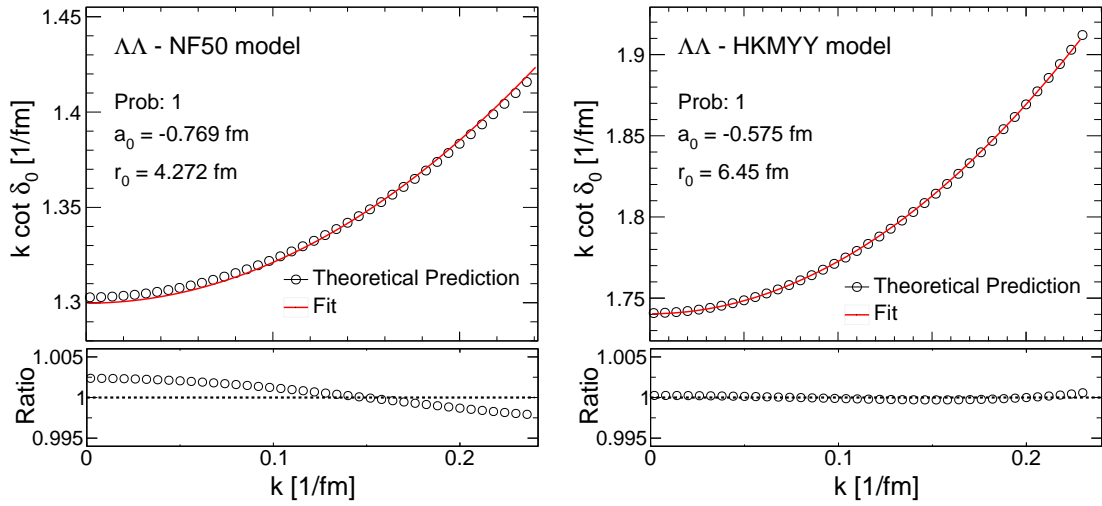
Another way to verify if the results from the two codes agree with each other is to obtain the *scattering observables*, which are the phase shift δ_0 , the scattering length a_0 and the effective range r_0 . The phase shift can be obtained from Eq. (3.24) for the code using the Schrödinger equation and from Eq. (3.57) for the code using Lippmann-Schwinger equation; a_0 and r_0 can be extracted from the effective range expansion (ERE) as

$$k \cot \delta_0 \approx -\frac{1}{a_0} + \frac{1}{2}r_0k^2. \quad (4.3)$$

Therefore, considering different values of δ_0 for different momenta k , it is possible to fit the right-hand side of the above equation. As an illustration, a fit was performed using the NF50 and the HKMYY models, as shown in Figure 4.3. The results are compatible with those in Ref. [29], which are reproduced in Table 4.1.

Table 4.1: Scattering observables from the calculations of Ref. [29] and from the calculations of the present work.

NF50 model			
	Morita et al. [29]	Schr Code	LS Code
a_0 (fm)	-0.772	-0.769	-0.769
r_0 (fm)	4.27	4.27	4.27
HKMYY model			
	Morita et al. [29]	Schr Code	LS Code
a_0 (fm)	-0.575	-0.575	-0.575
r_0 (fm)	6.45	6.45	6.45

Figure 4.3: Comparison of the fit adjusting the parameters on the right-hand side of Eq. (4.3) (red, full line) and the numerical results evaluated using the left-hand side of the same equation (black, dots), as a function of the relative momentum k for $\Lambda\Lambda$ pair using the NF50 model (left plot) and the HKMYY model (right plot).

The $\Lambda\Lambda$ femtoscopic correlations are still an exploratory subject in the field, although there are some experimental data that can guide the theoretical models to describe this interaction. One of them was performed by the STAR collaboration at RHIC, in AuAu collisions at $\sqrt{s_{NN}} = 200$ GeV. For comparing the numerical results with data it is necessary to take into account the λ factor, as it was done in Eqs. (2.44) and (2.97). The expression used by the STAR collaboration to obtain

the fitted parameters, for the scattering observables, is [41]

$$\begin{aligned}
C_{\text{STAR}}(k) = & \text{N} \left\{ 1 + \lambda \left[-\frac{1}{2} e^{-4k^2 R^2} + \frac{|f_0(k)|^2}{4R^2} \left(1 - \frac{r_0}{2\sqrt{\pi R}} \right) \right. \right. \\
& + \left. \frac{\text{Re} f_0(k)}{\sqrt{\pi R}} F_1(2kr) - \frac{\text{Im} f_0(k)}{2R} F_2(2kR) \right] \\
& \left. + a_{\text{res}} \exp \left[-4k^2 r_{\text{res}}^2 \right] \right\}, \tag{4.4}
\end{aligned}$$

where $\text{N} = 1.006 \pm 0.001$, $\lambda = 0.18 \pm 0.05$, $R = 2.96 \pm 0.38$ fm. The last term in the above expression is called *negative residual correlation* and is needed because of some small k discrepancies observed between the previous expression with data, possibly caused by decaying parents. The values for the parameters of this additional term are: $a_{\text{res}} = -0.044 \pm 0.004$ fm and $r_{\text{res}} = 0.04 \pm 0.43$ fm. Then, to compare the data from STAR collaboration to the numerical results of the present work, shown in Fig. 4.4, Eq. (2.101) is rewritten as

$$\begin{aligned}
C(k) = & \text{N} \left\{ 1 + \lambda \left[-\frac{1}{2} e^{-4k^2 R^2} + \frac{1}{2} \int d^3r S(r) \left(|\psi_0(k, r)|^2 - j_0^2(kr) \right) \right] \right. \\
& \left. + a_{\text{res}} \exp \left[-4k^2 r_{\text{res}}^2 \right] \right\}. \tag{4.5}
\end{aligned}$$

Also a study using Ref. [29] was performed, which the authors indicated that the value of λ proposed by the STAR collaboration should it be reviewed, considering effects of dacaying particles, the corrected value is $\lambda = (0.67)^2$ and the comparison it is show in Fig. 4.4.

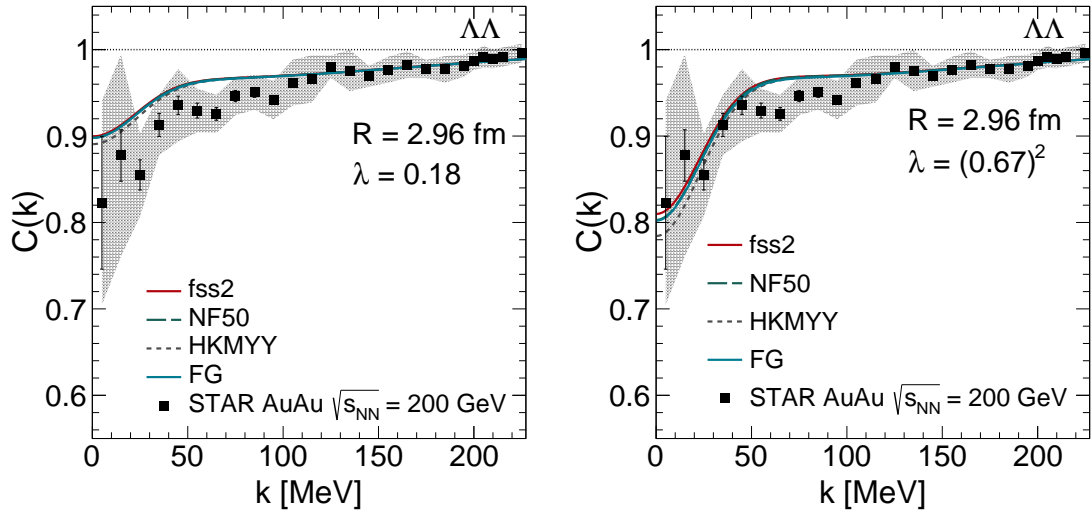


Figure 4.4: Comparison of the numerical results for the correlation function from Eq. (4.5), calculated in the present work using four potential models: fss2 (red, full line), NF50 (green, long dashed line), HKMYY (grey, short dashed line), FG (blue, full line), with $\lambda = 0.18$ (left plot), from Ref. [41], and $\lambda = (0.67)^2$ (right plot), from Ref. [29], and the data from STAR collaboration (black, dots) measured in AuAu collisions at $\sqrt{s_{NN}} = 200$ GeV [41].

More recent experimental data are available from pp collisions at $\sqrt{s_{NN}} = 13$ TeV and pPb collisions at $\sqrt{s_{NN}} = 5.02$ TeV obtained by the ALICE collaboration at the LHC [42]. To compare this data to the numerical results of the present work, shown in Figure 4.5, Eq. (2.101) is rewritten as

$$C(k) = 1 + \lambda \left[-\frac{1}{2} e^{-4k^2 R^2} + \frac{1}{2} \int d^3 r S(r) \left(|\psi_0(k, r)|^2 - j_0^2(kr) \right) \right] \quad (4.6)$$

where $\lambda = 0.338$ and $R = 1.182$ fm for pp collisions and $\lambda = 0.239$ and $R = 1.427$ fm for pPb collisions.

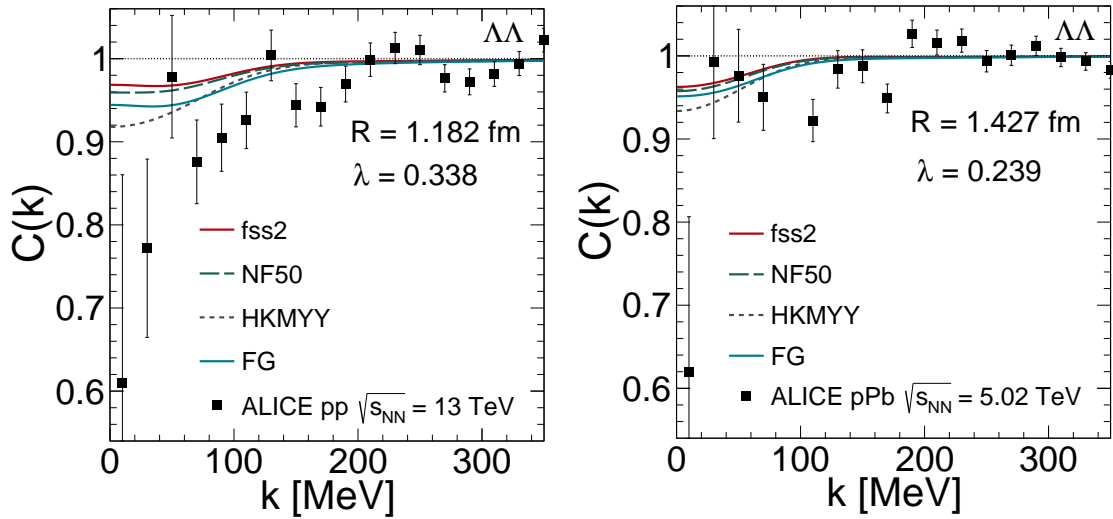


Figure 4.5: Comparison of the numerical results for the correlation function from Eq. (4.6), calculated in the present work using four distinct potential models: fss2 (red, full line), NF50 (green, long dashed line), HKMY (grey, short dashed line), FG (blue, full line) and the data from ALICE collaboration (black, square dots) measured in pp collisions at $\sqrt{s_{NN}} = 13$ TeV (left) and in pPb collisions at $\sqrt{s_{NN}} = 5.02$ TeV (right) [42].

Figures 4.4 and 4.5 show that the numerical results for the potential models that characterize the $\Lambda\Lambda$ correlation describe the overall behavior of experimental points of the correlation function. This is more evident for the pair relative momentum above ~ 150 MeV.

4.1.2 $p\Lambda$ correlation

The $p\Lambda$ correlation function can be obtained by the two-particle correlation function for non-identical spin- $1/2$ fermions derived in Chapter 2, as described in Eq. (2.103). In this case, the only contribution comes from the strong interaction (SI), with a singlet state ($S = 0$) term and a triplet state ($S = 1$) term,

$$C(k) = 1 + 4\pi \left[\left(\frac{1}{4}\right) \int_0^\infty dr r^2 S(r) \left(|\psi_0^S(k, r)|^2 - j_0^2(kr) \right) + \left(\frac{3}{4}\right) \int_0^\infty dr r^2 S(r) \left(|\psi_0^S(k, r)|^2 - j_0^2(kr) \right) \right]. \quad (4.7)$$

The contributions for three values of source width, R , using the Usmani potential, Eq. (3.85) and Eq. (3.86), are shown in Figure 4.6. Notice that the curves are in agreement with the correlation function results shown in Ref. [36].

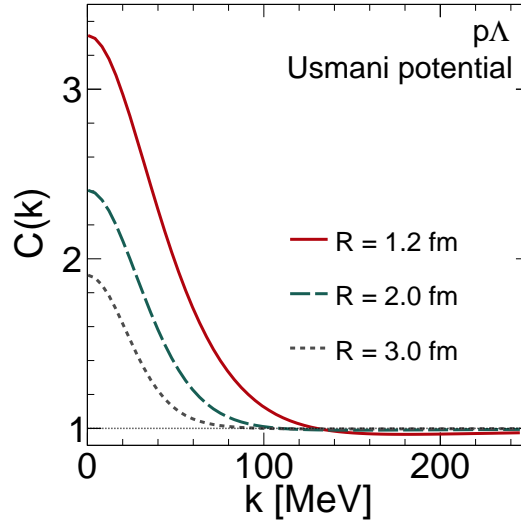


Figure 4.6: Two-particle correlation function for $p\Lambda$ particles for three values of the source width, $R = 1.2$ fm (red, full line), $R = 2.0$ fm (green, long dashed line) and $R = 3.0$ fm (grey, short dashed line), as a function of the relative momentum k , using the Usmani potential.

Similarly to what was done in the previous section, another important test for the code developed in this work is to obtain the scattering observables using expression (4.3). To illustrate that a fit was performed using the Usmani potential, shown in Figure 4.7. The results are compatible with those in Ref. [36], which are

reproduced in Table 4.2.

Table 4.2: Scattering observables for the results of Ref. [36] and for the results of the present work.

1S_0 channel		
	Mihaylov et al. [36]	Schr Code
a_0 (fm)	-2.88	-2.88
r_0 (fm)	2.92	2.92
3S_1 channel		
	Mihaylov et al. [36]	Schr Code
a_0 (fm)	-1.66	-1.66
r_0 (fm)	3.78	3.78

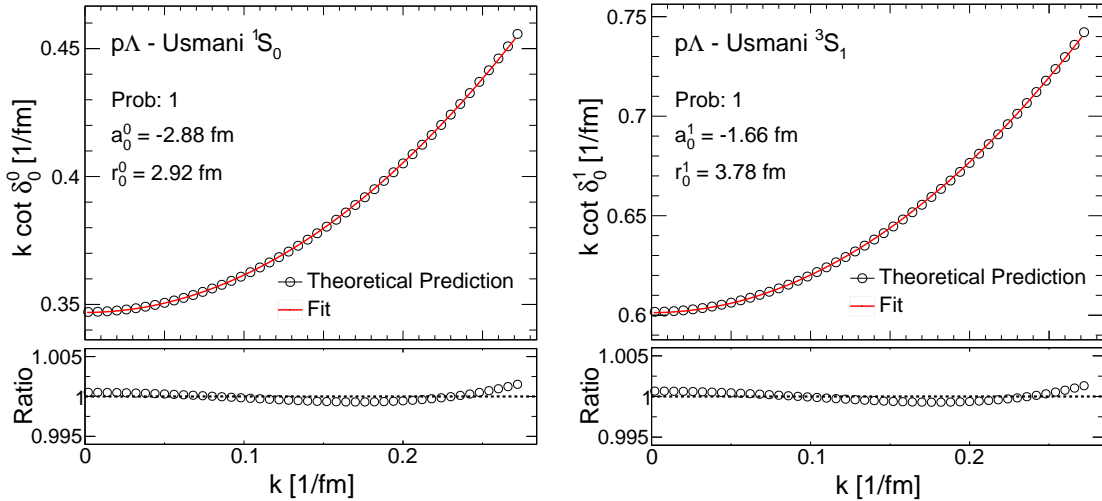


Figure 4.7: Comparison of the fit adjusting the parameters on the right-hand side of Eq. (4.3) (red, full line) and the numerical results evaluated using the left-hand side of the same equation (black, dots) as a function of the relative momentum k , for $p\Lambda$ particles, using the Usmani singlet term (left) and the Usmani triplet term (right).

Figure 4.8 shows the results from a study comparing the numerical calculations from the code that solves the Schrödinger equation and those corresponding to the expression of the Lednicky-Lyuboshitz (LL) model, in Eq. (2.80), for which the scattering observables were extracted from the fit to Figure 4.7 and using the parameters in Table 4.2. As expected, the LL model reproduce better the curve corresponding to higher value of the source width R , since the model is an approximation and one of the constraints is that $R \geq r_0$.

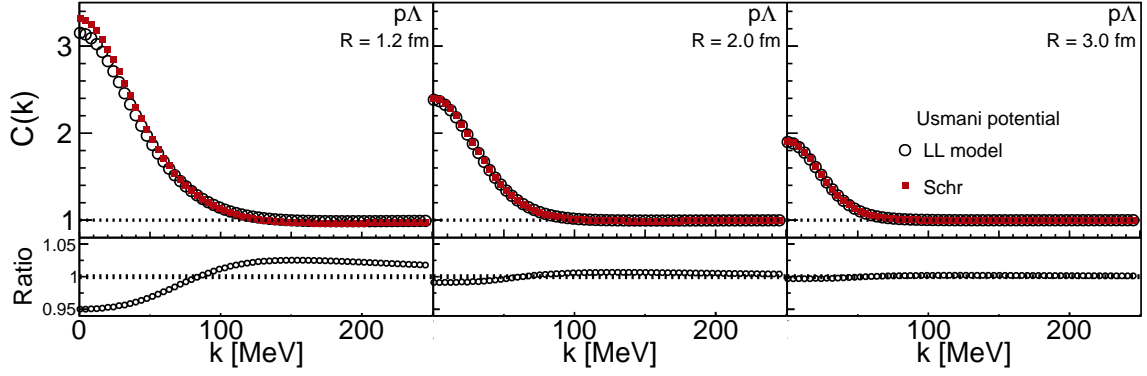


Figure 4.8: Comparison of the results for the correlation function from the code that solves the Schrödinger equation (red, dots) and those corresponding to the expression of the LL model (black, dots), as a function of the relative momentum k .

To compare the $p\Lambda$ correlation obtained from the numerical results of the present work, the experimental data from the ALICE collaboration in pp collisions at $\sqrt{s_{NN}} = 7$ TeV [43] was used. In this case, it is necessary to take into account the λ factor, as it was done in Eqs. (2.44) and (2.97), and Eq. (2.103) is rewritten as

$$C(k) = 1 + \lambda \left[4\pi \sum_S \rho_S \int d^3r S(r) \left(|\psi_0^S(k, r)|^2 - j_0^2(kr) \right) \right] \quad (4.8)$$

where $\lambda = 0.4713$ fm and $R = 1.125$ fm. The comparison of the results from the calculation correlation function and the corresponding experimental data points is shown in Figure 4.9.

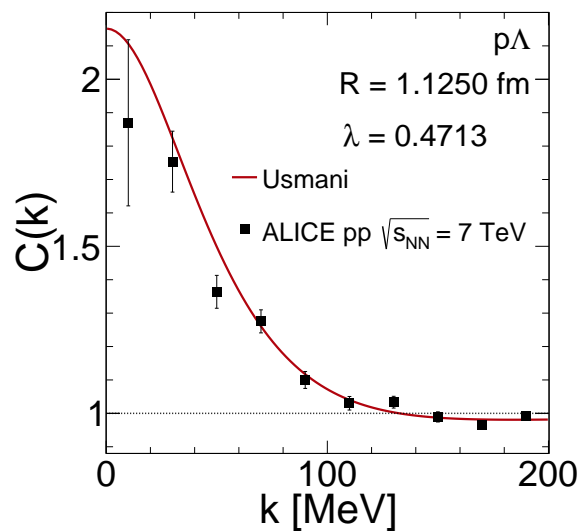


Figure 4.9: Comparison of the numerical results for the correlation function from Eq. (4.8), calculated in the present work using Usmani potential (red, full line) and the data points from ALICE collaboration (black, dots) for pp collisions at $\sqrt{s_{NN}} = 7$ TeV [43].

4.2 $D^0D^0, \bar{D}^0\bar{D}^0$ correlation

The femtosopic correlation function for D^0D^0 and $\bar{D}^0\bar{D}^0$ pairs can be obtained from the two-particle correlation function for identical bosons derived in Chapter 2, described by Eq. (2.102). In this expression, the quantum statistics (QS) contribution is written as

$$C_{\text{QS}}(k) = 1 + e^{-4k^2R^2}, \quad (4.9)$$

and the strong interaction (SI) contribution is written as

$$C_{\text{SI}}(k) = 1 + 8\pi \int_0^\infty dr r^2 S(r) \left[|\psi_0(k, r)|^2 - j_0^2(kr) \right], \quad (4.10)$$

where the total contribution (QS+SI) is explicit in Eq. (2.102). Since there is no theoretical or experimental guidelines in femtoscopy for $D^0D^0, \bar{D}^0\bar{D}^0$ correlation, in Fig. 4.10 a comparative plot was made for the strong interactions contributions to the femtosopic correlation function for a fixed value of source width, $R = 1.5$ fm, using the spin-spin plus long-range terms of the potential V_{hyp} plus $V_{\text{long-range}}$ in Eq. (3.101), the spin-spin term only V_{hyp} in Eq. (3.102), and the long-range term only $V_{\text{long-range}}$ in Eq. (3.103). The effect of the attractive character of the long-range potential in the correlation function tries to push the SI contribution to go greater than one, however the spin-spin term is still dominant under the SI contribution for the correlation function, as it can be seen in the red curve in Fig. 4.10. Because of that, in Fig. 4.11, the comparison will only be performed using the spin-spin plus long-range terms of the potential V_{hyp} plus $V_{\text{long-range}}$ in Eq. (3.101), and the spin-spin term of the potential V_{hyp} in Eq. (3.102).

The investigation of the femtosopic correlation function sensitivity to the potential terms was extended to different values of the source width, R . The results shown in Figure 4.12 for three values of R were obtained using the spin-spin plus long-range terms of the potential, V_{hyp} plus $V_{\text{long-range}}$, whereas those shown in Figure 4.13 were obtained only considering the spin-spin term of the potential V_{hyp} .

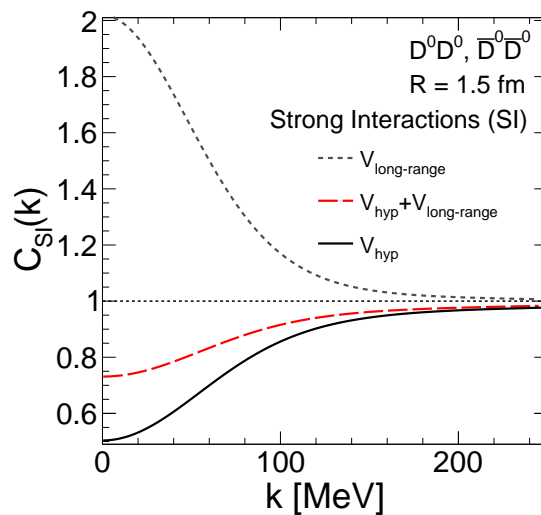


Figure 4.10: The strong interactions (SI) contribution for the femtoscopic correlation function of $D^0 D^0, \bar{D}^0 \bar{D}^0$ as a function of the relative momentum k , when considering as a potential with the long-range term (grey, short dashed line), spin-spin plus long-range term (red, long dashed line), $V_{\text{hyp}} + V_{\text{long-range}}$, and the spin-spin term only (black, full line), V_{hyp} .

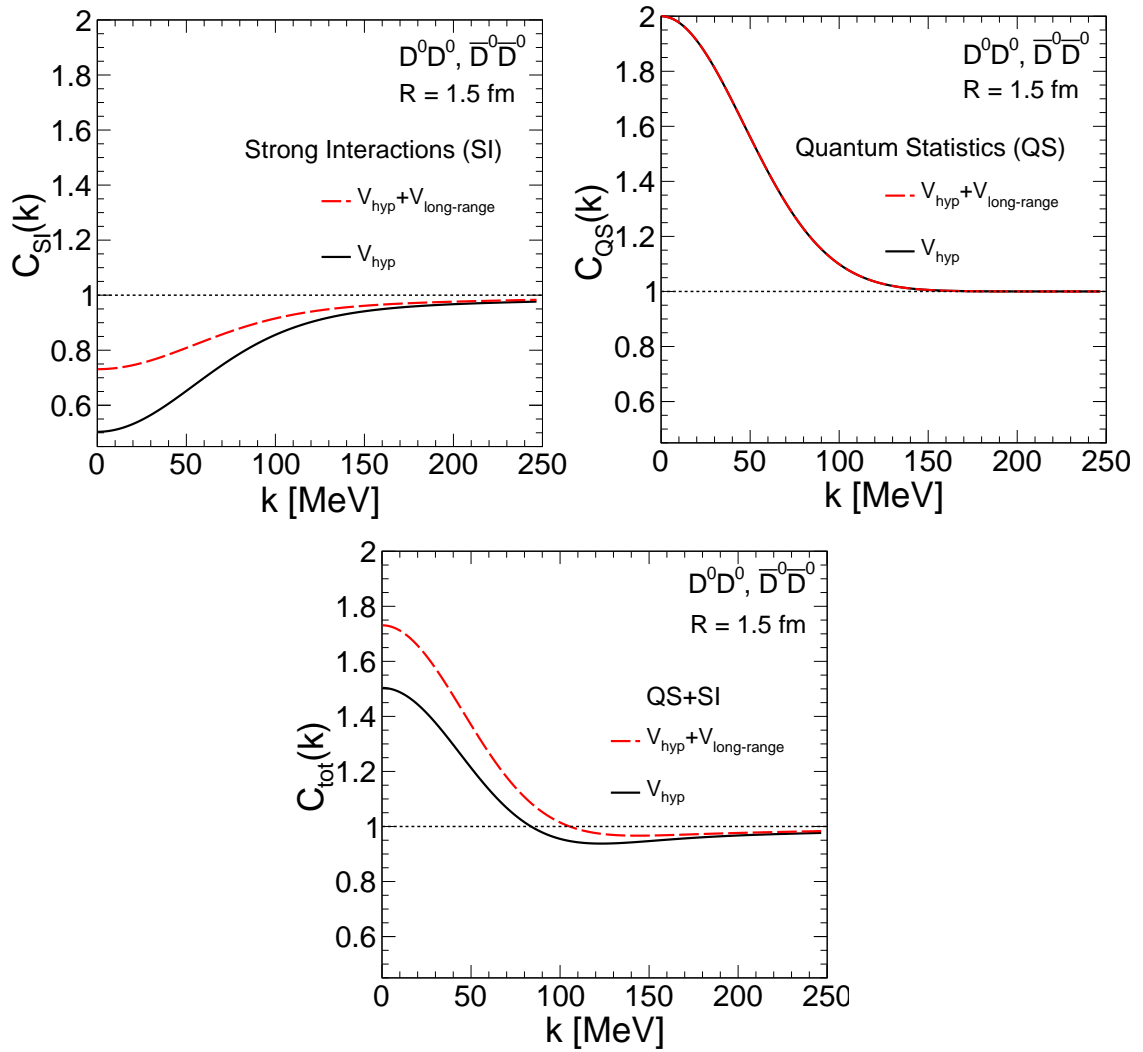


Figure 4.11: Femsoscopic correlation function of $D^0 D^0$, $D^0 \bar{D}^0$ as a function of the relative momentum k , when considering as a potential with the spin-spin plus long-range term (red, long dashed line), $V_{\text{hyp}} + V_{\text{long-range}}$, and the spin-spin term only (black, full line), V_{hyp} . The top left plot shows the strong interaction (SI) contribution, the one on the top right shows the quantum statistics (QS) contribution and, finally, the bottom plot shows the total correlation function (QS+SI) contribution.

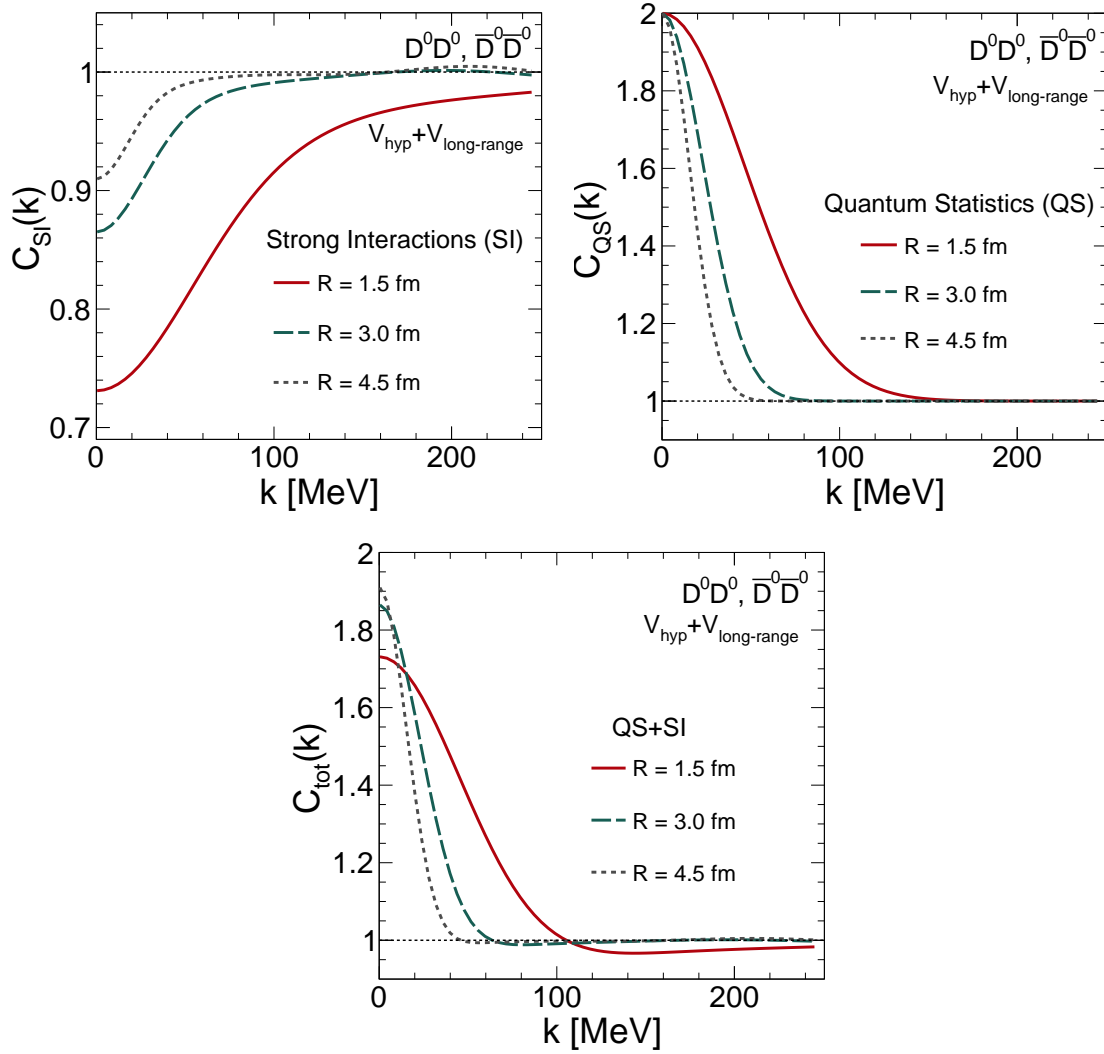


Figure 4.12: $D^0 D^0, \bar{D}^0 D^0$ correlation function versus the relative momentum for $R = 1.5$ fm (red, full line), $R = 3.0$ fm (green, long dashed line) and $R = 4.5$ fm (grey, short dashed line), considering the meson-meson potential with the spin-spin plus long-range terms. The plot on the top left shows the SI contribution, the one on the top right shows the QS contribution and the one on the bottom corresponds to the joint QS+SI contribution.

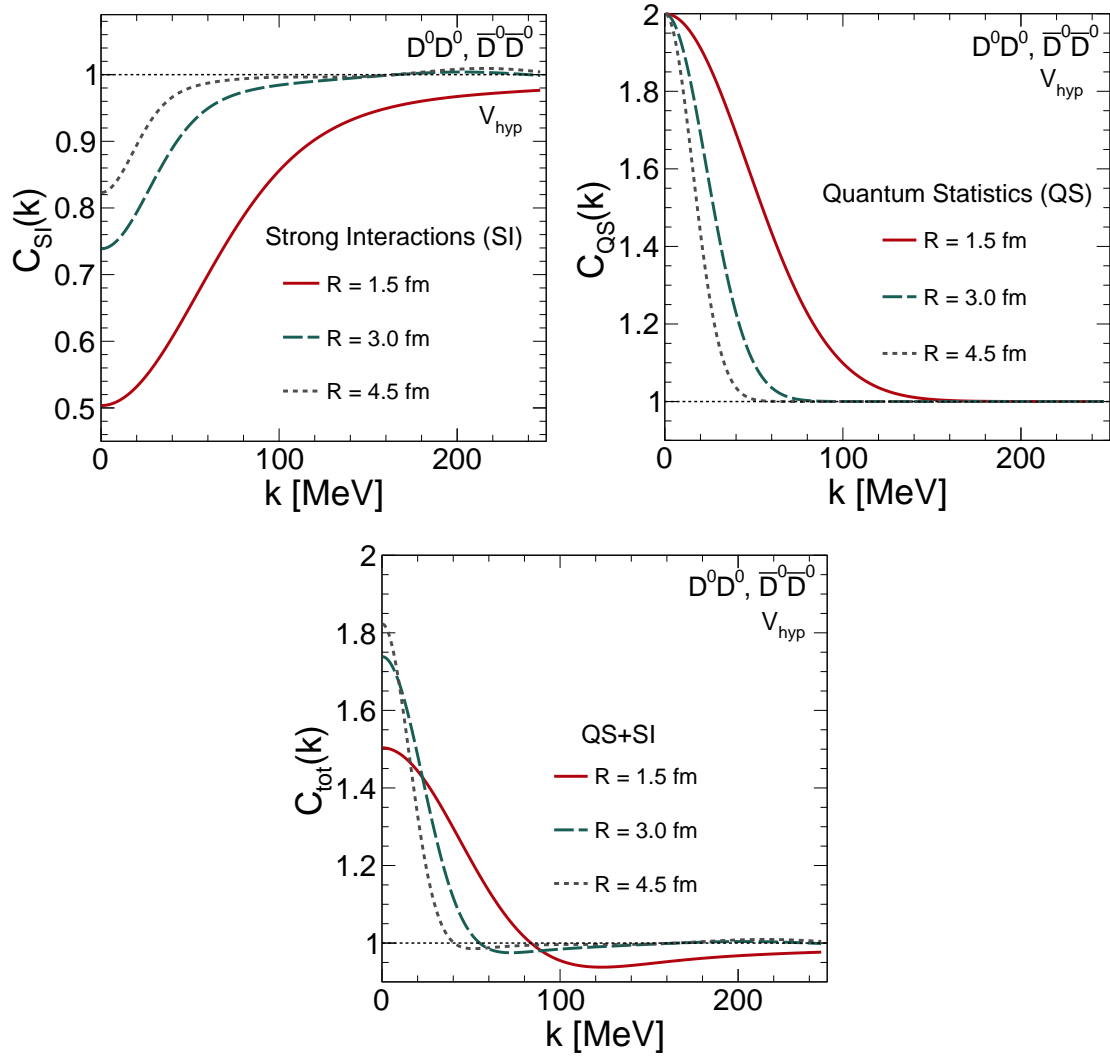


Figure 4.13: $D^0 D^0, \bar{D}^0 \bar{D}^0$ correlation function versus the relative momentum for $R = 1.5$ fm (red, full line), $R = 3.0$ fm (green, long dashed line) and $R = 4.5$ fm (grey, short dashed line), for the meson-meson potential with the spin-spin term only. The plot on the top left shows the SI contribution, the one on the top right the QS contribution, and the one on the bottom corresponds to the joint QS+SI contribution.

In Fig. 4.14, the plots containing the quantum statistics, strong interaction and total contributions of $C(k)$ for two values of source width, $R = 1.5$ fm and $R = 3.0$ fm, are displayed. It can be seen that the strong interaction has a more visible effect for a smaller value of R , as well as in Figures 4.12 and 4.13 because, for smaller values of the source width, the probability of the particles being emitted from closer points is larger and more likely the relative distance of the particles is smaller, where the short-range contribution of the potential predominates, resulting in a more pronounced effect on the particles correlation.

From these figures, it can be seen that the curve corresponding to the quantum statistics contribution goes above one, that, in femtoscopy it is referred to as an "attractive" correlation, in association with the behavior of QS correlations between identical mesons, as it was shown in Fig. 2.2. As can also be seen, the width of the Gaussian curve for the QS contribution is smaller for lower values of inverse R .

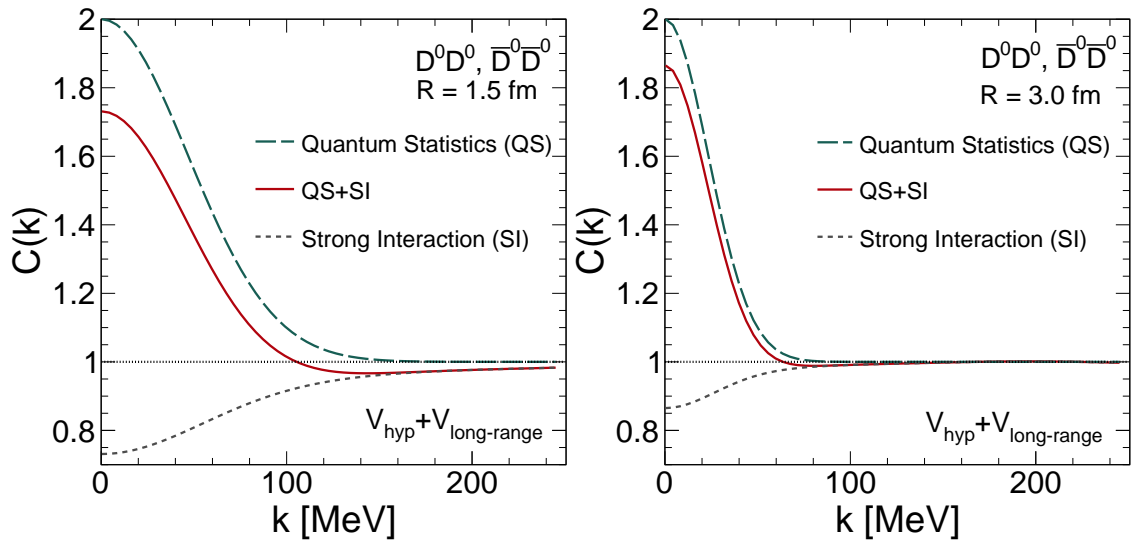


Figure 4.14: The two-particle correlation function contributions for $D^0 D^0, \bar{D}^0 \bar{D}^0$ that includes $V_{\text{hyp}} + V_{\text{long-range}}$ terms, from strong interaction (grey, short dashed line), total (red, full line) and quantum statistics (green, long dashed line) are shown as a function of the momentum k , using the source width as $R = 1.5$ fm (left) and $R = 3.0$ fm (right).

As it was done in the previous section, an interesting result is to obtain the scattering observables. For the case of the meson-meson potential, it is interesting to explore the values for the phase shift δ_0 as a connection with the experiment, as can be seen in Figure 4.15. A fit was performed using the effective range expansion for the meson-meson potential, Eq. (3.101), with the contributions from the spin-

spin plus long-range terms and the parameters scattering length $a_0 = 0.182$ fm and effective range $r_0 = 2.445$ fm was obtained, and is shown in Figure 4.16.

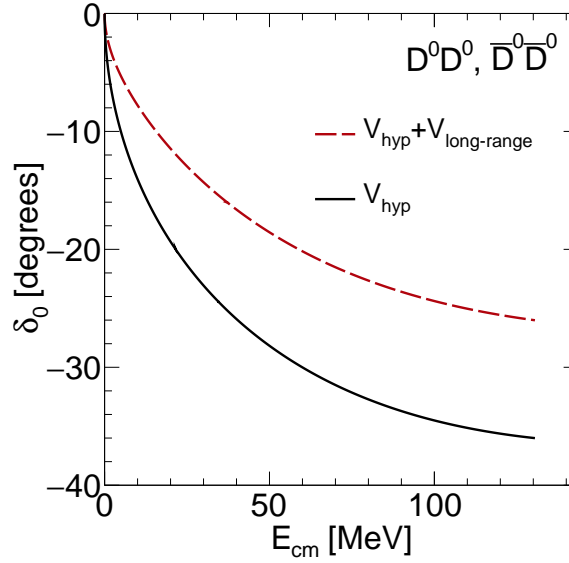


Figure 4.15: Comparison of the phase shift, as a function of the center-of-mass energy E_{cm} , of the D^0D^0 pair using the spin plus long-range term of the meson-meson potential (red, dashed line) and only the spin term of the meson-meson potential (black, full line).

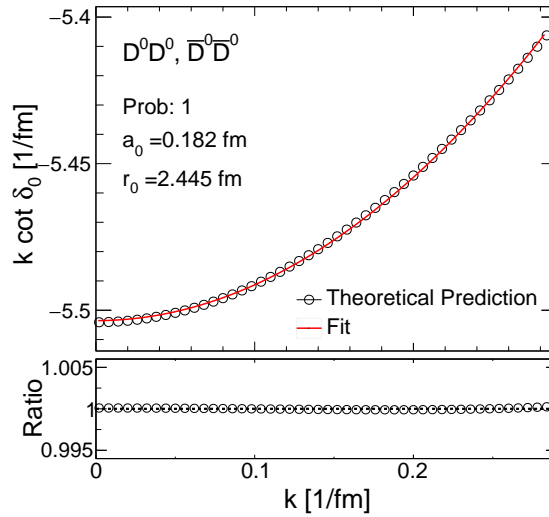


Figure 4.16: Comparison of the fit of the right-hand side to Eq. (4.3) (red, full line) and the numerical results evaluated using the left-hand side of the same equation (black, dots) as a function of the relative momentum k for D^0 particles.

In Figures 4.17 and 4.18, a study to compare the numerical results from

the code that solves the Lippmann-Schwinger equation (LS) and the one for the expression of the Lednicky-Lyuboshitz model (LL) was performed. An important point to remember is that the LL model is an approximation and has some constraints to take into account. One of them is to impose the correction term $\Delta C(k) = -\frac{r_0}{4\sqrt{\pi}R^3}|f_0(k)|^2$, Eq. (2.77), for the region where $V \neq 0$ (or non-asymptotic region). In Figure 4.17, a comparison of Eq. (2.96), with and without the correction $\Delta C(k)$ was performed, using the scattering amplitude written in terms of the effective range expansion (ERE), Eq. (2.79), which can be obtained using the scattering observables extracted from the fit of Figure 4.16. For low values of k , the LL model with the correction approximates better results from the LS approach, than the one without $\Delta C(k)$. As expected, and it was also shown in Figure 4.8 for the $p\Lambda$ case, the Lednicky-Lyuboshitz model reproduces better the curve for the higher value of the source width R , since one of the constraints that needs to be fulfilled is that $R \geq r_0$.

In Figure 4.18, a comparison of Eq. (2.96) without the correction $\Delta C(k)$, but using the scattering amplitude with the effective range expansion, as in Eq. (2.79), and without it, as in Eq. (2.78), since, the expansion has some limits [44]. As it can be seen both expressions are comparable, showing that the fit performed in Figure 4.16 returns satisfactory results.

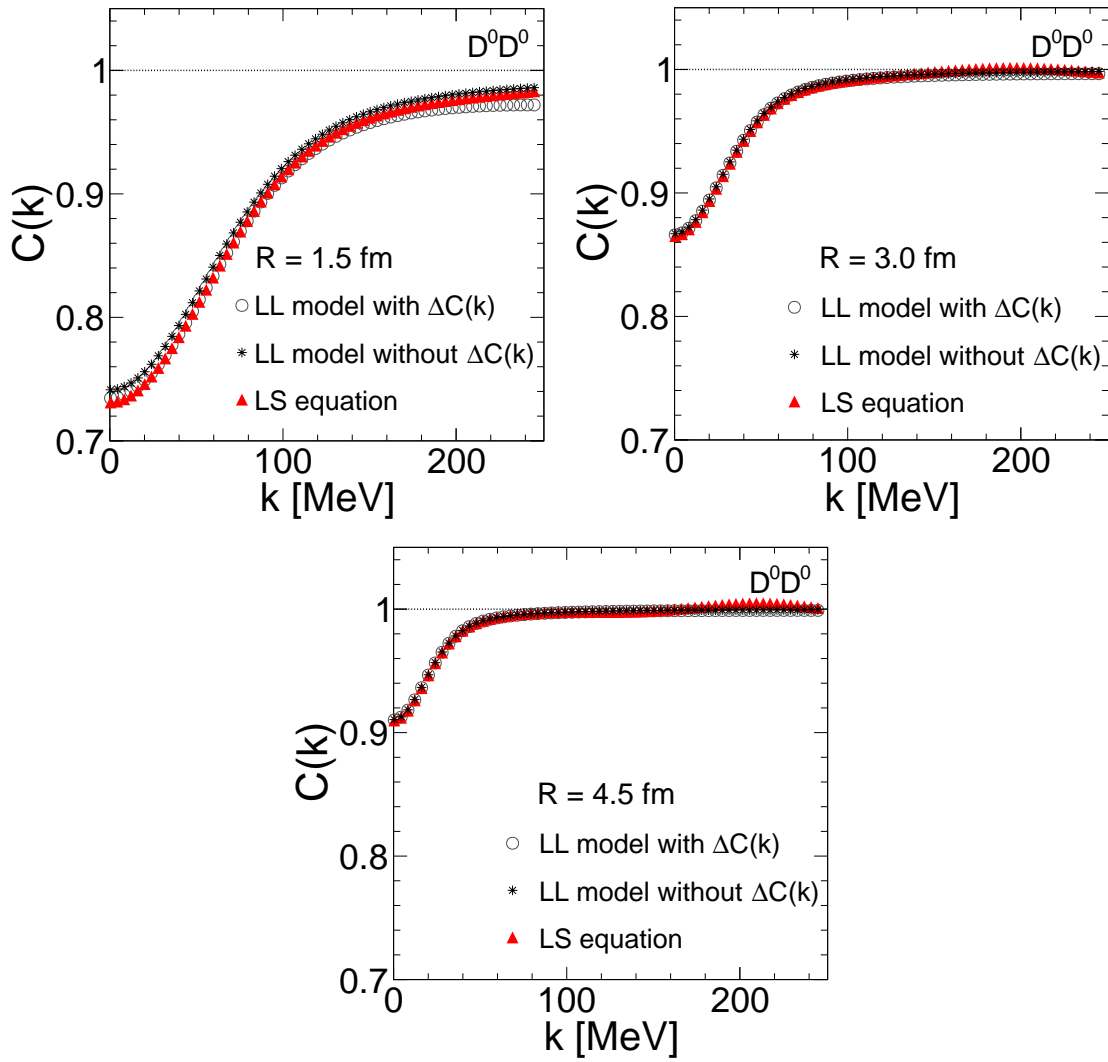


Figure 4.17: $D^0 D^0$, $\bar{D}^0 \bar{D}^0$ correlation function for $R = 1.5$ fm (top left plot), $R = 3.0$ fm (top right plot), $R = 4.5$ fm (bottom plot). The LL model with the correction $\Delta C(k)$ (grey, empty circle dots), the LL model without the correction $\Delta C(k)$ (black, asterisk dots) and the correlation function obtain from the LS equation code (red, triangle dots) are shown.

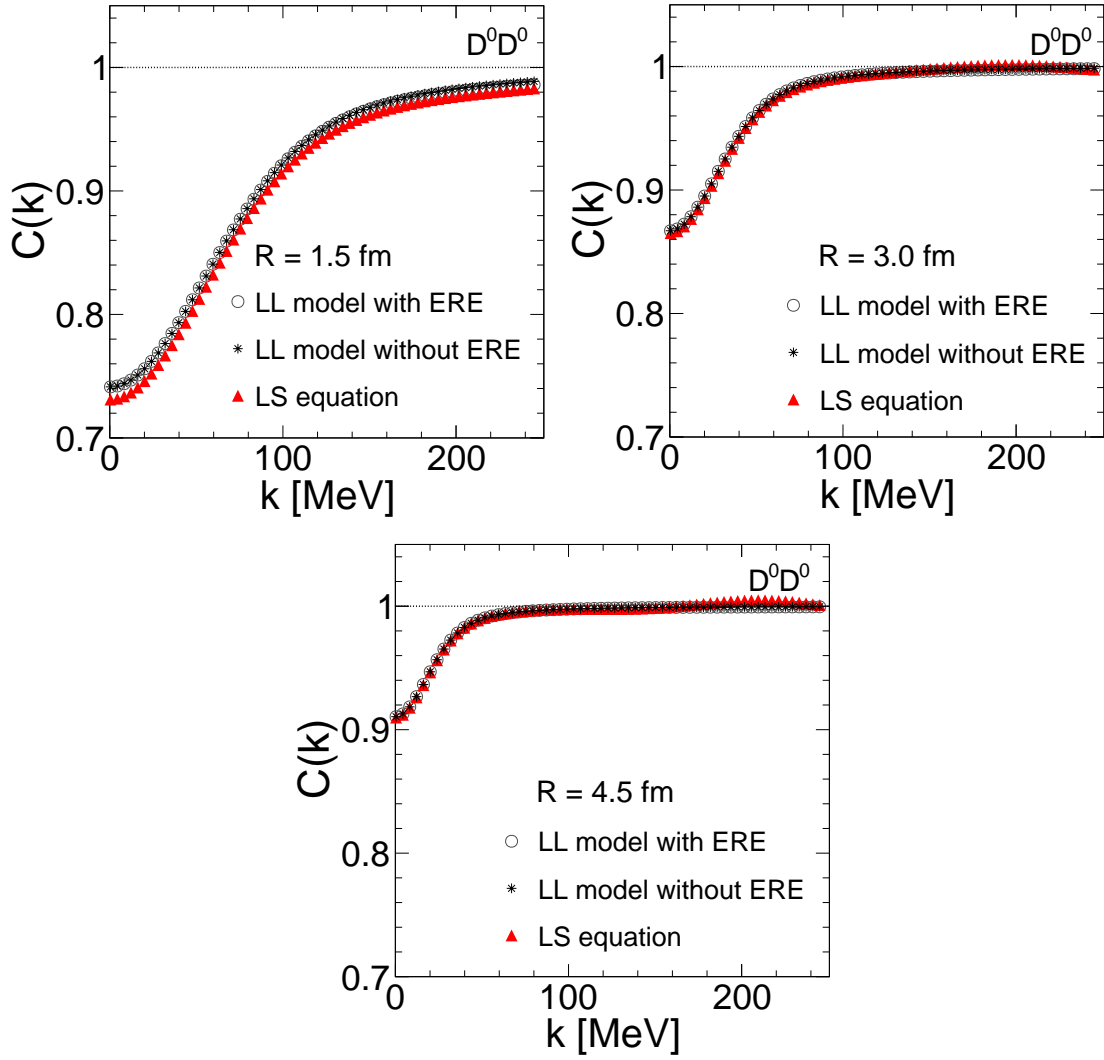


Figure 4.18: $D^0 D^0$, $\bar{D}^0 \bar{D}^0$ correlation function for $R = 1.5$ fm, top left, $R = 3.0$ fm, top right, $R = 4.5$ fm, bottom. Each plot is composed by the LL model without $\Delta C(k)$ and using the effective range expansion (ERE) (grey, empty circle dots), the LL model without $\Delta C(k)$ and without ERE (black, asterisk dots), and the correlation function obtained from the LS equation code (red, triangle dots).

In this Chapter, a study of a femtoscopic the $D^0 D^0$, $\bar{D}^0 \bar{D}^0$ correlations was performed with the contribution from the strong interactions was considering by using a meson-meson potential from a quark model [37, 38], as shown in Sec. (3.4.3). The effect is more visible for smaller values of source width R . Also, the scattering observables were obtained and used to perform a study in the limitation of the Lednicky-Lyuboshitz model.

Chapter 5

Conclusions and final remarks

Femtoscopy is known as a powerful tool to investigate the space-time dimensions of the region from which particles are emitted, in high energy collisions. Although originally derived for identical particle quantum statistics correlations, it is sensitive not only to quantum statistics, but also to final state interactions, such as Coulomb interactions, when considering charged particles and strong interactions between hadrons. In this work, femtoscopic correlations using identical and non-identical particles were studied and different contributions to the correlation function were derived.

In theoretical calculations the two-particle correlation function $C(k)$ can be approximated by a spatial integral over a source function and the norm squared of the total wave function $\Psi(\mathbf{k}, \mathbf{r})$ of the correlating particles. Therefore the first step in this study was to obtain numerically the total pair correlation function. For this purpose a code to solve the Schrödinger equation was developed for interactions with a local potential. The validation of this code was performed using two types of correlating pairs $p\Lambda$ and $\Lambda\Lambda$. Such correlations were measured by the ALICE collaborations at the LHC, and by the STAR collaboration at RHIC. The results of the calculations were then compared with those data and also with other theoretical results that are already in the literature. From the code for solving the Schrödinger equation the comparison of the numerically obtained correlation functions in the $p\Lambda$ and $\Lambda\Lambda$ cases are in agreement. Also, the comparison of the scattering observables obtained in this work with the ones in the literature mainly shows less than 0.5% of percentage error.

The absence of experimental data and theoretical description of D^0D^0 and $\bar{D}^0\bar{D}^0$ correlations motivated the development of a code that solves the Lippmann-Schwinger equation with a non-local potential to obtain the scattered wave function and, afterwards, the respective two-particle correlation function. The D^0 particles are an interesting object of study, as it is composed of a light quark u and

heavy quark c . Therefore, it can be employed to study heavy particle correlations and to instigate the investigation of new exotic bound states of matter as for example, molecular states. To certify that the code that solves the Lippmann-Schwinger equation was working properly, a validation was performed using the results obtained in this work for $\Lambda\Lambda$ particles correlations, using the code that solves the Schrödinger equation, with those obtained for the Lippmann-Schwinger equation.

The results obtained for D^0D^0 and $\bar{D}^0\bar{D}^0$ correlations show that the quantum statistics contribution reproduces the behavior of QS correlations between identical spin-zero bosons, since it is expected that the correlation function goes above one, which in femtoscopy is called an "attractive" correlation. It was shown that the effect of the strong interaction is more significant at smaller values of R , since the probability of emission of the particles from closer points is larger and more likely the relative distance of the pair is smaller, where the short-range contribution of the potential predominates.

In the development of this work, it was also possible to study the limitation of the Lednicky-Lyubulshitz model for describing final-state interactions and check its validity depending on the value of source size and inclusion of the correction term $\Delta C(k)$, using the scattering observables.

Finally, with this study, it was possible to show that femtoscopy can be used to study final-state interactions and give information about the shape of the particle correlation functions. Furthermore, the results in this work might be used for correlation studies of D^0D^0 and $\bar{D}^0\bar{D}^0$ in particle collider experiments, as a guideline. Regarding future perspectives of this work, other correlations could be studied to evaluate the efficiency of the quark model used in this dissertation, for instance, $K^+\bar{D}^0$ femtoscopic correlations, adjusting the parameters for the respective particles, such as the mesonic states and its constituent quarks. There is also the possibility to investigate D^0 mesons correlations using more complex descriptions, for example, potential models derived from effective field theory formalisms.

Appendix A

Elements of the meson-meson potential

In this Appendix, the calculations for the meson-meson potential, that are presented in Sec. 3.4.3, are shown in more detail, based on Sergio Szpigel's PhD Thesis [37] "*Interação Méson-méson no formalismo Fock-Tani*" and published in Ref. [38]. A hadronic interaction is mainly composed of a short-range and a long-range contribution. In this case, the short-range is equivalent to a contact interaction represented by a spin-spin term, and the long-range is described by a meson-exchange potential. In the following, the description of this two terms are divided in Secs. A.1 and A.2.

A.1 Short-range contribution

In Sec. 3.4.3, it was shown that for a meson-meson scattering, Eq. (3.87), the potential is given by a matrix element between the final and the initial state of the process, as it is done in Eq. (3.88). The evaluation of this previous expression results in six non-zero terms that is the contribution for the short-range interactions

$$\begin{aligned} V_{\text{mm}}^{\text{short-range}}(\alpha\beta; \gamma\delta) &= V^1(\alpha\beta; \gamma\delta) + V^2(\alpha\beta; \gamma\delta) + V^3(\alpha\beta; \gamma\delta) \\ &+ V^4(\alpha\beta; \gamma\delta) + V^5(\alpha\beta; \gamma\delta) + V^6(\alpha\beta; \gamma\delta), \end{aligned} \quad (\text{A.1})$$

where

$$V^j(\alpha\beta; \gamma\delta) = I_0^j I_{\text{spin}}^j(\alpha\beta; \gamma\delta) I_{\text{flavor}}^j(\alpha\beta; \gamma\delta) I_{\text{color}}^j(\alpha\beta; \gamma\delta) I_{\text{spatial}}^j(\alpha\beta; \gamma\delta). \quad (\text{A.2})$$

From Refs. [37] and [45] the I_j matrix elements are

$$\begin{aligned} I_0^1 &= I_0^2 = I_0^3 = I_0^4 = -\frac{1}{2}, \\ I_0^5 &= I_0^6 = -1. \end{aligned} \quad (\text{A.3})$$

$$\begin{aligned}
 I_{\text{color}}^1 &= I_{\text{color}}^2 = I_{\text{color}}^3 = I_{\text{color}}^4 = -\frac{4}{9}, \\
 I_{\text{color}}^5 &= I_{\text{color}}^6 = \frac{4}{9}.
 \end{aligned}
 \tag{A.4}$$

$$I_{\text{flavor}}^1 = I_{\text{flavor}}^2 = I_{\text{flavor}}^3 = I_{\text{flavor}}^4 = I_{\text{flavor}}^5 = I_{\text{flavor}}^6 = 1.
 \tag{A.5}$$

$$\begin{aligned}
 I_{\text{spin}}^1 &= I_{\text{spin}}^2 = I_{\text{spin}}^3 = I_{\text{spin}}^4 = -\frac{3}{8}, \\
 I_{\text{spin}}^5 &= I_{\text{spin}}^6 = \frac{3}{8}.
 \end{aligned}
 \tag{A.6}$$

The spatial factors are defined as [37]

$$I_{\text{spatial}}^j(\alpha\beta; \gamma\delta) = \langle P_\alpha P_\beta | \left(\hat{V}_{q\bar{Q}} + \hat{V}_{qq} + \hat{V}_{\bar{Q}\bar{Q}} \right) | P_\gamma P_\delta \rangle_j,
 \tag{A.7}$$

where $\hat{V}_{q\bar{Q}}$ is the quark-antiquark interaction term, \hat{V}_{qq} is the quark-quark interaction term and $\hat{V}_{\bar{Q}\bar{Q}}$ is the antiquark-antiquark term

$$\begin{aligned}
 \hat{V}_{q\bar{Q}} &= V(\mu\nu, \sigma\rho) q_\mu^\dagger \bar{Q}_\nu^\dagger \bar{Q}_\rho q_\sigma, \\
 \hat{V}_{qq} &= V(\mu\nu, \sigma\rho) q_\mu^\dagger q_\nu^\dagger q_\rho q_\sigma, \\
 \hat{V}_{\bar{Q}\bar{Q}} &= V(\mu\nu, \sigma\rho) \bar{Q}_\mu^\dagger \bar{Q}_\nu^\dagger \bar{Q}_\rho \bar{Q}_\sigma,
 \end{aligned}
 \tag{A.8}$$

$$V(\mu\nu, \sigma\rho) \Rightarrow \delta^{(3)}(\mathbf{p}'_1 + \mathbf{p}'_2 - \mathbf{p}_1 - \mathbf{p}_2) V(\mathbf{p}_1 - \mathbf{p}'_1).
 \tag{A.9}$$

The mesonic state is

$$|P_\alpha\rangle = \Phi_{\mathbf{P}_\alpha}^{\mu\nu} q_\mu^\dagger \bar{Q}_\nu^\dagger |0\rangle,
 \tag{A.10}$$

with q_μ^\dagger and \bar{Q}_ν^\dagger being the quark and antiquark creation operator, respectively and $\Phi_{\mathbf{P}_\alpha}^{\mu\nu}$ is the meson wave function.

The evaluation of Eq. (A.7) results in six principal terms that will represent the

short-range interactions

$$\begin{aligned}
 I_{\text{spatial}}^1(\alpha\beta; \gamma\delta) &= \Phi_{\alpha}^{*\mu'v'} \Phi_{\beta}^{*\mu\nu} V(\mu\nu, \sigma\rho) \Phi_{\gamma}^{\sigma\nu'} \Phi_{\delta}^{\mu'\rho}, \\
 I_{\text{spatial}}^2(\alpha\beta; \gamma\delta) &= \Phi_{\alpha}^{*\mu\nu} \Phi_{\beta}^{*\mu'v'} V(\mu\nu, \sigma\rho) \Phi_{\gamma}^{\mu'\rho} \Phi_{\delta}^{\sigma\nu'}, \\
 I_{\text{spatial}}^3(\alpha\beta; \gamma\delta) &= \Phi_{\alpha}^{*\mu\nu'} \Phi_{\beta}^{*\mu'v} V(\mu\nu, \sigma\rho) \Phi_{\gamma}^{\mu'v'} \Phi_{\delta}^{\sigma\rho}, \\
 I_{\text{spatial}}^4(\alpha\beta; \gamma\delta) &= \Phi_{\alpha}^{*\mu'v} \Phi_{\beta}^{*\mu\nu'} V(\mu\nu, \sigma\rho) \Phi_{\gamma}^{\sigma\rho} \Phi_{\delta}^{\mu'v'}, \\
 I_{\text{spatial}}^5(\alpha\beta; \gamma\delta) &= \Phi_{\alpha}^{*\mu\nu'} \Phi_{\beta}^{*\nu\rho'} V(\mu\nu, \sigma\rho) \Phi_{\gamma}^{\rho\nu'} \Phi_{\delta}^{\sigma\rho'}, \\
 I_{\text{spatial}}^6(\alpha\beta; \gamma\delta) &= \Phi_{\alpha}^{*\sigma'\mu} \Phi_{\beta}^{*\mu'v} V(\mu\nu, \sigma\rho) \Phi_{\gamma}^{\mu'\sigma} \Phi_{\delta}^{\sigma'\rho}.
 \end{aligned} \tag{A.11}$$

Expanding these expressions

$$\begin{aligned}
 I_{\text{spatial}}^1 &= \int d\mathbf{p}'_1 d\mathbf{p}'_2 d\mathbf{p}_1 d\mathbf{p}_2 d\mathbf{p}_3 d\mathbf{p}_4 \delta^{(3)}(\mathbf{p}'_1 + \mathbf{p}'_2 - \mathbf{p}_1 - \mathbf{p}_2) \\
 &\times \Phi_{\mathbf{P}_{\alpha}}^{*\mathbf{p}'_1\mathbf{p}'_2} \Phi_{\mathbf{P}_{\beta}}^{*\mathbf{p}_3\mathbf{p}_4} V(\mathbf{p}'_1 - \mathbf{p}_1) \Phi_{\mathbf{P}_{\delta}}^{\mathbf{p}_1\mathbf{p}_4} \Phi_{\mathbf{P}_{\gamma}}^{\mathbf{p}_3\mathbf{p}_2},
 \end{aligned} \tag{A.12}$$

$$\begin{aligned}
 I_{\text{spatial}}^2 &= \int d\mathbf{p}'_1 d\mathbf{p}'_2 d\mathbf{p}_1 d\mathbf{p}_2 d\mathbf{p}_3 d\mathbf{p}_4 \delta^{(3)}(\mathbf{p}'_1 + \mathbf{p}'_2 - \mathbf{p}_1 - \mathbf{p}_2) \\
 &\times \Phi_{\mathbf{P}_{\alpha}}^{*\mathbf{p}_3\mathbf{p}_4} \Phi_{\mathbf{P}_{\beta}}^{*\mathbf{p}'_1\mathbf{p}'_2} V(\mathbf{p}'_1 - \mathbf{p}_1) \Phi_{\mathbf{P}_{\delta}}^{\mathbf{p}_3\mathbf{p}_2} \Phi_{\mathbf{P}_{\gamma}}^{\mathbf{p}_1\mathbf{p}_4},
 \end{aligned} \tag{A.13}$$

$$\begin{aligned}
 I_{\text{spatial}}^3 &= \int d\mathbf{p}'_1 d\mathbf{p}'_2 d\mathbf{p}_1 d\mathbf{p}_2 d\mathbf{p}_3 d\mathbf{p}_4 \delta^{(3)}(\mathbf{p}'_1 + \mathbf{p}'_2 - \mathbf{p}_1 - \mathbf{p}_2) \\
 &\times \Phi_{\mathbf{P}_{\alpha}}^{*\mathbf{p}'_1\mathbf{p}_4} \Phi_{\mathbf{P}_{\beta}}^{*\mathbf{p}_3\mathbf{p}'_2} V(\mathbf{p}'_1 - \mathbf{p}_1) \Phi_{\mathbf{P}_{\delta}}^{\mathbf{p}_1\mathbf{p}_2} \Phi_{\mathbf{P}_{\gamma}}^{\mathbf{p}_3\mathbf{p}_4},
 \end{aligned} \tag{A.14}$$

$$\begin{aligned}
 I_{\text{spatial}}^4 &= \int d\mathbf{p}'_1 d\mathbf{p}'_2 d\mathbf{p}_1 d\mathbf{p}_2 d\mathbf{p}_3 d\mathbf{p}_4 \delta^{(3)}(\mathbf{p}'_1 + \mathbf{p}'_2 - \mathbf{p}_1 - \mathbf{p}_2) \\
 &\times \Phi_{\mathbf{P}_{\alpha}}^{*\mathbf{p}_3\mathbf{p}'_2} \Phi_{\mathbf{P}_{\beta}}^{*\mathbf{p}'_1\mathbf{p}_4} V(\mathbf{p}'_1 - \mathbf{p}_1) \Phi_{\mathbf{P}_{\delta}}^{\mathbf{p}_3\mathbf{p}_4} \Phi_{\mathbf{P}_{\gamma}}^{\mathbf{p}_1\mathbf{p}_2},
 \end{aligned} \tag{A.15}$$

$$\begin{aligned}
 I_{\text{spatial}}^5 &= \int d\mathbf{p}'_1 d\mathbf{p}'_2 d\mathbf{p}_1 d\mathbf{p}_2 d\mathbf{p}_3 d\mathbf{p}_4 \delta^{(3)}(\mathbf{p}'_1 + \mathbf{p}'_2 - \mathbf{p}_1 - \mathbf{p}_2) \\
 &\times \Phi_{\mathbf{P}_{\alpha}}^{*\mathbf{p}'_1\mathbf{p}_4} \Phi_{\mathbf{P}_{\beta}}^{*\mathbf{p}'_2\mathbf{p}_3} V(\mathbf{p}'_1 - \mathbf{p}_1) \Phi_{\mathbf{P}_{\delta}}^{\mathbf{p}_1\mathbf{p}_3} \Phi_{\mathbf{P}_{\gamma}}^{\mathbf{p}_2\mathbf{p}_4},
 \end{aligned} \tag{A.16}$$

$$\begin{aligned}
 I_{\text{spatial}}^6 &= \int d\mathbf{p}'_1 d\mathbf{p}'_2 \mathbf{p}_1 \mathbf{p}_2 \mathbf{p}_3 \mathbf{p}_4 \delta^{(3)}(\mathbf{p}'_1 + \mathbf{p}'_2 - \mathbf{p}_1 - \mathbf{p}_2) \\
 &\times \Phi_{\mathbf{P}_\alpha}^{*\mathbf{P}_3 \mathbf{P}'_1} \Phi_{\mathbf{P}_\beta}^{*\mathbf{P}_4 \mathbf{P}'_2} V(\mathbf{p}'_1 - \mathbf{p}_1) \Phi_{\mathbf{P}_\delta}^{\mathbf{P}_3 \mathbf{P}_2} \Phi_{\mathbf{P}_\gamma}^{\mathbf{P}_4 \mathbf{P}_1}.
 \end{aligned} \tag{A.17}$$

In order to be able to perform the spatial integrals analytically, the meson wave function $\Phi_{\mathbf{P}_\alpha}^{\mathbf{P}_i \mathbf{P}'_k}$ was used in a Gaussian form:

$$\Phi_{\mathbf{P}_\alpha}^{\mathbf{P}_i \mathbf{P}'_k} = \delta^{(3)}(\mathbf{P}_\alpha - \mathbf{p}_i - \mathbf{p}'_k) \left(\pi b_\alpha^2 \right)^{-3/4} e^{\left[-\frac{\bar{\mathbf{p}}}{2b_\alpha^2} \right]}, \tag{A.18}$$

where $\bar{\mathbf{p}} = \eta_\alpha \mathbf{p}_i - (1 - \eta_\alpha) \mathbf{p}_k$ and $\eta_\alpha = \frac{m_Q}{m_q + m_Q}$ is the parameter that will inform what is the meson of interest. Assuming $\mathbf{q} = \mathbf{p}'_1 - \mathbf{p}_1$ the expressions for the integrals will become

$$\begin{aligned}
 I_{\text{spatial}}^1(\alpha\beta; \gamma\delta) &= \delta^{(3)}(\mathbf{P}_\alpha + \mathbf{P}_\beta - \mathbf{P}_\gamma - \mathbf{P}_\delta) \left(\pi^4 b_\alpha^2 b_\beta^2 b_\gamma^2 b_\delta^2 \right)^{-3/4} \int d\mathbf{p}_1 d\mathbf{q} V(\mathbf{q}) \\
 &\times e^{-\frac{1}{2b_\alpha^2}(\mathbf{p}_1 + \mathbf{q} - (1 - \eta_\alpha)\mathbf{P}_\alpha)^2} e^{-\frac{1}{2b_\beta^2}(\mathbf{p}_1 - \mathbf{P}_\delta + \eta_\beta \mathbf{P}_\beta)^2} \\
 &\times e^{-\frac{1}{2b_\delta^2}(\mathbf{p}_1 - (1 - \eta_\delta)\mathbf{P}_\delta)^2} e^{-\frac{1}{2b_\gamma^2}(\mathbf{p}_1 + \mathbf{P}_\beta - \mathbf{P}_\delta - (1 - \eta_\gamma)\mathbf{P}_\gamma)^2},
 \end{aligned} \tag{A.19}$$

$$\begin{aligned}
 I_{\text{spatial}}^2(\alpha\beta; \gamma\delta) &= \delta^{(3)}(\mathbf{P}_\alpha + \mathbf{P}_\beta - \mathbf{P}_\gamma - \mathbf{P}_\delta) \left(\pi^4 b_\alpha^2 b_\beta^2 b_\gamma^2 b_\delta^2 \right)^{-3/4} \int d\mathbf{p}_1 d\mathbf{q} V(\mathbf{q}) \\
 &\times e^{-\frac{1}{2b_\alpha^2}(\mathbf{p}_1 - \mathbf{P}_\gamma + \eta_\alpha \mathbf{P}_\alpha)^2} e^{-\frac{1}{2b_\beta^2}(\mathbf{p}_1 + \mathbf{q} - (1 - \eta_\beta)\mathbf{P}_\beta)^2} \\
 &\times e^{-\frac{1}{2b_\delta^2}(\mathbf{p}_1 + \mathbf{P}_\alpha - \mathbf{P}_\gamma - (1 - \eta_\delta)\mathbf{P}_\delta)^2} e^{-\frac{1}{2b_\gamma^2}(\mathbf{p}_1 - (1 - \eta_\gamma)\mathbf{P}_\gamma)^2},
 \end{aligned} \tag{A.20}$$

$$\begin{aligned}
 I_{\text{spatial}}^3(\alpha\beta; \gamma\delta) &= \delta^{(3)}(\mathbf{P}_\alpha + \mathbf{P}_\beta - \mathbf{P}_\gamma - \mathbf{P}_\delta) \left(\pi^4 b_\alpha^2 b_\beta^2 b_\gamma^2 b_\delta^2 \right)^{-3/4} \int d\mathbf{p}_1 d\mathbf{q} V(\mathbf{q}) \\
 &\times e^{-\frac{1}{2b_\alpha^2}(\mathbf{p}_1 + \mathbf{q} - (1 - \eta_\alpha)\mathbf{P}_\alpha)^2} e^{-\frac{1}{2b_\beta^2}(\mathbf{p}_1 + \mathbf{q} + \mathbf{P}_\gamma - \mathbf{P}_\alpha - (1 - \eta_\beta)\mathbf{P}_\beta)^2} \\
 &\times e^{-\frac{1}{2b_\delta^2}(\mathbf{p}_1 - (1 - \eta_\delta)\mathbf{P}_\delta)^2} e^{-\frac{1}{2b_\gamma^2}(\eta_\gamma(\mathbf{p}_1 + \mathbf{q} + \mathbf{P}_\gamma - \mathbf{P}_\alpha) - (1 - \eta_\gamma)(\mathbf{P}_\alpha - \mathbf{p}_1 - \mathbf{q}))^2},
 \end{aligned} \tag{A.21}$$

$$\begin{aligned}
 I_{\text{spatial}}^4(\alpha\beta; \gamma\delta) &= \delta^{(3)}(\mathbf{P}_\alpha + \mathbf{P}_\beta - \mathbf{P}_\gamma - \mathbf{P}_\delta) \left(\pi^4 b_\alpha^2 b_\beta^2 b_\gamma^2 b_\delta^2 \right)^{-3/4} \int d\mathbf{p}_1 d\mathbf{q} V(\mathbf{q}) \\
 &\times e^{-\frac{1}{2b_\alpha^2}(\mathbf{p}_1 + \mathbf{q} + \mathbf{P}_\delta - \mathbf{P}_\beta - (1-\eta_\alpha)\mathbf{P}_\alpha)^2} e^{-\frac{1}{2b_\beta^2}(\mathbf{p}_1 + \mathbf{q} - (1-\eta_\beta)\mathbf{P}_\beta)^2} \\
 &\times e^{-\frac{1}{2b_\delta^2}(\eta_\delta(\mathbf{p}_1 + \mathbf{q} + \mathbf{P}_\delta - \mathbf{P}_\beta) - (1-\eta_\delta)(\mathbf{P}_\beta - \mathbf{p}_1 - \mathbf{q}))^2} e^{-\frac{1}{2b_\gamma^2}(\mathbf{p}_1 - (1-\eta_\gamma)\mathbf{P}_\gamma)^2},
 \end{aligned} \tag{A.22}$$

$$\begin{aligned}
 I_{\text{spatial}}^5(\alpha\beta; \gamma\delta) &= \delta^{(3)}(\mathbf{P}_\alpha + \mathbf{P}_\beta - \mathbf{P}_\gamma - \mathbf{P}_\delta) \left(\pi^4 b_\alpha^2 b_\beta^2 b_\gamma^2 b_\delta^2 \right)^{-3/4} \int d\mathbf{p}_1 d\mathbf{q} V(\mathbf{q}) \\
 &\times e^{-\frac{1}{2b_\alpha^2}(\mathbf{p}_1 + \mathbf{q} - (1-\eta_\alpha)\mathbf{P}_\alpha)^2} e^{-\frac{1}{2b_\beta^2}(\mathbf{p}_1 - \mathbf{P}_\delta + \eta_\beta\mathbf{P}_\beta)^2} \\
 &\times e^{-\frac{1}{2b_\delta^2}(\mathbf{p}_1 - (1-\eta_\delta)\mathbf{P}_\delta)^2} e^{-\frac{1}{2b_\gamma^2}(\mathbf{p}_1 + \mathbf{q} - \mathbf{P}_\alpha + \eta_\gamma\mathbf{P}_\gamma)^2},
 \end{aligned} \tag{A.23}$$

$$\begin{aligned}
 I_{\text{spatial}}^6(\alpha\beta; \gamma\delta) &= \delta^{(3)}(\mathbf{P}_\alpha + \mathbf{P}_\beta - \mathbf{P}_\gamma - \mathbf{P}_\delta) \left(\pi^4 b_\alpha^2 b_\beta^2 b_\gamma^2 b_\delta^2 \right)^{-3/4} \int d\mathbf{p}_1 d\mathbf{q} V(\mathbf{q}) \\
 &\times e^{-\frac{1}{2b_\alpha^2}(\mathbf{p}_1 + \mathbf{q} - (1-\eta_\alpha)\mathbf{P}_\alpha)^2} e^{-\frac{1}{2b_\beta^2}(\mathbf{p}_1 - \mathbf{P}_\gamma + (1-\eta_\beta)\mathbf{P}_\beta)^2} \\
 &\times e^{-\frac{1}{2b_\delta^2}(\mathbf{p}_1 + \mathbf{q} - \mathbf{P}_\alpha + (1-\eta_\delta)\mathbf{P}_\delta)^2} e^{-\frac{1}{2b_\gamma^2}(\mathbf{p}_1 - (1-\eta_\gamma)\mathbf{P}_\gamma)^2}.
 \end{aligned} \tag{A.24}$$

It is convenient to evaluate these integrals in the center-of-mass (CM) and in the pair rest frame, which is

$$\mathbf{P}_\gamma = -\mathbf{P}_\delta = \mathbf{p},$$

$$\mathbf{P}_\alpha = -\mathbf{P}_\beta = \mathbf{p}',$$

where \mathbf{p}' is the pair incident relative momentum and \mathbf{p} is the pair outgoing relative momentum. Considering also the simplest case of identical particle, that is

$$b_\alpha = b_\beta = b_\gamma = b_\delta = b,$$

$$\eta_\alpha = \eta_\beta = \eta_\gamma = \eta_\delta = \eta,$$

replacing those assumptions in the expressions for I_{spatial}^j become

$$\begin{aligned}
 I_{\text{spatial}}^1(\alpha\beta; \gamma\delta) &= \frac{1}{\pi^3 b^6} \int d\mathbf{p}_1 d\mathbf{q} V(\mathbf{q}) \\
 &\times e^{-\frac{1}{2b^2}(\mathbf{p}_1+\mathbf{q}-(1-\eta)\mathbf{p}')^2} e^{-\frac{1}{2b^2}(\mathbf{p}_1+\mathbf{p}-\eta\mathbf{p}')^2} \\
 &\times e^{-\frac{1}{2b^2}(\mathbf{p}_1+(1-\eta)\mathbf{p})^2} e^{-\frac{1}{2b^2}(\mathbf{p}_1-\mathbf{p}'+\eta\mathbf{p})^2}, \quad (\text{A.25})
 \end{aligned}$$

$$\begin{aligned}
 I_{\text{spatial}}^2(\alpha\beta; \gamma\delta) &= \frac{1}{\pi^3 b^6} \int d\mathbf{p}_1 d\mathbf{q} V(\mathbf{q}) \\
 &\times e^{-\frac{1}{2b^2}(\mathbf{p}_1+\mathbf{q}+(1-\eta)\mathbf{p}')^2} e^{-\frac{1}{2b^2}(\mathbf{p}_1-\mathbf{p}+\eta\mathbf{p}')^2} \\
 &\times e^{-\frac{1}{2b^2}(\mathbf{p}_1-(1-\eta)\mathbf{p})^2} e^{-\frac{1}{2b^2}(\mathbf{p}_1+\mathbf{p}'-\eta\mathbf{p})^2}, \quad (\text{A.26})
 \end{aligned}$$

$$\begin{aligned}
 I_{\text{spatial}}^3(\alpha\beta; \gamma\delta) &= \frac{1}{\pi^3 b^6} \int d\mathbf{p}_1 d\mathbf{q} V(\mathbf{q}) \\
 &\times e^{-\frac{1}{2b^2}(\mathbf{p}_1+\mathbf{q}-(1-\eta)\mathbf{p}')^2} e^{-\frac{1}{2b^2}(\mathbf{p}_1+\mathbf{q}+\mathbf{p}-(1-\eta)\mathbf{p}')^2} \\
 &\times e^{-\frac{1}{2b^2}(\mathbf{p}_1+(1-\eta)\mathbf{p})^2} e^{-\frac{1}{2b^2}(\mathbf{p}_1+\mathbf{q}-\mathbf{p}'+\eta\mathbf{p})^2}, \quad (\text{A.27})
 \end{aligned}$$

$$\begin{aligned}
 I_{\text{spatial}}^4(\alpha\beta; \gamma\delta) &= \frac{1}{\pi^3 b^6} \int d\mathbf{p}_1 d\mathbf{q} V(\mathbf{q}) \\
 &\times e^{-\frac{1}{2b^2}(\mathbf{p}_1+\mathbf{q}+(1-\eta)\mathbf{p}')^2} e^{-\frac{1}{2b^2}(\mathbf{p}_1+\mathbf{q}-\mathbf{p}+\eta\mathbf{p}')^2} \\
 &\times e^{-\frac{1}{2b^2}(\mathbf{p}_1-(1-\eta)\mathbf{p})^2} e^{-\frac{1}{2b^2}(\mathbf{p}_1+\mathbf{q}-\eta\mathbf{p}+\mathbf{p}')^2}, \quad (\text{A.28})
 \end{aligned}$$

$$\begin{aligned}
 I_{\text{spatial}}^5(\alpha\beta; \gamma\delta) &= \frac{1}{\pi^3 b^6} \int d\mathbf{p}_1 d\mathbf{q} V(\mathbf{q}) \\
 &\times e^{-\frac{1}{2b^2}(\mathbf{p}_1+\mathbf{q}-(1-\eta)\mathbf{p}')^2} e^{-\frac{1}{2b^2}(\mathbf{p}_1+\mathbf{p}-\eta\mathbf{p}')^2} \\
 &\times e^{-\frac{1}{2b^2}(\mathbf{p}_1+(1-\eta)\mathbf{p})^2} e^{-\frac{1}{2b^2}(\mathbf{p}_1+\mathbf{q}-\mathbf{p}'+\eta\mathbf{p})^2}, \quad (\text{A.29})
 \end{aligned}$$

$$\begin{aligned}
 I_{\text{spatial}}^6(\alpha\beta; \gamma\delta) &= \frac{1}{\pi^3 b^6} \int d\mathbf{p}_1 d\mathbf{q} V(\mathbf{q}) \\
 &\times e^{-\frac{1}{2b^2}(\mathbf{p}_1 + \mathbf{q} - (1-\eta)\mathbf{p}')^2} e^{-\frac{1}{2b^2}(\mathbf{p}_1 - \mathbf{p} - (1-\eta)\mathbf{p}')^2} \\
 &\times e^{-\frac{1}{2b^2}(\mathbf{p}_1 - \eta\mathbf{p})^2} e^{-\frac{1}{2b^2}(\mathbf{p}_1 + \mathbf{q} - \mathbf{p}' - (1-\eta)\mathbf{p})^2}. \tag{A.30}
 \end{aligned}$$

By expanding all these terms it is easy to see that the argument of the integrals are gaussians, and the integrals can be solved using

$$\begin{aligned}
 I &= \int d\mathbf{p} \left[e^{-a\mathbf{p}^2 + \mathbf{p} \cdot \mathbf{Q}} \right] \\
 &= \left(\frac{\pi}{a} \right)^{3/2} e^{\frac{\mathbf{Q}^2}{4a}}. \tag{A.31}
 \end{aligned}$$

For the contact interaction $V(q)$ is constant, $V(q) = V$. Therefore, performing the integral over \mathbf{p}_1 and \mathbf{q} :

$$\begin{aligned}
 I_{\text{spatial}}^1(\alpha\beta; \gamma\delta) &= \frac{8}{3\sqrt{3}} V \\
 &\times \exp \left[-\frac{1}{2b^2} 2\eta^2 (\mathbf{p}^2 + \mathbf{p}'^2) - \frac{1}{2b^2} (1-2\eta) (\mathbf{p} + \mathbf{p}')^2 \right] \\
 &\times \exp \left[\frac{1}{2b^2} \frac{1}{3} (\mathbf{p} + (1-2\eta)\mathbf{p}')^2 \right], \tag{A.32}
 \end{aligned}$$

$$\begin{aligned}
 I_{\text{spatial}}^2(\alpha\beta; \gamma\delta) &= \frac{8}{3\sqrt{3}} V \\
 &\times \exp \left[-\frac{1}{2b^2} 2\eta^2 (\mathbf{p}^2 + \mathbf{p}'^2) - \frac{1}{2b^2} (1-2\eta) (\mathbf{p} + \mathbf{p}')^2 \right] \\
 &\times \exp \left[\frac{1}{2b^2} \frac{1}{3} (\mathbf{p} + (1-2\eta)\mathbf{p}')^2 \right], \tag{A.33}
 \end{aligned}$$

$$\begin{aligned}
 I_{\text{spatial}}^3(\alpha\beta; \gamma\delta) &= \frac{8}{3\sqrt{3}} V \\
 &\times \exp \left[-\frac{1}{2b^2} 2\eta^2 (\mathbf{p}^2 + \mathbf{p}'^2) - \frac{1}{2b^2} (1-2\eta) (\mathbf{p} + \mathbf{p}')^2 \right] \\
 &\times \exp \left[\frac{1}{2b^2} \frac{1}{3} ((1-2\eta)\mathbf{p} + \mathbf{p}')^2 \right], \tag{A.34}
 \end{aligned}$$

$$\begin{aligned}
 I_{\text{spatial}}^4(\alpha\beta; \gamma\delta) &= \frac{8}{3\sqrt{3}}V \\
 &\times \exp\left[-\frac{1}{2b^2}2\eta^2(\mathbf{p}^2 + \mathbf{p}'^2) - \frac{1}{2b^2}(1-2\eta)(\mathbf{p} + \mathbf{p}')^2\right] \\
 &\times \exp\left[\frac{1}{2b^2}\frac{1}{3}((1-2\eta)\mathbf{p} - \mathbf{p}')^2\right], \tag{A.35}
 \end{aligned}$$

$$I_{\text{spatial}}^5(\alpha\beta; \gamma\delta) = V \exp\left[-\frac{1}{2b^2}\eta^2(\mathbf{p} - \mathbf{p}')^2\right], \tag{A.36}$$

$$I_{\text{spatial}}^6(\alpha\beta; \gamma\delta) = V \exp\left[-\frac{1}{2b^2}(1-\eta^2)(\mathbf{p} + \mathbf{p}')^2\right]. \tag{A.37}$$

Replacing all the matrix elements I^j in Eq. (A.2) and using $V = V_{\text{hyp}}$, from Eq. (3.92), it is possible to have an expression for the spin-spin term contribution

$$\begin{aligned}
 V^{\text{hyp}}(\mathbf{p}, \mathbf{p}') &= V^1(\mathbf{p}, \mathbf{p}') + V^2(\mathbf{p}, \mathbf{p}') + V^3(\mathbf{p}, \mathbf{p}') \\
 &+ V^4(\mathbf{p}, \mathbf{p}') + V^5(\mathbf{p}, \mathbf{p}') + V^6(\mathbf{p}, \mathbf{p}'), \tag{A.38}
 \end{aligned}$$

with

$$\begin{aligned}
 V^1(\mathbf{p}, \mathbf{p}') &= \left(\frac{1}{2}\right) \left(\frac{1}{9}\right) \frac{8}{3\sqrt{3}} \left(\frac{1}{(2\pi)^3} \frac{8\pi\alpha_s}{m_q m_Q}\right) \\
 &\times \exp\left[-\frac{1}{2b^2}(2\eta^2(\mathbf{p}^2 + \mathbf{p}'^2) + (1-2\eta)(\mathbf{p} + \mathbf{p}')^2)\right] \\
 &\times \exp\left[\frac{1}{2b^2}\frac{1}{3}(\mathbf{p} + (1-2\eta)\mathbf{p}')^2\right], \tag{A.39}
 \end{aligned}$$

$$\begin{aligned}
 V^2(\mathbf{p}, \mathbf{p}') &= \left(\frac{1}{2}\right) \left(\frac{1}{9}\right) \frac{8}{3\sqrt{3}} \left(\frac{1}{(2\pi)^3} \frac{8\pi\alpha_s}{m_q m_Q}\right) \\
 &\times \exp\left[-\frac{1}{2b^2}(2\eta^2(\mathbf{p}^2 + \mathbf{p}'^2) + (1-2\eta)(\mathbf{p} + \mathbf{p}')^2)\right] \\
 &\times \exp\left[\frac{1}{2b^2}\frac{1}{3}(\mathbf{p} + (1-2\eta)\mathbf{p}')^2\right], \tag{A.40}
 \end{aligned}$$

$$\begin{aligned}
 V^3(\mathbf{p}, \mathbf{p}') &= \left(\frac{1}{2}\right) \left(\frac{1}{9}\right) \frac{8}{3\sqrt{3}} \left(\frac{1}{(2\pi)^3} \frac{8\pi\alpha_s}{m_q m_Q}\right) \\
 &\times \exp\left[-\frac{1}{2b^2} \left(2\eta^2(\mathbf{p}^2 + \mathbf{p}'^2) + (1 - 2\eta)(\mathbf{p} + \mathbf{p}')^2\right)\right] \\
 &\times \exp\left[\frac{1}{2b^2} \frac{1}{3} \left((1 - 2\eta)\mathbf{p} + \mathbf{p}'\right)^2\right], \tag{A.41}
 \end{aligned}$$

$$\begin{aligned}
 V^4(\mathbf{p}, \mathbf{p}') &= \left(\frac{1}{2}\right) \left(\frac{1}{9}\right) \frac{8}{3\sqrt{3}} \left(\frac{1}{(2\pi)^3} \frac{8\pi\alpha_s}{m_q m_Q}\right) \\
 &\times \exp\left[-\frac{1}{2b^2} \left(2\eta^2(\mathbf{p}^2 + \mathbf{p}'^2) + (1 - 2\eta)(\mathbf{p} + \mathbf{p}')^2\right)\right] \\
 &\times \exp\left[\frac{1}{2b^2} \frac{1}{3} \left((1 - 2\eta)\mathbf{p} + \mathbf{p}'\right)^2\right], \tag{A.42}
 \end{aligned}$$

$$\begin{aligned}
 V^5(\mathbf{p}, \mathbf{p}') &= \left(\frac{1}{9}\right) \left(\frac{1}{(2\pi)^3} \frac{8\pi\alpha_s}{m_q m_Q}\right) \\
 &\times \exp\left[-\frac{1}{2b^2} \left(\eta^2(\mathbf{p} - \mathbf{p}')^2\right)\right], \tag{A.43}
 \end{aligned}$$

$$\begin{aligned}
 V^6(\mathbf{p}, \mathbf{p}') &= \left(\frac{1}{9}\right) \left(\frac{1}{(2\pi)^3} \frac{8\pi\alpha_s}{m_Q m_Q}\right) \\
 &\times \exp\left[-\frac{1}{2b^2} \left((1 - \eta)^2(\mathbf{p} + \mathbf{p}')^2\right)\right]. \tag{A.44}
 \end{aligned}$$

A.2 Long-range contribution

Besides the six terms that appear evaluating Eq.(A.7), there is another one that will represent the long-range interactions given by

$$I_{\text{spatial}}^{\text{long-range}} = \Phi_{\alpha}^{*\mu\nu'} \Phi_{\beta}^{*v\mu'} V(\mu\nu, \sigma\rho) \Phi_{\gamma}^{\sigma\mu'} \Phi_{\delta}^{\rho\mu'}, \tag{A.45}$$

Expanding this expression

$$\begin{aligned}
 I_{\text{spatial}}^{\text{long-range}} &= \int d\mathbf{p}'_1 d\mathbf{p}'_2 d\mathbf{p}_1 d\mathbf{p}_2 d\mathbf{p}_3 d\mathbf{p}_4 \delta^{(3)}(\mathbf{p}'_1 + \mathbf{p}'_2 - \mathbf{p}_1 - \mathbf{p}_2) \\
 &\times \Phi_{\mathbf{P}'_1}^{*\mathbf{P}'_1\mathbf{P}_3} \Phi_{\mathbf{P}'_2}^{*\mathbf{P}'_2\mathbf{P}_4} V(\mathbf{p}'_1 - \mathbf{p}_1) \Phi_{\mathbf{P}'_3}^{\mathbf{P}_1\mathbf{P}_3} \Phi_{\mathbf{P}'_4}^{\mathbf{P}_2\mathbf{P}_4}. \tag{A.46}
 \end{aligned}$$

Applying the center-of-mass frame

$$\begin{aligned}
 I_{\text{spatial}}^{\text{long-range}} &= \frac{1}{\pi^3 b^6} V(\mathbf{p}' - \mathbf{p}) \int d\mathbf{p}'_2 d\mathbf{p}_1 \\
 &\times e^{-\frac{1}{2b^2}(\mathbf{p}_1 - \mathbf{p} - \eta\mathbf{p}')^2} e^{-\frac{1}{2b^2}(\mathbf{p}'_2 + (1-\eta)\mathbf{p}')^2} \\
 &\times e^{-\frac{1}{2b^2}(\mathbf{p}_1 - (1-\eta)\mathbf{p})^2} e^{-\frac{1}{2b^2}(\mathbf{p}'_2 + \mathbf{p}' - \eta\mathbf{p})^2}, \tag{A.47}
 \end{aligned}$$

and performing the integral using the expression (3.93) for the $V(\mathbf{p} - \mathbf{p}')$, it is possible to have a final equation for the long-range contribution

$$V^{\text{long-range}}(\mathbf{p}' - \mathbf{p}) = \frac{g^2}{(2\pi)^3} \frac{e^{-\frac{1}{2b^2}\eta^2(\mathbf{p}' - \mathbf{p})^2}}{(\mathbf{p}' - \mathbf{p})^2 + m_\sigma^2}. \tag{A.48}$$

Bibliography

- [1] R. Hanbury-Brown and R. Q. Twiss, “A New type of interferometer for use in radio astronomy”, *The London, Edinburgh, and Dublin Philosophical Magazine and Journal of Science* **45** (1954), no. 366, 663–682,
[doi:10.1080/14786440708520475](https://doi.org/10.1080/14786440708520475).
- [2] R. H. Brown and R. Q. Twiss, “Correlation between photons in two coherent beams of light”, *Nature* **177** (1956), no. 4497, 27–29,
[doi:10.1038/177027a0](https://doi.org/10.1038/177027a0).
- [3] R. Hanbury-Brown and R. Q. Twiss, “A test of a new type of stellar interferometer on sirius”, *Nature* **178** (1956), no. 4541, 1046–1048,
[doi:10.1038/1781046a0](https://doi.org/10.1038/1781046a0).
- [4] G. S. L. W. Goldhaber, G. and A. Pais, “Influence of Bose-Einstein Statistics on the Antiproton-Proton Annihilation Process”, *Physical Review* **120** (1960), no. 1, 300, [doi:10.1103/PhysRev.120.300](https://doi.org/10.1103/PhysRev.120.300).
- [5] M. A. Lisa, S. Pratt, R. Soltz, and U. Wiedemann, “FEMTOSCOPY IN RELATIVISTIC HEAVY ION COLLISIONS: Two Decades of Progress”, *Annual Review of Nuclear and Particle Science* **55** (2005), no. 1, 357–402,
[doi:10.1146/annurev.nucl.55.090704.151533](https://doi.org/10.1146/annurev.nucl.55.090704.151533).
- [6] C.-Y. Wong, “Introduction to High-Energy Heavy-Ion Collisions”. World Scientific, 1994.
- [7] S. S. Padula, “HBT interferometry: Historical perspective”, *Braz. J. Phys.* **35** (2005) 70, [doi:10.1590/S0103-97332005000100005](https://doi.org/10.1590/S0103-97332005000100005).
- [8] W. Florkowski, “Phenomenology of Ultra-Relativistic Heavy-Ion Collisions”. ISBN 978.
- [9] M. Steinpreis, “Neutral Kaon Femtoscopy in Pb-Pb Collisions at $\sqrt{s_{NN}} = 2.76$ TeV at the LHC with ALICE”. PhD thesis.
- [10] D. Anchishkin, U. W. Heinz, and P. Renk, “Final state interactions in two particle interferometry”, *Phys. Rev. C* **57** (1998) 1428–1439,
[doi:10.1103/PhysRevC.57.1428](https://doi.org/10.1103/PhysRevC.57.1428), [arXiv:nucl-th/9710051](https://arxiv.org/abs/nucl-th/9710051).

- [11] O. W. Arnold, "Study of the hyperon-nucleon interaction via femtoscopy in elementary systems with HADES and ALICE". PhD thesis, Munich, Tech. U., 2017.
- [12] S. E. Koonin, "Proton pictures of high-energy nuclear collisions", *Physics Letters B* **70** (1977), no. 1, 43–47,
[doi:https://doi.org/10.1016/0370-2693\(77\)90340-9](https://doi.org/10.1016/0370-2693(77)90340-9).
- [13] J. Buxton, "ΛK and Ξ–K Femtoscopy in Pb-Pb Collisions at from the LHC ALICE Collaboration". PhD thesis, Ohio State U., 2019.
- [14] F. B. Yano and S. E. Koonin, "Determining Pion Source Parameters in Relativistic Heavy Ion Collisions", *Phys. Lett. B* **78** (1978) 556–559,
[doi:10.1016/0370-2693\(78\)90638-X](https://doi.org/10.1016/0370-2693(78)90638-X).
- [15] S. Pratt, "Pion interferometry for exploding sources", *Phys. Rev. Lett.* **53** (Sep, 1984) 1219–1221, [doi:10.1103/PhysRevLett.53.1219](https://doi.org/10.1103/PhysRevLett.53.1219).
- [16] M. G. Bowler, "Coulomb corrections to bose-einstein corrections have greatly exaggerated", *Physics Letters B* **270** (1991), no. 1, 69–74,
[doi:10.1016/0370-2693\(91\)91541-3](https://doi.org/10.1016/0370-2693(91)91541-3).
- [17] R. Lednicky and V. L. Lyuboshits, "Final state interaction effect on pairing correlations between particles with small relative momenta", *Yad. Fiz.* **35** (1981) 1316–1330.
- [18] R. H. Landau, "Quantum mechanics II: a second course in quantum theory". John Wiley & Sons, 2008.
- [19] W. H. J. Arfken, G. B. and F. E. Harris, "Chapter 15 - legendre functions", in *Mathematical Methods for Physicists (Seventh Edition)*, pp. 715–772. Academic Press, Boston, seventh edition edition, 2013.
[doi:10.1016/B978-0-12-384654-9.00015-3](https://doi.org/10.1016/B978-0-12-384654-9.00015-3).
- [20] W. H. J. Arfken, G. B. and F. E. Harris, "Chapter 14 - bessel functions", in *Mathematical Methods for Physicists (Seventh Edition)*, pp. 643–713. Academic Press, Boston, seventh edition edition, 2013.
[doi:10.1016/B978-0-12-384654-9.00014-1](https://doi.org/10.1016/B978-0-12-384654-9.00014-1).
- [21] H. A. Bethe, "Theory of the effective range in nuclear scattering", *Phys. Rev.* **76** (Jul, 1949) 38–50, [doi:10.1103/PhysRev.76.38](https://doi.org/10.1103/PhysRev.76.38).

- [22] A. F. R. d. T. Piza, “Chapter 10 - Espalhamento por um potencial de curto alcance”. EdUSP, 2003.
- [23] S. Cho et al., “Exotic hadrons from heavy ion collisions”, *Progress in Particle and Nuclear Physics* **95** (Jul, 2017) 279–322,
[doi:10.1016/j.pnpnp.2017.02.002](https://doi.org/10.1016/j.pnpnp.2017.02.002).
- [24] D. J. Griffiths, “Introduction to quantum mechanics”. Prentice Hall, second edi, 2010.
- [25] L. D. Landau and E. M. Lifshitz, “Quantum mechanics: non-relativistic theory”, volume 3. Elsevier, 2013.
- [26] R. Landau, M. Paez, and C. C. Bordeianu, “Computational Physics: Problem Solving with Computers: Second Edition”, volume 51. 01, 2007.
[doi:10.1063/1.882306](https://doi.org/10.1063/1.882306).
- [27] E. F. Redish and K. Stricker-Bauer, “Off-energy-shell behavior of realistic potential models”, *Phys. Rev. C* **36** (Aug, 1987) 513–532,
[doi:10.1103/PhysRevC.36.513](https://doi.org/10.1103/PhysRevC.36.513).
- [28] L. Tomio and S. K. Adhikari, “Method for scattering equations. ii. iterative solution”, *Phys. Rev. C* **22** (Jul, 1980) 28–35,
[doi:10.1103/PhysRevC.22.28](https://doi.org/10.1103/PhysRevC.22.28).
- [29] K. Morita, T. Furumoto, and A. Ohnishi, “Lambda-lambda interaction from relativistic heavy-ion collisions”, *Physical Review C* **91** (Feb, 2015)
[doi:10.1103/physrevc.91.024916](https://doi.org/10.1103/physrevc.91.024916).
- [30] M. M. Nagels, T. A. Rijken, and J. J. de Swart, “Baryon-baryon scattering in a one-boson-exchange-potential approach. iii. a nucleon-nucleon and hyperon-nucleon analysis including contributions of a nonet of scalar mesons”, *Phys. Rev. D* **20** (Oct, 1979) 1633–1645,
[doi:10.1103/PhysRevD.20.1633](https://doi.org/10.1103/PhysRevD.20.1633).
- [31] Y. Fujiwara, Y. Suzuki, and C. Nakamoto, “Baryon-baryon interactions in the SU(6) quark model and their applications to light nuclear systems”, *Progress in Particle and Nuclear Physics* **58** (Apr, 2007) 439–520,
[doi:10.1016/j.pnpnp.2006.08.001](https://doi.org/10.1016/j.pnpnp.2006.08.001).

- [32] E. Hiyama et al., “Four-body cluster structure of $A = 7 - 10$ double- Λ hypernuclei”, *Phys. Rev. C* **66** (Aug, 2002) 024007, [doi:10.1103/PhysRevC.66.024007](https://doi.org/10.1103/PhysRevC.66.024007).
- [33] I. Filikhin and A. Gal, “Faddeev–Yakubovsky calculations for light Lambda-Lambda hypernuclei”, *Nuclear Physics A* **707** (Sep, 2002) 491–509, [doi:10.1016/s0375-9474\(02\)01008-4](https://doi.org/10.1016/s0375-9474(02)01008-4).
- [34] A. Bodmer and Q. Usmani, “Binding energies of hypernuclei and Λ -nuclear interactions”, *Nuclear Physics A* **450** (1986) 257–274, [doi:10.1134/S154747710606001X](https://doi.org/10.1134/S154747710606001X).
- [35] F. Wang and S. Pratt, “Lambda-Proton Correlations in Relativistic Heavy Ion Collisions”, *Phys. Rev. Lett.* **83** (Oct, 1999) 3138–3141, [doi:10.1103/PhysRevLett.83.3138](https://doi.org/10.1103/PhysRevLett.83.3138).
- [36] D. L. Mihaylov et al., “A femtosopic correlation analysis tool using the schrödinger equation (cats)”, *The European Physical Journal C* **78** (May, 2018) [doi:10.1140/epjc/s10052-018-5859-0](https://doi.org/10.1140/epjc/s10052-018-5859-0).
- [37] S. Szpigel, “Interação méson-méson no formalismo Fock-Tani”. PhD thesis, Universidade de São Paulo, 1995.
- [38] D. Hadjimichef, G. Krein, S. Szpigel, and J. S. da Veiga, “Mapping of composite hadrons into elementary hadrons and effective hadronic Hamiltonians”, *Annals Phys.* **268** (1998) 105–148, [doi:10.1006/aphy.1998.5825](https://doi.org/10.1006/aphy.1998.5825), [arXiv:hep-ph/9805459](https://arxiv.org/abs/hep-ph/9805459).
- [39] T. F. Caramés et al., “Hadronic molecules with a \bar{D} meson in a medium”, *Phys. Rev. D* **94** (Aug, 2016) 034009, [doi:10.1103/PhysRevD.94.034009](https://doi.org/10.1103/PhysRevD.94.034009).
- [40] Particle Data Group Collaboration, “Review of Particle Physics”, *PTEP* **2020** (2020), no. 8, 083C01, [doi:10.1093/ptep/ptaa104](https://doi.org/10.1093/ptep/ptaa104).
- [41] STAR Collaboration, “ $\Lambda\Lambda$ Correlation Function in Au+Au collisions at $\sqrt{s_{NN}} = 200$ GeV”, *Phys. Rev. Lett.* **114** (2015), no. 2, 022301, [doi:10.1103/PhysRevLett.114.022301](https://doi.org/10.1103/PhysRevLett.114.022301), [arXiv:1408.4360](https://arxiv.org/abs/1408.4360).
- [42] S. Acharya et al., “Study of the $\Lambda\Lambda$ interaction with femtoscopy correlations in pp and p–Pb collisions at the LHC”, *Physics Letters B* **797** (Oct, 2019) 134822, [doi:10.1016/j.physletb.2019.134822](https://doi.org/10.1016/j.physletb.2019.134822).

- [43] S. Acharya et al., “p-p, p- Λ , and Λ - Λ correlations studied via femtoscopy in pp reactions at $\sqrt{s} = 7$ TeV”, *Physical Review C* **99** (Feb, 2019) [doi:10.1103/physrevc.99.024001](https://doi.org/10.1103/physrevc.99.024001).
- [44] S. K. Adhikari, “Improved effective-range expansions for small and large values of scattering length”, *European Journal of Physics* **39** (aug, 2018) 055403, [doi:10.1088/1361-6404/aad620](https://doi.org/10.1088/1361-6404/aad620).
- [45] T. Barnes and E. S. Swanson, “Diagrammatic approach to meson-meson scattering in the nonrelativistic quark potential model”, *Phys. Rev. D* **46** (Jul, 1992) 131–159, [doi:10.1103/PhysRevD.46.131](https://doi.org/10.1103/PhysRevD.46.131).